



CERN-PH-EP-2014-210

Submitted to: JHEP

Search for neutral Higgs bosons of the minimal supersymmetric standard model in pp collisions at $\sqrt{s} = 8$ TeV with the ATLAS detector

The ATLAS Collaboration

Abstract

A search for the neutral Higgs bosons predicted by the Minimal Supersymmetric Standard Model (MSSM) is reported. The analysis is performed on data from proton–proton collisions at a centre-of-mass energy of 8 TeV collected with the ATLAS detector at the Large Hadron Collider. The samples used for this search were collected in 2012 and correspond to integrated luminosities in the range 19.5–20.3 fb⁻¹. The MSSM Higgs bosons are searched for in the $\tau\tau$ final state. No significant excess over the expected background is observed, and exclusion limits are derived for the production cross section times branching fraction of a scalar particle as a function of its mass. The results are also interpreted in the MSSM parameter space for various benchmark scenarios.

Search for neutral Higgs bosons of the minimal supersymmetric standard model in pp collisions at $\sqrt{s} = 8$ TeV with the ATLAS detector

ABSTRACT: A search for the neutral Higgs bosons predicted by the Minimal Supersymmetric Standard Model (MSSM) is reported. The analysis is performed on data from proton–proton collisions at a centre-of-mass energy of 8 TeV collected with the ATLAS detector at the Large Hadron Collider. The samples used for this search were collected in 2012 and correspond to integrated luminosities in the range $19.5\text{--}20.3\text{ fb}^{-1}$. The MSSM Higgs bosons are searched for in the $\tau\tau$ final state. No significant excess over the expected background is observed, and exclusion limits are derived for the production cross section times branching fraction of a scalar particle as a function of its mass. The results are also interpreted in the MSSM parameter space for various benchmark scenarios.

Contents

1	Introduction	1
2	The ATLAS detector	3
3	Data and Monte Carlo simulation samples	4
4	Object reconstruction	5
5	Search channels	6
5.1	The $h/H/A \rightarrow \tau_e\tau_\mu$ channel	7
5.2	The $h/H/A \rightarrow \tau_{\text{lep}}\tau_{\text{had}}$ channel	11
5.3	The $h/H/A \rightarrow \tau_{\text{had}}\tau_{\text{had}}$ channel	16
6	Systematic uncertainties	19
7	Results	22
8	Summary	26

1 Introduction

The discovery of a scalar particle at the Large Hadron Collider (LHC) [1, 2] has provided important insight into the mechanism of electroweak symmetry breaking. Experimental studies of the new particle [3–7] demonstrate consistency with the Standard Model (SM) Higgs boson [8–13]. However, it remains possible that the discovered particle is part of an extended scalar sector, a scenario that is favoured by a number of theoretical arguments [14, 15].

The Minimal Supersymmetric Standard Model (MSSM) [16–20] is an extension of the SM, which provides a framework addressing naturalness, gauge coupling unification, and the existence of dark matter. The Higgs sector of the MSSM contains two Higgs doublets, which results in five physical Higgs bosons after electroweak symmetry breaking. Of these bosons, two are neutral and CP-even (h , H), one is neutral and CP-odd (A),¹ and the remaining two are charged (H^\pm). At tree level, the mass of the light scalar Higgs boson, m_h , is restricted to be smaller than the Z boson mass, m_Z . This bound is weakened due to radiative corrections up to a maximum allowed value of $m_h \sim 135$ GeV. Only two additional parameters are needed with respect to the SM at tree level to describe the MSSM Higgs

¹By convention the lighter CP-even Higgs boson is denoted h , the heavier CP-even Higgs boson is denoted H . The masses of the three bosons are denoted in the following as m_h , m_H and m_A for h , H and A , respectively.

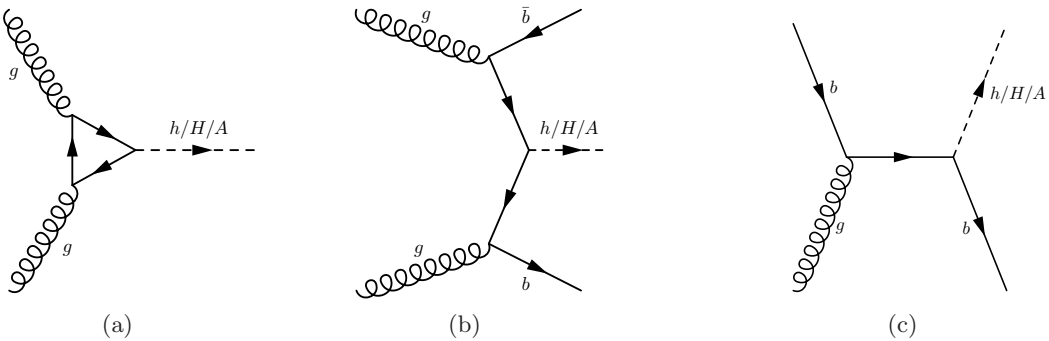


Figure 1. Example Feynman diagrams for (a) gluon fusion and (b) b -associated production in the four-flavour scheme and (c) five-flavour scheme of a neutral MSSM Higgs boson.

sector. These can be chosen to be the mass of the CP-odd Higgs boson, m_A , and the ratio of the vacuum expectation values of the two Higgs doublets, $\tan\beta$. Beyond lowest order, the MSSM Higgs sector depends on additional parameters, which are fixed at specific values in various MSSM benchmark scenarios. For example, in the m_h^{\max} scenario the radiative corrections are chosen such that m_h is maximized for a given $\tan\beta$ and M_{SUSY} [21, 22].² This results for $M_{\text{SUSY}} = 1 \text{ TeV}$ in $m_h \sim 130 \text{ GeV}$ for large m_A and $\tan\beta$. In addition, in the same region the heavy Higgs bosons, H , A and H^\pm , are approximately mass degenerate and h has properties very similar to a SM Higgs boson with the same mass. This feature is generic in the MSSM Higgs sector: a decoupling limit exists defined by $m_A \gg m_Z$ in which the heavy Higgs bosons have similar masses and the light CP-even Higgs boson in practice becomes identical to a SM Higgs boson with the same mass.

The discovery of a SM-like Higgs boson, with mass that is now measured to be $125.36 \pm 0.37 \text{ (stat)} \pm 0.18 \text{ (syst)} \text{ GeV}$ [24], has prompted the definition of additional MSSM scenarios [23]. Most notably, the $m_h^{\text{mod}+}$ and $m_h^{\text{mod}-}$ scenarios are similar to the m_h^{\max} scenario, apart from the fact that the choice of radiative corrections is such that the maximum light CP-even Higgs boson mass is $\sim 126 \text{ GeV}$. This choice increases the region of the parameter space that is compatible with the observed Higgs boson being the lightest CP-even Higgs boson of the MSSM with respect to the m_h^{\max} scenario. There are many other MSSM parameter choices beyond these scenarios that are also compatible with the observed SM Higgs boson, for instance, refs. [25, 26].

The couplings of the MSSM Higgs bosons to down-type fermions are enhanced with respect to the SM for large $\tan\beta$ values resulting in increased branching fractions to τ leptons and b -quarks, as well as a higher cross section for Higgs boson production in association with b -quarks. This has motivated a variety of searches in $\tau\tau$ and bb final states at LEP [27], the Tevatron [28–30] and the LHC [31–33].

This paper presents the results of a search for a neutral MSSM Higgs boson in the $\tau\tau$ decay mode using $19.5\text{--}20.3 \text{ fb}^{-1}$ of proton–proton collision data collected with the ATLAS detector [34] in 2012 at a centre-of-mass energy of 8 TeV. Higgs boson production through

²The supersymmetry scale, M_{SUSY} , is defined here as the mass of the third generation squarks following refs. [21–23].

gluon fusion or in association with b -quarks is considered (see figure 1), with the latter mode dominating for high $\tan\beta$ values. The results of the search are interpreted in various MSSM scenarios.

The ATLAS search for the SM Higgs boson in the $\tau\tau$ channel [35] is similar to that described here. Important differences between the two searches are that they are optimized for different production mechanisms and Higgs boson mass ranges. Additionally, the three Higgs bosons of the MSSM, which can have different masses, are considered in this search. In particular the couplings to b -quarks and vector bosons are different between the SM and MSSM. The b -associated production mode is dominant for the H and A bosons and is enhanced for the h boson with respect to the SM for large parts of the MSSM parameter space. Furthermore, the coupling of the H boson to vector bosons is suppressed with respect to those for a SM Higgs boson with the same mass and the coupling of the A boson to vector bosons is zero at lowest order, due to the assumption of CP symmetry conservation. Hence, vector boson fusion production and production in association with a vector boson, which contribute significantly to the SM Higgs boson searches, are much less important with respect to the SM. Finally, for high m_A the search for the heavy H and A bosons is more sensitive in constraining the MSSM parameter space than the search for the h boson. As a consequence, this search has little sensitivity to the production of a SM Higgs boson with a mass around 125 GeV. For consistency, the SM Higgs signal is not considered part of the SM background, as the MSSM contains a SM-like Higgs boson for large parts of the parameter space.

2 The ATLAS detector

The ATLAS experiment [34] at the LHC is a multi-purpose particle detector with a forward-backward symmetric cylindrical geometry and a near 4π coverage in solid angle. It consists of an inner tracking detector surrounded by a thin superconducting solenoid providing a 2 T axial magnetic field, electromagnetic and hadronic calorimeters, and a muon spectrometer. The inner tracking detector covers the pseudorapidity range³ $|\eta| < 2.5$. It consists of silicon pixel, silicon micro-strip, and transition radiation tracking detectors. Lead/liquid-argon (LAr) sampling calorimeters provide electromagnetic (EM) energy measurements with high granularity. A hadronic (iron/scintillator-tile) calorimeter covers the central pseudorapidity range ($|\eta| < 1.7$). The end-cap and forward regions are instrumented with LAr calorimeters for both the EM and hadronic energy measurements up to $|\eta| = 4.9$. The muon spectrometer surrounds the calorimeters and is based on three large air-core toroid superconducting magnets with eight coils each. Its bending power is in the range 2.0–7.5 Tm. It includes a system of precision tracking chambers and fast detectors for triggering. A three-level trigger system is used to select events. The first-level trigger is

³ ATLAS uses a right-handed coordinate system with its origin at the nominal interaction point (IP) in the centre of the detector and the z -axis along the beam pipe. The x -axis points from the IP to the centre of the LHC ring, and the y -axis points upwards. Cylindrical coordinates (r, ϕ) are used in the transverse plane, ϕ being the azimuthal angle around the beam pipe. The pseudorapidity is defined in terms of the polar angle θ as $\eta = -\ln \tan(\theta/2)$. Angular distance is measured in units of $\Delta R \equiv \sqrt{(\Delta\eta)^2 + (\Delta\phi)^2}$.

implemented in hardware. It is designed to use a subset of the detector information to reduce the accepted rate to at most 75 kHz. This is followed by two software-based trigger levels that together reduce the accepted event rate to 400 Hz on average, depending on the data-taking conditions, during 2012.

3 Data and Monte Carlo simulation samples

The data used in this search were recorded by the ATLAS experiment during the 2012 LHC run with proton–proton collisions at a centre-of-mass energy of 8 TeV. They correspond to an integrated luminosity of 19.5–20.3 fb⁻¹, depending on the search channel.

Simulated samples of signal and background events were produced using various event generators. The presence of multiple interactions occurring in the same or neighbouring bunch crossings (pile-up) was accounted for, and the ATLAS detector was modelled using GEANT4 [36, 37].

The Higgs boson production mechanisms considered in this analysis are gluon fusion and b -associated production. The cross sections for these processes were calculated using HIGLU [38], GGH@NNLO [39] and SUSHI [39–54]. For b -associated production, four-flavour [55, 56] and five-flavour [44] cross-section calculations are combined [57]. The masses, couplings and branching fractions of the Higgs bosons are computed with FEYNHIGGS [50, 51, 53]. Gluon fusion production is simulated with POWHEG Box 1.0 [58], while b -associated production is simulated with SHERPA 1.4.1 [59]. For a mass of $m_A = 150$ GeV and $\tan \beta = 20$, the ratio of the gluon fusion to b associated production modes is approximately 0.5 for A and H production and three for h production. For a mass of $m_A = 300$ GeV and $\tan \beta = 30$, the ratio of production modes becomes approximately 0.1 for A and H production and 50 for h production. For both samples the CT10 [60] parton distribution function set is used. Signal samples are generated using the A boson production mode at discrete values of m_A , with the mass steps chosen by taking the $\tau\tau$ mass resolution into account. The signal model is then constructed by combining three mass samples, one for each of the h , H and A bosons, with appropriately scaled cross sections and branching fractions. The cross sections and branching fractions, as well as the masses of the h and H bosons, depend on m_A , $\tan \beta$ and the MSSM scenario under study. The differences in the kinematic properties of the decays of CP-odd and CP-even Higgs bosons are expected to be negligible for this search. Thus the efficiencies and acceptances from the A boson simulated samples are applicable to all neutral Higgs bosons.

Background samples of W and Z bosons produced in association with jets are produced using ALPGEN 2.14 [61], while the high-mass Z/γ^* tail is modelled separately using PYTHIA8 [62, 63] since in the high-mass range the current analysis is rather insensitive to the modelling of b -jet production. WW production is modelled with ALPGEN and WZ and ZZ production is modelled with HERWIG 6.520 [64]. The simulation of top pair production uses POWHEG and MC@NLO 4.01 [65], and single-top processes are generated with ACERMC 3.8 [66]. All simulated background samples use the CTEQ6L1 [67] parton distribution function set, apart from MC@NLO, which uses CT10.

For all the simulated event samples, the parton shower and hadronization are simulated with HERWIG, PYTHIA8 or SHERPA. PYTHIA8 is used for POWHEG-generated samples, SHERPA for the b -associated signal production and HERWIG for the remaining samples. Decays of τ leptons are generated with TAUOLA [68], SHERPA or PYTHIA8. PHOTOS [69] or SHERPA provide additional radiation from charged leptons.

$Z/\gamma^* \rightarrow \tau\tau$ events form an irreducible background that is particularly important when considering low-mass Higgs bosons ($m_A \lesssim 200$ GeV). It is modelled with $Z/\gamma^* \rightarrow \mu^+\mu^-$ events from data, where the muon tracks and the associated calorimeter cells are replaced by the corresponding simulated signature of a τ lepton decay. The two τ leptons are simulated by TAUOLA. The procedure takes into account the effect of τ polarization and spin correlations [70]. In the resulting sample, the τ lepton decays and the response of the detector are modelled by the simulation, while the underlying event kinematics and all other properties are obtained from data. This τ -embedded $Z/\gamma^* \rightarrow \mu^+\mu^-$ sample is validated as described in refs. [31, 35]. The $\mu\mu$ event selection requires two isolated muons in the rapidity range $|\eta| < 2.5$, where the leading muon has $p_T > 20$ GeV, the subleading muon $p_T > 15$ GeV and the invariant mass is in the range $m_{\mu\mu} > 40$ GeV. This results in an almost pure $Z/\gamma^* \rightarrow \mu^+\mu^-$ sample, which, however, has some contribution from $t\bar{t}$ and diboson production. The contamination from these backgrounds that pass the original $\mu\mu$ event selection and, after replacement of the muons by tau leptons, enter the final event selection are estimated using simulation. Further details can be found in section 6. $Z/\gamma^* \rightarrow \tau\tau$ events in the invariant mass range $m_{\tau\tau} < 40$ GeV are modelled using ALPGEN simulated events.

4 Object reconstruction

Electron candidates are formed from energy deposits in the electromagnetic calorimeter associated with a charged-particle track measured in the inner detector. Electrons are selected if they have a transverse energy $E_T > 15$ GeV, lie within $|\eta| < 2.47$, but outside the transition region between the barrel and end-cap calorimeters ($1.37 < |\eta| < 1.52$), and meet the “medium” identification requirements defined in ref. [71]. Additional isolation criteria, based on tracking and calorimeter information, are used to suppress backgrounds from misidentified jets or semileptonic decays of heavy quarks. In particular, the sum of the calorimeter deposits in a cone of size $\Delta R = 0.2$ around the electron direction is required to be less than 6 (8)% of the electron E_T for the $\tau_{\text{lep}}\tau_{\text{had}}$ ($\tau_{\text{lep}}\tau_{\text{lep}}$) final state. Similarly, the scalar sum of the transverse momentum of tracks with $p_T > 1$ GeV in a cone of size $\Delta R = 0.4$ with respect to the electron direction is required to be less than 6% of the electron E_T .

Muon candidates are reconstructed by associating an inner detector track with a muon spectrometer track [72]. For this analysis, the reconstructed muons are required to have a transverse momentum $p_T > 10$ GeV and to lie within $|\eta| < 2.5$. Additional track-quality and track-isolation criteria are required to further suppress backgrounds from cosmic rays, hadrons punching through the calorimeter, or muons from semileptonic decays of heavy quarks. The muon calorimetric and track isolation criteria use the same cone sizes and

generally the same threshold values with respect to the muon p_T as in the case of electrons - only for the case of the $\tau_{\text{lep}}\tau_{\text{lep}}$ final state is the muon calorimetric isolation requirement changed to be less than 4% of the muon momentum.

Jets are reconstructed using the anti- k_t algorithm [73] with a radius parameter $R = 0.4$, taking topological clusters [74] in the calorimeter as input. The jet energy is calibrated using a combination of test-beam results, simulation and *in situ* measurements [75]. Jets must satisfy $E_T > 20$ GeV and $|\eta| < 4.5$. To reduce the effect of pile-up, it is required that, for jets within $|\eta| < 2.4$ and $E_T < 50$ GeV, at least half of the transverse momentum, as measured by the associated charged particles, be from particles matched to the primary vertex.⁴

A multivariate discriminant is used to tag jets, reconstructed within $|\eta| < 2.5$, originating from a b -quark [76]. The b -jet identification has an average efficiency of 70% in simulated $t\bar{t}$ events, whereas the corresponding light-quark jet misidentification probability is approximately 0.7%, but varies as a function of the jet p_T and η [77].

Hadronic decays of τ leptons (τ_{had}) [78] are reconstructed starting from topological clusters in the calorimeter. A τ_{had} candidate must lie within $|\eta| < 2.5$, have a transverse momentum greater than 20 GeV, one or three associated tracks and a charge of ± 1 . Information on the collimation, isolation, and shower profile is combined into a multivariate discriminant against backgrounds from jets. Dedicated algorithms that reduce the number of electrons and muons misreconstructed as hadronic τ decays are applied. In this analysis, two τ_{had} identification selections are used —“loose” and “medium”— with efficiencies of about 65% and 55%, respectively.

When different objects selected according to the criteria mentioned above overlap with each other geometrically (within $\Delta R = 0.2$) only one of them is considered. The overlap is resolved by selecting muon, electron, τ_{had} and jet candidates in this order of priority.

The missing transverse momentum is defined as the negative vectorial sum of the muon momenta and energy deposits in the calorimeters [79]. The magnitude of the missing transverse momentum is denoted by E_T^{miss} . Clusters of calorimeter-cell energy deposits belonging to jets, τ_{had} candidates, electrons, and photons, as well as cells that are not associated with any object, are treated separately in the missing transverse momentum calculation. The energy deposits in calorimeter cells that are not matched to any object are weighted by the fraction of unmatched tracks associated with the primary vertex, in order to reduce the effect of pile-up on the E_T^{miss} resolution. The contributions of muons to missing transverse momentum are calculated differently for isolated and non-isolated muons, to account for the energy deposited by muons in the calorimeters.

5 Search channels

The following $\tau\tau$ decay modes are considered in this search: $\tau_e\tau_\mu$ (6%), $\tau_e\tau_{\text{had}}$ (23%), $\tau_\mu\tau_{\text{had}}$ (23%) and $\tau_{\text{had}}\tau_{\text{had}}$ (42%), where τ_e and τ_μ represent the two leptonic τ decay modes and the percentages in the parentheses denote the corresponding $\tau\tau$ branching fractions.

⁴The primary vertex is taken to be the reconstructed vertex with the highest Σp_T^2 of the associated tracks.

The selections defined for each of the channels and described in sections 5.1–5.3 are such that there are no events common to any two of these channels.

Events are collected using several single- and combined-object triggers. The single-electron and single-muon triggers require an isolated lepton with a p_T threshold of 24 GeV. The single- τ_{had} trigger implements a p_T threshold of 125 GeV. The following combined-object triggers are used: an electron–muon trigger with lepton p_T thresholds of 12 GeV and 8 GeV for electrons and muons, respectively, and a $\tau_{\text{had}}\tau_{\text{had}}$ trigger with p_T thresholds of 38 GeV for each hadronically decaying τ lepton.

With two τ leptons in the final state, it is not possible to infer the neutrino momenta from the reconstructed missing transverse momentum vector and, hence, the $\tau\tau$ invariant mass. Two approaches are used. The first method used is the Missing Mass Calculator (MMC) [80]. This algorithm assumes that the missing transverse momentum is due entirely to the neutrinos, and performs a scan over the angles between the neutrinos and the visible τ lepton decay products. The MMC mass, $m_{\tau\tau}^{\text{MMC}}$, is defined as the most likely value chosen by weighting each solution according to probability density functions that are derived from simulated τ lepton decays. As an example, the MMC resolution,⁵ assuming a Higgs boson with mass $m_A = 150$ GeV, is about 30% for $\tau_e\tau_\mu$ events. The resolution is about 20% for $\tau_{\text{lep}}\tau_{\text{had}}$ events ($\tau_{\text{lep}} = \tau_e$ or τ_μ) for Higgs bosons with a mass in the range 150 – 350 GeV. The second method uses the $\tau\tau$ total transverse mass, defined as:

$$m_{\text{T}}^{\text{total}} = \sqrt{m_{\text{T}}^2(\tau_1, \tau_2) + m_{\text{T}}^2(\tau_1, E_{\text{T}}^{\text{miss}}) + m_{\text{T}}^2(\tau_2, E_{\text{T}}^{\text{miss}})} ,$$

where the transverse mass, m_{T} , between two objects with transverse momenta $p_{\text{T}1}$ and $p_{\text{T}2}$ and relative angle $\Delta\phi$ is given by

$$m_{\text{T}} = \sqrt{2p_{\text{T}1}p_{\text{T}2}(1 - \cos \Delta\phi)} .$$

As an example, the $m_{\text{T}}^{\text{total}}$ mass resolution assuming a Higgs boson with mass $m_A = 350$ GeV for $\tau_{\text{had}}\tau_{\text{had}}$ events is approximately 30%. While the MMC exhibits a better $\tau\tau$ mass resolution for signal events, multi-jet background events tend to be reconstructed at lower masses with $m_{\text{T}}^{\text{total}}$, leading to better overall discrimination between signal and background for topologies dominated by multi-jet background.

5.1 The $h/H/A \rightarrow \tau_e\tau_\mu$ channel

Events in the $h/H/A \rightarrow \tau_e\tau_\mu$ channel are selected using either single-electron or electron–muon triggers. The data sample corresponds to an integrated luminosity of 20.3 fb⁻¹. Exactly one isolated electron and one isolated muon of opposite charge are required, with lepton p_T thresholds of 15 GeV for electrons and 10 GeV for muons. Electrons with p_T in the range 15–25 GeV are from events selected by the electron–muon trigger, whereas electrons with $p_T > 25$ GeV are from events selected by the single-electron trigger. Events containing hadronically decaying τ leptons, satisfying the “loose” τ_{had} identification criterion, are vetoed.

⁵The resolution of the mass reconstruction is estimated by dividing the root mean square of the mass distribution by its mean.

To increase the sensitivity of this channel, the events are split into two categories based on the presence (“tag category”) or absence (“veto category”) of a b -tagged jet. The tag category requires exactly one jet satisfying the b -jet identification criterion. In addition, a number of kinematic requirements are imposed to reduce the background from top quark decays. The azimuthal angle between the electron and the muon, $\Delta\phi(e, \mu)$, must be greater than 2.0 (see figure 2(a)). The sum of the cosines of the azimuthal angles between the leptons and the missing transverse momentum, $\Sigma \cos \Delta\phi \equiv \cos(\phi(e) - \phi(E_T^{\text{miss}})) + \cos(\phi(\mu) - \phi(E_T^{\text{miss}}))$, must be greater than -0.2 . The scalar sum of the p_T of jets with $p_T > 30$ GeV must be less than 100 GeV. Finally, the scalar sum of the p_T of the leptons and the E_T^{miss} must be below 125 GeV. The veto category is defined by requiring that no jet satisfies the b -jet identification criterion. Because the top quark background is smaller in this category, the imposed kinematic selection requirements, $\Delta\phi(e, \mu) > 1.6$ and $\Sigma \cos \Delta\phi > -0.4$ (see figure 2(b)), are looser than in the tag category.

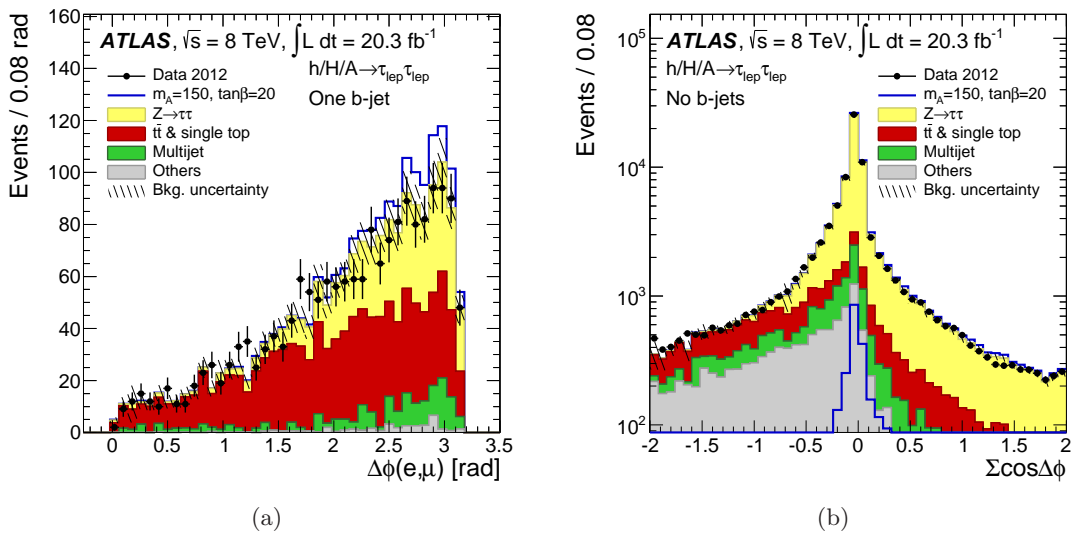


Figure 2. Kinematic distributions for the $h/H/A \rightarrow \tau_e \tau_\mu$ channel: (a) the $\Delta\phi(e, \mu)$ distribution after the tag category selection criteria apart from the $\Delta\phi(e, \mu)$ requirement and (b) the $\Sigma \cos \Delta\phi$ distribution after the b -jet veto requirement. The data are compared to the background expectation and a hypothetical MSSM signal ($m_A = 150$ GeV and $\tan\beta = 20$). In (b) the assumed signal is shown twice: as a distribution in the bottom of the plot and on top of the total background prediction. The background uncertainty includes statistical and systematic uncertainties.

The most important background processes in this channel are $Z/\gamma^* + \text{jets}$, $t\bar{t}$, and multi-jet production. The $Z/\gamma^* \rightarrow \tau\tau$ background is estimated using the τ -embedded $Z/\gamma^* \rightarrow \mu^+ \mu^-$ sample outlined in section 3. It is normalized using the NNLO $Z/\gamma^* + \text{jets}$ cross section calculated with FEWZ [81] and a simulation estimate of the efficiency of the trigger, lepton η and p_T , and identification requirements. The $t\bar{t}$ background is estimated from simulation with the normalization taken from a data control region enriched in $t\bar{t}$ events, defined by requiring two b -tagged jets. The $W + \text{jet}$ background, where one of the leptons results from a misidentified jet, is estimated using simulation. Smaller backgrounds

	Tag category	Veto category
Signal ($m_A = 150$ GeV, $\tan \beta = 20$)		
$h \rightarrow \tau\tau$	8.7 ± 1.9	244 ± 11
$H \rightarrow \tau\tau$	65 ± 14	882 ± 45
$A \rightarrow \tau\tau$	71 ± 15	902 ± 48
$Z/\gamma^* \rightarrow \tau\tau + \text{jets}$	418 ± 28	54700 ± 3800
Multi-Jet	100 ± 21	4180 ± 670
$t\bar{t}$ and single top	421 ± 46	2670 ± 360
Others	25.8 ± 7.4	4010 ± 280
Total background	965 ± 59	65500 ± 3900
Data	904	65917

Table 1. Number of events observed in the $h/H/A \rightarrow \tau_e\tau_\mu$ channel and the predicted background and signal. The predicted signal event yields correspond to the parameter choice $m_A = 150$ GeV and $\tan \beta = 20$. The row labelled ‘‘Others’’ includes events from diboson production, $Z/\gamma^* \rightarrow ee/\mu\mu$ and $W+\text{jets}$ production. Combined statistical and systematic uncertainties are quoted. The signal prediction does not include the uncertainty due to the cross-section calculation.

from single-top and diboson production are also estimated from simulation.

The multi-jet background is estimated from data using a two-dimensional sideband method. The event sample is split into four regions according to the charge product of the $e\mu$ pair and the isolation requirements on the electron and muon. Region A (B) contains events where both leptons pass the isolation requirements and are of opposite (same) charge, while region C (D) contains events where both leptons fail the isolation requirements and are also of opposite (same) charge. This way, A is the signal region, while B , C , and D are control regions. Event contributions to the B , C and D control regions from processes other than multi-jet production are estimated using simulation and subtracted. The final prediction for the multi-jet contribution to the signal region, A , is given by the background-subtracted data in region B , scaled by the opposite-sign to same-sign ratio measured in regions C and D , $r_{C/D} \equiv n_C/n_D$. Systematic uncertainties on the prediction are estimated from the stability of $r_{C/D}$ under variations of the lepton isolation requirement.

Table 1 shows the number of observed $\tau_e\tau_\mu$ events, the predicted background, and the signal prediction for the MSSM m_h^{\max} scenario [21, 22] parameter choice $m_A = 150$ GeV and $\tan \beta = 20$. The total combined statistical and systematic uncertainties on the predictions are also quoted on table 1. The observed event yields are compatible with the expected yields from SM processes. The MMC mass is used as the discriminating variable in this channel, and is shown in figure 3 for the tag and veto categories separately.

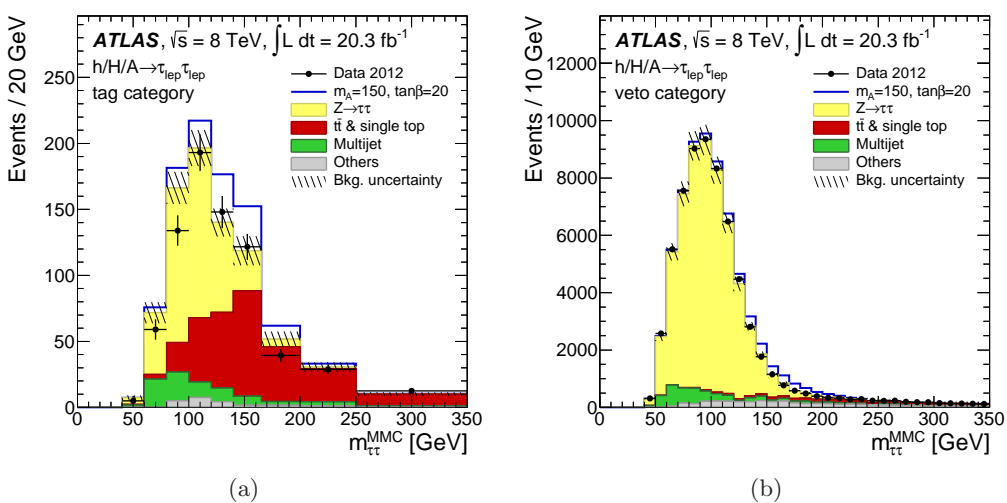


Figure 3. MMC mass distributions for the $h/H/A \rightarrow \tau_e\tau_\mu$ channel. The MMC mass is shown for (a) the tag and (b) the veto categories. The data are compared to the background expectation and a hypothetical MSSM signal ($m_A = 150$ GeV and $\tan\beta = 20$). The contributions of the diboson, $Z/\gamma^* \rightarrow ee/\mu\mu$, and $W + \text{jets}$ background processes are combined and labelled “Others”. The background uncertainty includes statistical and systematic uncertainties.

5.2 The $h/H/A \rightarrow \tau_{\text{lep}}\tau_{\text{had}}$ channel

Events in the $h/H/A \rightarrow \tau_{\text{lep}}\tau_{\text{had}}$ channel are selected using single-electron or single-muon triggers. The data sample corresponds to an integrated luminosity of 20.3 fb^{-1} . Events are required to contain an electron or a muon with $p_T > 26 \text{ GeV}$ and an oppositely charged τ_{had} with $p_T > 20 \text{ GeV}$ satisfying the “medium” τ_{had} identification criterion. Events must not contain additional electrons or muons. The event selection is optimized separately for low- and high-mass Higgs bosons in order to exploit differences in kinematics and background composition.

The low-mass selection targets the parameter space with $m_A < 200 \text{ GeV}$. It includes two orthogonal categories: the tag category and the veto category. In the tag category there must be at least one jet tagged as a b -jet. Events that contain one or more jets with $p_T > 30 \text{ GeV}$, without taking into account the leading b -jet, are rejected. In addition, the transverse mass of the lepton and the transverse missing momentum is required to not exceed 45 GeV . These requirements serve to reduce the otherwise dominant $t\bar{t}$ background. In the veto category there must be no jet tagged as a b -jet. Two additional selection requirements are applied to reduce the $W + \text{jets}$ background. First, the transverse mass of the lepton and the missing transverse momentum must be below 60 GeV . Secondly, the sum of the azimuthal angles $\Sigma\Delta\phi \equiv \Delta\phi(\tau_{\text{had}}, E_T^{\text{miss}}) + \Delta\phi(\tau_{\text{lep}}, E_T^{\text{miss}})$, must have a value less than 3.3 (see figure 4(a)). Finally, in the $\tau_\mu\tau_{\text{had}}$ channel of the veto category, dedicated requirements based on kinematic and shower shape properties of the τ_{had} candidate are applied to reduce the number of muons faking hadronic τ lepton decays.

The high-mass selection targets $m_A \geq 200 \text{ GeV}$. It requires $\Sigma\Delta\phi < 3.3$, in order to reduce the $W + \text{jets}$ background. The hadronic and leptonic τ lepton decays are required to be back-to-back: $\Delta\phi(\tau_{\text{lep}}, \tau_{\text{had}}) > 2.4$. In addition, the transverse momentum difference between the τ_{had} and the lepton, $\Delta p_T \equiv p_T(\tau_{\text{had}}) - p_T(\text{lepton})$, must be above 45 GeV (see figure 4(b)). This requirement takes advantage of the fact that a τ_{had} tends to have a higher visible transverse momentum than a τ_{lep} due to the presence of more neutrinos in the latter decay.

In the low-mass categories, the electron and muon channels are treated separately and combined statistically. For the high-mass category, they are treated as a single channel to improve the statistical robustness.

The most important SM background processes in this channel are $Z/\gamma^* + \text{jets}$, $W + \text{jets}$, multi-jet production, top (including both $t\bar{t}$ and single top) and diboson production. The τ -embedded $Z/\gamma^* \rightarrow \mu^+\mu^-$ sample is used to estimate the $Z/\gamma^* \rightarrow \tau\tau$ background. It is normalized in the same way as in the $\tau_{\text{lep}}\tau_{\text{lep}}$ channel. The rate at which electrons are misidentified as τ_{had} , important mostly for $Z \rightarrow ee$ decays, was estimated from data in ref. [78]. The contribution of diboson processes is small and estimated from simulation. Events originating from $W + \text{jets}$, $Z(\rightarrow \ell\ell) + \text{jets}$ ($\ell = e, \mu$), $t\bar{t}$ and single-top production, in which a jet is misreconstructed as τ_{had} , are estimated from simulated samples with normalization estimated by comparing event yields in background-dominated control regions in data. Separate regions are defined for each of the background sources in each of the low-mass tag, low-mass veto, and high-mass categories. Systematic uncertainties are derived

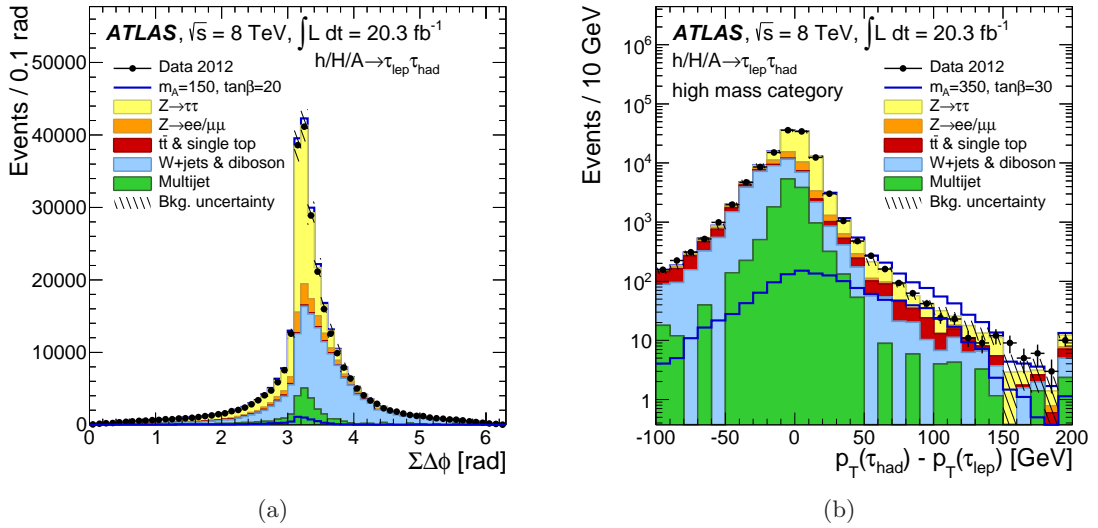


Figure 4. Kinematic distributions for the $h/H/A \rightarrow \tau_{\text{lep}}\tau_{\text{had}}$ channel: (a) the $\Sigma\Delta\phi$ distribution after the kinematic requirements on the τ_{lep} and τ_{had} and (b) the distribution of $\Delta p_T \equiv p_T(\tau_{\text{had}}) - p_T(\text{lepton})$ for the high-mass category for the combined $\tau_e\tau_{\text{had}}$ and $\tau_\mu\tau_{\text{had}}$ final states. In (b) all the $\tau_{\text{lep}}\tau_{\text{had}}$ high-mass selection criteria are applied apart from the $\Delta p_T > 45$ GeV requirement. The data are compared to the background expectation and a hypothetical MSSM signal: $m_A = 150$ GeV, $\tan\beta = 20$ for (a) and $m_A = 350$ GeV, $\tan\beta = 30$ for (b). The assumed signal is shown twice: as a distribution in the bottom of the plot and on top of the total background prediction. The background uncertainty includes statistical and systematic uncertainties.

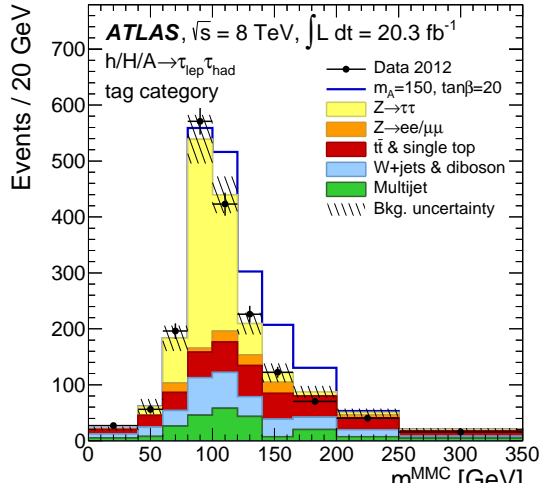
using alternative definitions for the control regions. The multi-jet background is estimated with a two-dimensional sideband method, similar to the one employed for the $\tau_e\tau_\mu$ channel, using the product of the lepton (e or μ) and τ_{had} charges and lepton isolation. The systematic uncertainty on the predicted event yield is estimated by varying the definitions of the regions used, and by testing the stability of the $r_{C/D}$ ratio across the $m_{\tau\tau}^{\text{MMC}}$ range.

Table 2 shows the number of observed $\tau_{\text{lep}}\tau_{\text{had}}$ events, the predicted background, and the signal prediction for the MSSM m_h^{max} scenario. The signal MSSM parameters are $m_A = 150$ GeV, $\tan\beta = 20$ for the low-mass categories and $m_A = 350$ GeV, $\tan\beta = 30$ for the high mass category. The total combined statistical and systematic uncertainties on the predictions are also quoted in table 2. The observed event yields are compatible with the expected yields from SM processes within the uncertainties. The MMC mass is used as the final mass discriminant in this channel and is shown in figures 5 and 6 for the low- and high-mass categories, respectively.

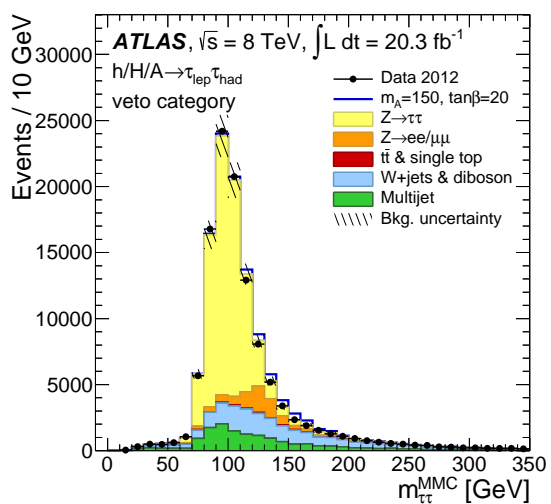
Low-mass categories				
	Tag category		Veto category	
	e channel	μ channel	e channel	μ channel
Signal ($m_A = 150$ GeV, $\tan \beta = 20$)				
$h \rightarrow \tau\tau$	10.5 ± 2.8	10.5 ± 2.6	194 ± 13	192 ± 14
$H \rightarrow \tau\tau$	86 ± 26	86 ± 24	836 ± 60	822 ± 61
$A \rightarrow \tau\tau$	94 ± 29	94 ± 27	840 ± 64	825 ± 62
$Z \rightarrow \tau\tau + \text{jets}$	403 ± 39	425 ± 42	31700 ± 2800	38400 ± 3300
$Z \rightarrow \ell\ell + \text{jets}$ ($\ell = e, \mu$)	72 ± 24	33 ± 14	5960 ± 920	2860 ± 510
$W + \text{jets}$	158 ± 44	185 ± 58	9100 ± 1300	9800 ± 1400
Multi-jet	185 ± 35	66 ± 31	11700 ± 490	3140 ± 430
$t\bar{t}$ and single top	232 ± 36	236 ± 34	533 ± 91	535 ± 98
Diboson	9.1 ± 2.3	10.0 ± 2.5	466 ± 40	468 ± 42
Total background	1059 ± 81	955 ± 86	59500 ± 3300	55200 ± 3600
Data	1067	947	60351	54776

High-mass category	
Signal ($m_A = 350$ GeV, $\tan \beta = 30$)	
$h \rightarrow \tau\tau$	5.60 ± 0.68
$H \rightarrow \tau\tau$	157 ± 13
$A \rightarrow \tau\tau$	152 ± 13
$Z \rightarrow \tau\tau + \text{jets}$	380 ± 50
$Z \rightarrow \ell\ell + \text{jets}$ ($\ell = e, \mu$)	34.9 ± 7.3
$W + \text{jets}$	213 ± 40
Multi-jet	57 ± 20
$t\bar{t}$ and single top	184 ± 26
Diboson	30.1 ± 4.8
Total background	900 ± 72
Data	920

Table 2. Numbers of events observed in the $h/H/A \rightarrow \tau_{\text{lep}}\tau_{\text{had}}$ channel and the predicted background and signal. The predicted signal event yields correspond to the parameter choice $m_A = 150$ GeV, $\tan \beta = 20$ for the low-mass categories and $m_A = 350$ GeV, $\tan \beta = 30$ for the high-mass category. Combined statistical and systematic uncertainties are quoted. The signal prediction does not include the uncertainty due to the cross-section calculation.



(a)



(b)

Figure 5. The MMC mass distributions for the low-mass categories of the $h/H/A \rightarrow \tau_{\text{lep}}\tau_{\text{had}}$ channel. Tag (a) and veto (b) categories are shown for the combined $\tau_e\tau_{\text{had}}$ and $\tau_\mu\tau_{\text{had}}$ final states. The data are compared to the background expectation and a hypothetical MSSM signal ($m_A = 150$ GeV and $\tan\beta = 20$). The background uncertainty includes statistical and systematic uncertainties.

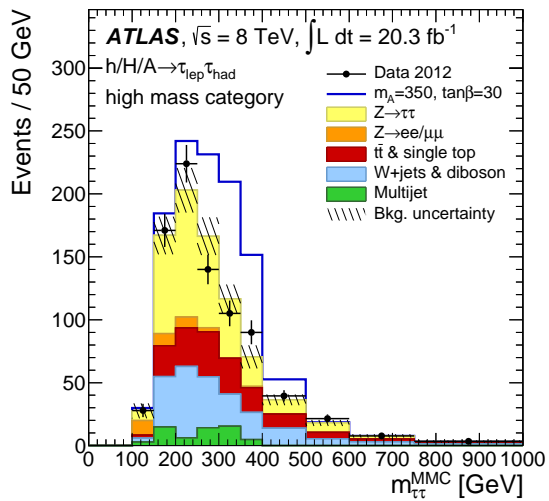


Figure 6. The MMC mass distribution for the high-mass category of the $h/H/A \rightarrow \tau_{\text{lep}}\tau_{\text{had}}$ channel is shown for the combined $\tau_e\tau_{\text{had}}$ and $\tau_\mu\tau_{\text{had}}$ final states. The data are compared to the background expectation and a hypothetical MSSM signal ($m_A = 350$ GeV and $\tan\beta = 30$). The background uncertainty includes statistical and systematic uncertainties.

5.3 The $h/H/A \rightarrow \tau_{\text{had}}\tau_{\text{had}}$ channel

Events in the $h/H/A \rightarrow \tau_{\text{had}}\tau_{\text{had}}$ channel are selected using either a single- τ_{had} trigger or a $\tau_{\text{had}}\tau_{\text{had}}$ trigger. The data sample corresponds to an integrated luminosity of 19.5 fb^{-1} . Events are required to contain at least two τ_{had} , identified using the “loose” identification criterion. If more than two τ_{had} are present, the two with the highest p_T values are considered. Events containing an electron or muon are rejected to ensure orthogonality with the other channels. The two τ_{had} are required to have $p_T > 50 \text{ GeV}$, have opposite electric charges, and to be back-to-back in the azimuthal plane ($\Delta\phi > 2.7$). Two event categories are defined as follows. The single- τ_{had} trigger category (STT category) includes the events selected by the single- τ_{had} trigger which contain at least one τ_{had} with $p_T > 150 \text{ GeV}$ (see figure 7(a)). The $\tau_{\text{had}}\tau_{\text{had}}$ trigger category (DTT category) includes the events selected by the $\tau_{\text{had}}\tau_{\text{had}}$ trigger, with the leading τ_{had} required to have p_T less than 150 GeV , to ensure orthogonality with the STT category, and with both τ leptons satisfying the “medium” identification criterion. In addition, events in the DTT category are required to have $E_T^{\text{miss}} > 10 \text{ GeV}$, and the scalar sum of transverse energy of all deposits in the calorimeter to be greater than 160 GeV (see figure 7(b)).

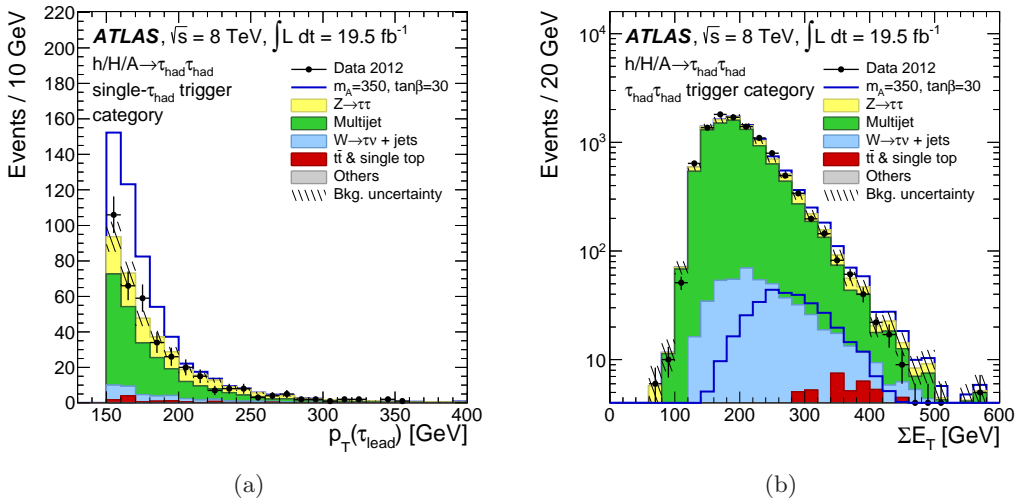


Figure 7. Kinematic distributions for the $h/H/A \rightarrow \tau_{\text{had}}\tau_{\text{had}}$ channel: (a) the transverse momentum of the highest- p_T τ_{had} for the STT category and (b) the scalar sum of transverse energy of all deposits, ΣE_T , in the DTT category, before the application of this requirement. The data are compared to the background expectation and a hypothetical MSSM signal ($m_A = 350 \text{ GeV}$ and $\tan\beta = 30$). The background labelled “Others” includes events from diboson production, $Z \rightarrow \ell\ell$ and $W \rightarrow \ell\nu$ with $\ell = e, \mu$. In (b) the assumed signal is shown twice: as a distribution in the bottom of the plot and on top of the total background prediction. The background uncertainty includes statistical and systematic uncertainties.

The dominant background in this channel is multi-jet production and for this reason m_T^{total} is used as the final discriminant. Other background samples include $Z/\gamma^* + \text{jets}$, $W + \text{jets}$, $t\bar{t}$ and diboson.

The multi-jet background is estimated separately for the STT and DTT categories. In the STT category, a control region is obtained by requiring the next-to-highest- p_T τ_{had} to fail the “loose” τ_{had} identification requirement, thus obtaining a high-purity sample of multi-jet events. The probability of a jet to be misidentified as a τ_{had} is measured in a high purity sample of dijet events in data, as a function of the number of associated tracks with the jet and the jet p_T . These efficiencies are used to obtain the shape and the normalization of the multi-jet background from the control region with the next-to-highest- p_T τ_{had} that fails the τ_{had} identification requirement. The systematic uncertainty on the method is obtained by repeating the multijet estimation, but requiring either a same-sign or opposite-sign between the two jets. The difference between the calculated efficiencies for the two measurements is then taken as the systematic uncertainty. This procedure has some sensitivity to differences related to whether the jets in the dijet sample are quark- or gluon-initiated. The resulting uncertainty is on average 11%. A two-dimensional sideband method is used in the DTT category by defining four regions based on the charge product of the two τ_{had} and the $E_T^{\text{miss}} > 10 \text{ GeV}$ requirement. A systematic uncertainty is derived by measuring the variation of the ratio of opposite-sign to same-sign $\tau_{\text{had}}\tau_{\text{had}}$ pairs for different sideband region definitions, as well as across the m_T^{total} range, and amounts to 5%.

The remaining backgrounds are modelled using simulation. Non-multi-jet processes with jets misidentified as τ_{had} are dominated by $W(\rightarrow \tau\nu) + \text{jets}$. In such events the τ_{had} identification requirements are only applied to the τ_{had} from the W decay and not the jet that may be misidentified as the second τ_{had} . Instead the event is weighted using misidentification probabilities, measured in a control region in data, to estimate the background yield. $Z/\gamma^* + \text{jets}$ background is also estimated using simulation. Due to the small number of remaining events after the p_T thresholds of the τ_{had} trigger requirements, the τ -embedded $Z \rightarrow \mu\mu$ sample is not used.

Table 3 shows the number of observed $\tau_{\text{had}}\tau_{\text{had}}$ events, the predicted background, and the signal prediction for the MSSM m_h^{max} scenario parameter choice $m_A = 350 \text{ GeV}$, $\tan \beta = 30$. The total combined statistical and systematic uncertainties on the predictions are also quoted in table 3. The observed event yields are compatible with the expected yields from SM processes within the uncertainties. The distributions of the total transverse mass are shown in figure 8 for the STT and the DTT categories separately.

	Single- τ_{had} trigger (STT) category	$\tau_{\text{had}}\tau_{\text{had}}$ trigger (DTT) category
Signal ($m_A = 350$ GeV, $\tan \beta = 30$)		
$h \rightarrow \tau\tau$	0.042 ± 0.039	11.2 ± 4.5
$H \rightarrow \tau\tau$	95 ± 18	182 ± 27
$A \rightarrow \tau\tau$	82 ± 16	158 ± 24
Multi-jet	216 ± 25	6770 ± 430
$Z/\gamma^* \rightarrow \tau\tau$	113 ± 18	750 ± 210
$W(\rightarrow \tau\nu) + \text{jets}$	34 ± 8.1	410 ± 100
$t\bar{t}$ and single top	10.2 ± 4.4	76 ± 26
Others	0.50 ± 0.20	3.40 ± 0.80
Total background	374 ± 32	8010 ± 490
Data	373	8225

Table 3. Number of events observed in the $h/H/A \rightarrow \tau_{\text{had}}\tau_{\text{had}}$ channel and the predicted background and signal. The predicted signal event yields correspond to the parameter choice $m_A = 350$ GeV, $\tan \beta = 30$. The row labelled “Others” includes events from diboson production, $Z \rightarrow \ell\ell$ and $W \rightarrow \ell\nu$ with $\ell = e, \mu$. Combined statistical and systematic uncertainties are quoted. The signal prediction does not include the uncertainty due to the cross-section calculation.

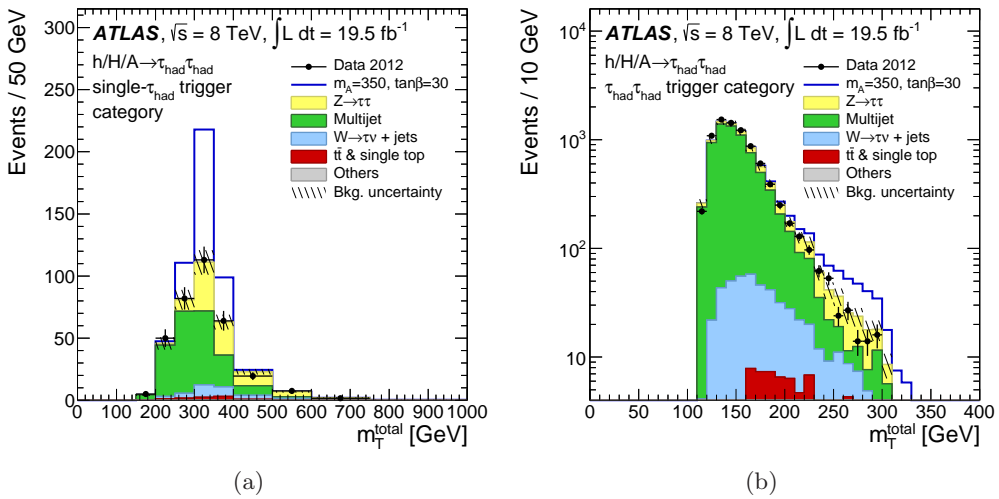


Figure 8. Total transverse mass distributions for (a) STT and (b) DTT categories of the $h/H/A \rightarrow \tau_{\text{had}}\tau_{\text{had}}$ channel. The data are compared to the background expectation and a hypothetical MSSM signal ($m_A = 350$ GeV and $\tan \beta = 30$). The background labelled “Others” includes events from diboson production, $Z \rightarrow \ell\ell$ and $W \rightarrow \ell\nu$ with $\ell = e, \mu$. The background uncertainty includes statistical and systematic uncertainties.

6 Systematic uncertainties

The event yields for several of the backgrounds in this search are estimated using control samples in data as described in section 5 and their associated uncertainties are discussed there. In this section, the remaining uncertainties are discussed and the overall effect of the systematic uncertainties is presented. Many of the systematic uncertainties affect both the signal and background estimates based on MC. These correlations are used in the limit calculation described in section 7.

Signal cross-section uncertainties are taken from the study in ref. [82]. Typical uncertainty values are in the range 10–15% for gluon fusion and 15–20% for b -associated production.

The uncertainty on the signal acceptance from the parameters used in the event generation of signal and background samples is also considered. This is done by evaluating the change in acceptance after varying the factorisation and renormalisation scale parameters, parton distribution function choices, and if applicable, conditions for the matching of the partons used in the fixed-order calculation and the parton shower. The uncertainty on the signal acceptance is largest in the tag category for b -associated production, where it is about 13%.

Uncertainties for single-boson and diboson production cross sections are estimated for missing higher-order corrections, parton distribution functions and the value of the strong coupling constant, and are considered wherever applicable. Acceptance uncertainties for these background processes are estimated in the same way as for signal. The most important theoretical uncertainties on the background are the Z +jets cross section and acceptance, which affect the normalization by about 7%.

The uncertainty on the integrated luminosity is 2.8%. It is derived, following the same methodology as that detailed in ref. [83], from a preliminary calibration of the luminosity scale derived from beam-separation scans performed in November 2012.

The single- τ_{had} and $\tau_{\text{had}}\tau_{\text{had}}$ trigger efficiencies are studied in $Z \rightarrow \tau\tau$ events. Their uncertainties are in the range 3–25% depending on the number of the tracks matched to the τ_{had} , the τ_{had} pseudorapidity and p_{T} , as well as the data-taking period. They are estimated with a method similar to the one in ref. [84] and updated for the 2012 data-taking conditions.

The τ_{had} identification efficiency is measured using $Z \rightarrow \tau\tau$ events. The uncertainty is in the range 3–10%, depending on the τ_{had} pseudorapidity and the number of tracks matched to the τ lepton [78]. Extrapolated uncertainties are used for τ_{had} candidates with transverse momenta above those accessible in $Z \rightarrow \tau\tau$ events.

The τ_{had} energy scale uncertainty is estimated by propagating the single-particle response to the individual τ_{had} decay products (neutral and charged pions). This uncertainty is in the range 2–4% [85] depending on p_{T} , pseudorapidity and the number of associated tracks.

The jet energy scale (JES) and resolution uncertainties are described in refs. [75, 86]. The JES is established by exploiting the p_{T} balance between a jet and a reference object

such as a Z boson or a photon. The uncertainty range is between 3% and 7%, depending on the p_T and pseudorapidity.

The b -jet identification efficiency uncertainty range is from 2% to 8%, depending on the jet p_T . The estimation of this uncertainty is based on a study that uses $t\bar{t}$ events in data [76].

The E_T^{miss} uncertainties are derived by propagating all energy scale uncertainties of reconstructed objects. Additionally, the uncertainty on the scale for energy deposits outside reconstructed objects and the resolution uncertainties are considered [87].

Electron and muon reconstruction, identification, isolation and trigger efficiency uncertainties are estimated from data in refs. [72, 88]. Uncertainties related to the electron energy scale and resolution and to the muon momentum scale and resolution are also estimated from data [72, 89] and taken into account.

Systematic uncertainties associated with the τ -embedded $Z/\gamma^* \rightarrow \mu^+\mu^- + \text{jets}$ data event sample are examined in refs. [31, 35]. Two are found to be the most significant: the uncertainty due to the muon selection, which is estimated by varying the muon isolation requirement used in selecting the $Z/\gamma^* \rightarrow \mu^+\mu^- + \text{jets}$ events, and the uncertainty from the subtraction of the calorimeter cell energy associated with the muon. The embedded sample contains a small contamination of $t\bar{t}$ events at high MMC values. This is found to have a non-negligible influence in the $\tau_{\text{lep}}\tau_{\text{had}}$ tag and high-mass categories only. The effect on the search result is found to be very small in the tag category since other background contributions are dominant in the relevant MMC region. Its effect is taken into account by adding an additional uncertainty of 50% to the $Z \rightarrow \tau\tau$ background for MMC values exceeding 135 GeV. For the high-mass category, the estimated background level is subtracted from the data and an uncertainty contribution of the same size is applied.

The relative effect of each of the systematic uncertainties can be seen by their influence on the signal strength parameter, μ , defined as the ratio of the fitted to the assumed signal cross section times branching fraction (see also section 7). The effects of the most important sources of systematic uncertainty are shown for two signal assumptions: table 4 shows a low-mass pseudoscalar boson hypothesis ($m_A = 150$ GeV, $\tan\beta = 5.7$) and table 5 a high-mass pseudoscalar boson hypothesis ($m_A = 350$ GeV, $\tan\beta = 14$). The $\tan\beta$ values chosen correspond to the observed limits for the respective m_A assumptions (see section 7). The size of the systematic uncertainty on μ varies strongly with $\tan\beta$. In these tables, “Multi-jet background” entries refer to uncertainties inherent to the methods used in estimation of the multi-jet background in the various channels of this search. The largest contribution comes from the stability of the ratio of opposite-sign to same-sign events used in the two-dimensional sideband extrapolation method for the multi-jet background estimation.

Source of uncertainty	Uncertainty on μ (%)
Lepton-to- τ_{had} fake rate	14
τ_{had} energy scale	12
Jet energy scale and resolution	11
Electron reconstruction & identification	8.1
Simulated backgrounds cross section and acceptance	7.5
Luminosity	7.4
Muon reconstruction & identification	7.2
b -jet identification	6.6
Jet-to- τ_{had} fake rate for electroweak processes ($\tau_{\text{lep}}\tau_{\text{had}}$)	6.2
Multi-jet background ($\tau_{\text{lep}}\tau_{\text{lep}}$, $\tau_{\text{lep}}\tau_{\text{had}}$)	6.1
Associated with the τ -embedded $Z \rightarrow \mu\mu$ sample	5.3
Signal acceptance	2.0
$e\mu$ trigger	1.5
τ_{had} identification	0.8

Table 4. The effect of the most important sources of uncertainty on the signal strength parameter, μ , for the signal hypothesis of $m_A = 150$ GeV, $\tan\beta = 5.7$. For this signal hypothesis only the $h/H/A \rightarrow \tau_{\text{lep}}\tau_{\text{had}}$ and $h/H/A \rightarrow \tau_e\tau_\mu$ channels are used.

Source of uncertainty	Uncertainty on μ (%)
τ_{had} energy scale	15
Multi-jet background ($\tau_{\text{had}}\tau_{\text{had}}$, $\tau_{\text{lep}}\tau_{\text{had}}$)	9.8
τ_{had} identification	7.9
Jet-to- τ_{had} fake rate for electroweak processes	7.6
τ_{had} trigger	7.4
Simulated backgrounds cross section and acceptance	6.6
Signal acceptance	4.7
Luminosity	4.1
Associated with the τ -embedded $Z \rightarrow \mu\mu$ sample	1.2
Lepton identification	0.7

Table 5. The effect of the most important sources of uncertainty on the signal strength parameter, μ , for the signal hypothesis of $m_A = 350$ GeV, $\tan\beta = 14$. For this signal hypothesis only the $h/H/A \rightarrow \tau_{\text{lep}}\tau_{\text{had}}$ and $h/H/A \rightarrow \tau_{\text{had}}\tau_{\text{had}}$ channels are used.

7 Results

The results from the channels studied in this search are combined to improve the sensitivity to MSSM Higgs boson production. Each of the channels used here is optimized for a specific Higgs boson mass regime. In particular, the $\tau_e\tau_\mu$ channel, the $\tau_{\text{lep}}\tau_{\text{had}}$ tag category, and the $\tau_{\text{lep}}\tau_{\text{had}}$ veto category are used for the range $90 \leq m_A < 200$ GeV. The $\tau_{\text{lep}}\tau_{\text{had}}$ high mass category and the $\tau_{\text{had}}\tau_{\text{had}}$ channel are used for $m_A \geq 200$ GeV. The event selection in these categories is such that the low mass categories, i.e. those that target $90 \leq m_A < 200$ GeV, are sensitive to the production of all three MSSM Higgs bosons, h , H and A . In contrast, the categories that target $m_A \geq 200$ GeV are sensitive only to H and A production.

The parameter of interest in this search is the signal strength, μ , defined as the ratio of the fitted signal cross section times branching fraction to the signal cross section times branching fraction predicted by the particular MSSM signal assumption. The value $\mu = 0$ corresponds to the absence of signal, whereas the value $\mu = 1$ suggests signal presence as predicted by the theoretical model under study. The statistical analysis of the data employs a binned likelihood function constructed as the product of Poisson probability terms as an estimator of μ . Signal and background predictions depend on systematic uncertainties, which are parameterized as nuisance parameters and are constrained using Gaussian functions. The binned likelihood function is constructed in bins of the MMC mass for the $\tau_e\tau_\mu$ and the $\tau_{\text{lep}}\tau_{\text{had}}$ channels and in bins of total transverse mass for the $\tau_{\text{had}}\tau_{\text{had}}$ channel.

Since the data are in good agreement with the predicted background yields, exclusion limits are calculated. The significance of any small observed excess in data is evaluated by quoting p -values to quantify the level of consistency of the data with the $\mu=0$ hypothesis. Exclusion limits use the modified frequentist method known as CL_s [90]. Both the exclusion limits and p -values are calculated using the asymptotic approximation [91]. The test statistic used for the exclusion limits derivation is the \tilde{q}_μ test statistic and for the p -values the q_0 test statistic⁶ [91].

The lowest local p -values are calculated assuming a single scalar boson ϕ with narrow natural width with respect to the experimental mass resolution. The lowest local p -value for the combination of all channels corresponds to 0.20, or 0.8σ in terms of Gaussian standard deviations, at $m_\phi = 200$ GeV. For the individual channels, the lowest local p -value in $\tau_{\text{had}}\tau_{\text{had}}$ is 0.10 (or 1.3σ) at $m_\phi = 250$ GeV and for the $\tau_{\text{lep}}\tau_{\text{had}}$ 0.10 (or 1.3σ)

⁶The definition of the test statistics used in this search is the following:

$$\tilde{q}_\mu = \begin{cases} -2 \ln(\mathcal{L}(\mu, \hat{\theta}) / \mathcal{L}(0, \hat{\theta})) & \text{if } \hat{\mu} < 0 \\ -2 \ln(\mathcal{L}(\mu, \hat{\theta}) / \mathcal{L}(\hat{\mu}, \hat{\theta})) & \text{if } 0 \leq \hat{\mu} \leq \mu \\ 0 & \text{if } \hat{\mu} > \mu \end{cases}$$

and

$$q_0 = \begin{cases} -2 \ln(\mathcal{L}(0, \hat{\theta}) / \mathcal{L}(\hat{\mu}, \hat{\theta})) & \text{if } \hat{\mu} \geq 0 \\ 0 & \text{if } \hat{\mu} < 0 \end{cases}$$

where $\mathcal{L}(\mu, \theta)$ denotes the binned likelihood function, μ is the parameter of interest (i.e. the signal strength parameter), and θ denotes the nuisance parameters. The pair $(\hat{\mu}, \hat{\theta})$ corresponds to the global maximum of the likelihood, whereas $(x, \hat{\theta})$ corresponds to a conditional maximum in which μ is fixed to a given value x .

at $m_\phi = 90$ GeV. In the $\tau_{\text{lep}}\tau_{\text{lep}}$ channel there is no excess in the mass region used for the combination ($90 \leq m_\phi < 200$ GeV).

Expected and observed 95% confidence level (CL) upper limits for the combination of all channels are shown in figure 9(a) for the MSSM m_h^{\max} scenario with $M_{\text{SUSY}} = 1$ TeV [21, 22]. In this figure, the theoretical MSSM Higgs cross-section uncertainties are not included in the reported result, but their impact is shown separately, by recalculating the upper limits again after considering the relevant $\pm 1\sigma$ variations. Figure 9(b) shows the upper limits for each channel separately for comparison. The best $\tan\beta$ constraint for the combined search excludes $\tan\beta > 5.4$ for $m_A = 140$ GeV, whereas, as an example, $\tan\beta > 37$ is excluded for $m_A = 800$ GeV. Figure 9(a) shows also contours of constant m_h and m_H for the MSSM m_h^{\max} scenario. Assuming that the light CP-even Higgs boson of the MSSM has a mass of about 125 GeV and taking into consideration the 3 GeV uncertainty in the m_h calculation in the MSSM [23], only the parameter space that is compatible with $122 < m_h < 128$ GeV is allowed. From this consideration it is concluded that if the light CP-even Higgs boson of the MSSM is identified with the particle discovered at the LHC, then for this particular MSSM scenario $m_A < 160$ GeV is excluded for all $\tan\beta$ values. Similarly, $\tan\beta > 10$ and $\tan\beta < 4$ are excluded for all m_A values. Figure 10 shows the expected and observed upper limits for the MSSM $m_h^{\text{mod}+}$ and $m_h^{\text{mod}-}$ scenarios [23]. Again, the combination of all channels is shown and the impact of signal cross-section uncertainties is shown separately. Under the assumption that the light CP-even Higgs boson of the MSSM is identified with the particle discovered at the LHC and taking into account the same considerations as in the m_h^{\max} scenario case, the region with $m_A < 200$ GeV is excluded for all $\tan\beta$ values, whereas $\tan\beta < 5.5$ is excluded for all values of m_A for both the MSSM $m_h^{\text{mod}+}$ and $m_h^{\text{mod}-}$ scenarios.

The outcome of the search is further interpreted in the case of a single scalar boson ϕ , with narrow width relative to the experimental mass resolution, produced in either the gluon fusion or b -associated production mode and decaying to $\tau\tau$. Figure 11 shows 95% CL upper limits on the cross section times the $\tau\tau$ branching fraction based on this interpretation. The exclusion limits for the production cross section times the branching fraction for a scalar boson decaying to $\tau\tau$ are shown as a function of the scalar boson mass. The excluded cross section times branching fraction values range from $\sigma \times BR > 29$ pb at $m_\phi = 90$ GeV to $\sigma \times BR > 7.4$ fb at $m_\phi = 1000$ GeV for a scalar boson produced via gluon fusion. The exclusion range for the b -associated production mechanism ranges from $\sigma \times BR > 6.4$ pb at $m_\phi = 90$ GeV to $\sigma \times BR > 7.2$ fb at $m_\phi = 1000$ GeV.

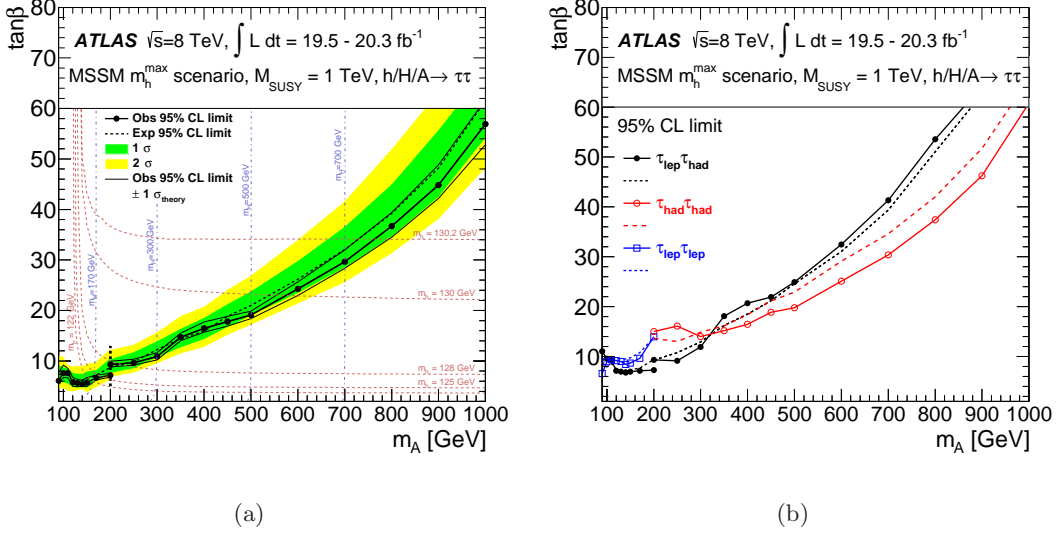


Figure 9. Expected (dashed line) and observed (solid line with markers) 95% CL upper limits on $\tan\beta$ as a function of m_A for the m_h^{\max} scenario of the MSSM (a) for the combination of all channels and (b) for each channel separately. Values of $\tan\beta$ above the lines are excluded. The vertical dashed line at 200 GeV in (a) indicates the transition point between low- and high-mass categories. Lines of constant m_h and m_H are also shown in (a) in red and blue colour, respectively. For more information, see text.

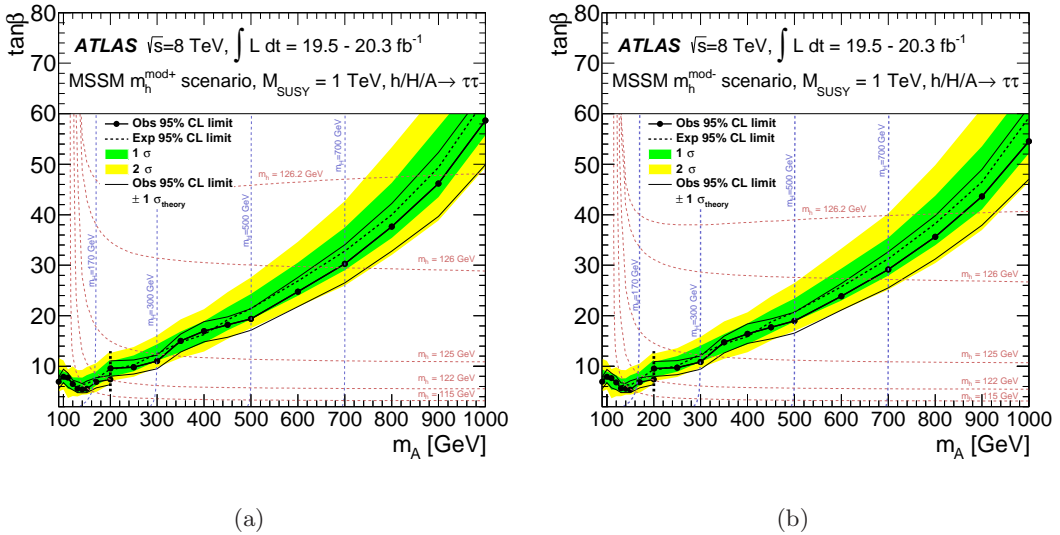


Figure 10. Expected (dashed line) and observed (solid line with markers) 95% CL upper limits on $\tan\beta$ as a function of m_A for (a) the $m_h^{\text{mod}+}$ and (b) the $m_h^{\text{mod}-}$ benchmark scenarios of the MSSM. The same notation as in figure 9(a) is used.

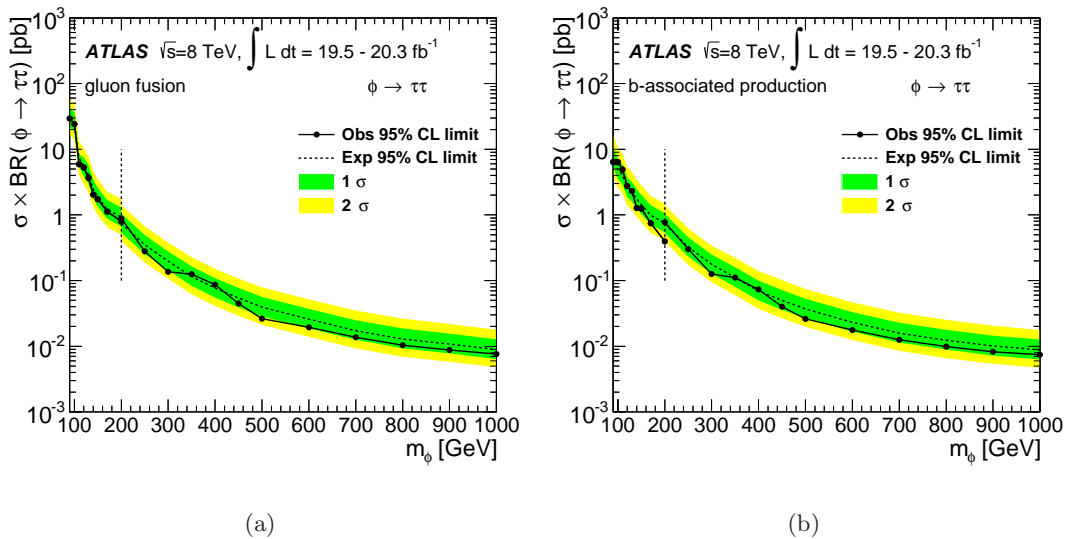


Figure 11. Expected (dashed bold line) and observed (solid bold line) 95% CL upper limits on the cross section of a scalar boson ϕ produced via (a) gluon fusion and (b) in association with b -quarks times the branching fraction into τ pairs. The vertical dashed line indicates the transition point between low- and high-mass categories.

8 Summary

A search is presented for the neutral Higgs bosons of the Minimal Supersymmetric Standard Model in proton–proton collisions at the centre-of-mass energy of 8 TeV with the ATLAS experiment at the LHC. The integrated luminosity used in the search is 19.5–20.3 fb^{−1}. The search uses the $\tau\tau$ final state. In particular, the following cases are considered: one τ lepton decays to an electron and the other to a muon ($\tau_e\tau_\mu$), one τ lepton decays to an electron or muon and the other hadronically ($\tau_{\text{lep}}\tau_{\text{had}}$) and finally both τ leptons decay hadronically ($\tau_{\text{had}}\tau_{\text{had}}$). The sensitivity is improved by performing a categorisation based on expected Higgs boson mass and production mechanisms. The search finds no indication of an excess over the expected background in the channels considered and 95% CL limits are set, which provide tight constraints in the MSSM parameter space. In particular, in the context of the MSSM m_h^{\max} scenario the lowest $\tan\beta$ constraint excludes $\tan\beta > 5.4$ for $m_A = 140$ GeV. Upper limits for the production cross section times $\tau\tau$ branching fraction of a scalar boson versus its mass, depending on the production mode, are also presented. The excluded cross section times $\tau\tau$ branching fraction ranges from about 30 pb to about 7 fb depending on the Higgs boson mass and the production mechanism.

Acknowledgements

We thank CERN for the very successful operation of the LHC, as well as the support staff from our institutions without whom ATLAS could not be operated efficiently.

We acknowledge the support of ANPCyT, Argentina; YerPhI, Armenia; ARC, Australia; BMWFW and FWF, Austria; ANAS, Azerbaijan; SSTC, Belarus; CNPq and FAPESP, Brazil; NSERC, NRC and CFI, Canada; CERN; CONICYT, Chile; CAS, MOST and NSFC, China; COLCIENCIAS, Colombia; MSMT CR, MPO CR and VSC CR, Czech Republic; DNRF, DNSRC and Lundbeck Foundation, Denmark; EPLANET, ERC and NSRF, European Union; IN2P3-CNRS, CEA-DSM/IRFU, France; GNSF, Georgia; BMBF, DFG, HGF, MPG and AvH Foundation, Germany; GSRT and NSRF, Greece; ISF, MINERVA, GIF, I-CORE and Benoziyo Center, Israel; INFN, Italy; MEXT and JSPS, Japan; CNRST, Morocco; FOM and NWO, Netherlands; BRF and RCN, Norway; MNiSW and NCN, Poland; GRICES and FCT, Portugal; MNE/IFA, Romania; MES of Russia and ROSATOM, Russian Federation; JINR; MSTD, Serbia; MSSR, Slovakia; ARRS and MIZŠ, Slovenia; DST/NRF, South Africa; MINECO, Spain; SRC and Wallenberg Foundation, Sweden; SER, SNSF and Cantons of Bern and Geneva, Switzerland; NSC, Taiwan; TAEK, Turkey; STFC, the Royal Society and Leverhulme Trust, United Kingdom; DOE and NSF, United States of America.

The crucial computing support from all WLCG partners is acknowledged gratefully, in particular from CERN and the ATLAS Tier-1 facilities at TRIUMF (Canada), NDGF (Denmark, Norway, Sweden), CC-IN2P3 (France), KIT/GridKA (Germany), INFN-CNAF (Italy), NL-T1 (Netherlands), PIC (Spain), ASGC (Taiwan), RAL (UK) and BNL (USA) and in the Tier-2 facilities worldwide.

References

- [1] ATLAS Collaboration, *Observation of a new particle in the search for the Standard Model Higgs boson with the ATLAS detector at the LHC*, *Phys. Lett. B* **716** (2012) 1–29, [[arXiv:1207.7214](#)].
- [2] CMS Collaboration, *Observation of a new boson at a mass of 125 GeV with the CMS experiment at the LHC*, *Phys. Lett. B* **716** (2012) 30–61, [[arXiv:1207.7235](#)].
- [3] ATLAS Collaboration, *Measurements of Higgs boson production and couplings in diboson final states with the ATLAS detector at the LHC*, *Phys. Lett. B* **726** (2013) 88–119, [[arXiv:1307.1427](#)].
- [4] ATLAS Collaboration, *Evidence for the spin-0 nature of the Higgs boson using ATLAS data*, *Phys. Lett. B* **726** (2013) 120–144, [[arXiv:1307.1432](#)].
- [5] CMS Collaboration, *Evidence for the direct decay of the 125 GeV Higgs boson to fermions*, *Nature Phys.* **10** (2014) [[arXiv:1401.6527](#)].
- [6] CMS Collaboration, *Measurement of the properties of a Higgs boson in the four-lepton final state*, *Phys. Rev. D* **89** (2014) 092007, [[arXiv:1312.5353](#)].
- [7] CMS Collaboration, *Measurement of Higgs boson production and properties in the WW decay channel with leptonic final states*, *JHEP* **01** (2014) 096, [[arXiv:1312.1129](#)].
- [8] F. Englert and R. Brout, *Broken symmetry and the mass of gauge vector mesons*, *Phys. Rev. Lett.* **13** (1964) 321–323.
- [9] P. W. Higgs, *Broken symmetries, massless particles and gauge fields*, *Phys. Lett.* **12** (1964) 132–133.
- [10] P. W. Higgs, *Broken symmetries and the masses of gauge bosons*, *Phys. Rev. Lett.* **13** (1964) 508–509.
- [11] P. W. Higgs, *Spontaneous symmetry breakdown without massless bosons*, *Phys. Rev.* **145** (1966) 1156–1163.
- [12] G. Guralnik, C. Hagen, and T. Kibble, *Global conservation laws and massless particles*, *Phys. Rev. Lett.* **13** (1964) 585–587.
- [13] T. Kibble, *Symmetry breaking in non-Abelian gauge theories*, *Phys. Rev.* **155** (1967) 1554–1561.
- [14] A. Djouadi, *The Anatomy of electro-weak symmetry breaking. II. The Higgs bosons in the minimal supersymmetric model*, *Phys. Rept.* **459** (2008) 1–241, [[hep-ph/0503173](#)].
- [15] *Theory and phenomenology of two-Higgs-doublet models*, *Phys. Rept.* **516** (2012) 1–102, [[arXiv:1106.0034](#)].
- [16] P. Fayet, *Supersymmetry and Weak, Electromagnetic and Strong Interactions*, *Phys. Lett. B* **64** (1976) 159.
- [17] P. Fayet, *Spontaneously Broken Supersymmetric Theories of Weak, Electromagnetic and Strong Interactions*, *Phys. Lett. B* **69** (1977) 489.
- [18] G. R. Farrar and P. Fayet, *Phenomenology of the Production, Decay, and Detection of New Hadronic States Associated with Supersymmetry*, *Phys. Lett. B* **76** (1978) 575–579.
- [19] P. Fayet, *Relations Between the Masses of the Superpartners of Leptons and Quarks, the Goldstino Couplings and the Neutral Currents*, *Phys. Lett. B* **84** (1979) 416.

- [20] S. Dimopoulos and H. Georgi, *Softly Broken Supersymmetry and SU(5)*, *Nucl. Phys. B* **193** (1981) 150.
- [21] S. Heinemeyer, W. Hollik, and G. Weiglein, *Constraints on tan Beta in the MSSM from the upper bound on the mass of the lightest Higgs boson*, *JHEP* **06** (2000) 009, [[hep-ph/9909540](#)].
- [22] M. Carena, S. Heinemeyer, C. E. M. Wagner and G. Weiglein, *Suggestions for benchmark scenarios for MSSM Higgs boson searches at hadron colliders*, *Eur. Phys. J. C* **26** (2003) 601, [[hep-ph/0202167](#)].
- [23] M. Carena, S. Heinemeyer, O. Stål, C. Wagner, and G. Weiglein, *MSSM Higgs Boson Searches at the LHC: Benchmark Scenarios after the Discovery of a Higgs-like Particle*, *Eur. Phys. J. C* **73** (2013) 2552, [[arXiv:1302.7033](#)].
- [24] *Measurement of the Higgs boson mass from the $H \rightarrow \gamma\gamma$ and $H \rightarrow ZZ^* \rightarrow 4\ell$ channels with the ATLAS detector using 25 fb^{-1} of pp collision data*, [arXiv:1406.3827](#).
- [25] P. Bechtle et al., *MSSM Interpretations of the LHC Discovery: Light or Heavy Higgs?*, *Eur. Phys. J. C* **73** (2013) 2354, [[arXiv:1211.1955](#)].
- [26] A. Arbey, M. Battaglia, A. Djouadi, and F. Mahmoudi, *The Higgs sector of the phenomenological MSSM in the light of the Higgs boson discovery*, *JHEP* **09** (2012) 107, [[arXiv:1207.1348](#)].
- [27] ALEPH, DELPHI, L3, and OPAL Collaborations, S. Schael et al., *Search for neutral MSSM Higgs bosons at LEP*, *Eur. Phys. J. C* **47** (2006) 547–587, [[hep-ex/0602042](#)].
- [28] Tevatron New Phenomena & Higgs Working Group Collaboration, B. Doug et al., *Combined CDF and D0 upper limits on MSSM Higgs boson production in $\tau\tau$ final states with up to 2.2 fb^{-1}* , [arXiv:1003.3363](#).
- [29] CDF Collaboration, T. Aaltonen et al., *Search for Higgs bosons predicted in two-Higgs-doublet models via decays to τ lepton pairs in 1.96 TeV proton–antiproton collisions*, *Phys. Rev. Lett.* **103** (2009) 201801, [[arXiv:0906.1014](#)].
- [30] D0 Collaboration, V. M. Abazov et al., *Search for Higgs bosons decaying to τ pairs in $p\bar{p}$ collisions with the D0 detector*, *Phys. Rev. Lett.* **101** (2008) 071804, [[arXiv:0805.2491](#)].
- [31] ATLAS Collaboration, *Search for the neutral Higgs bosons of the minimal supersymmetric standard model in pp collisions at $\sqrt{s} = 7$ TeV with the ATLAS detector*, *JHEP* **02** (2013) 095, [[arXiv:1211.6956](#)].
- [32] CMS Collaboration, *Search for neutral MSSM Higgs bosons decaying to a pair of tau leptons in pp collisions*, [arXiv:1408.3316](#).
- [33] LHCb Collaboration, R. Aaij et al., *Limits on neutral Higgs boson production in the forward region in pp collisions at $\sqrt{s} = 7$ TeV*, *JHEP* **05** (2013) 132, [[arXiv:1304.2591](#)].
- [34] ATLAS Collaboration, *The ATLAS experiment at the CERN Large Hadron Collider*, *JINST* **3** (2008) S08003.
- [35] ATLAS Collaboration, *Search for the Standard Model Higgs boson in the $H \rightarrow \tau\tau$ decay mode in $\sqrt{s}=7$ TeV pp collisions with ATLAS*, *JHEP* **09** (2012) 070, [[arXiv:1206.5971](#)].
- [36] ATLAS Collaboration, *The ATLAS simulation infrastructure*, *Eur. Phys. J. C* **70** (2010) 823–874, [[arXiv:1005.4568](#)].
- [37] GEANT4 Collaboration, S. Agostinelli et al., *GEANT4 - a simulation toolkit*, *Nucl. Instrum. Meth. A* **506** (2003) 250–303.

- [38] M. Spira, *HIGLU: A program for the calculation of the total Higgs production cross section at hadron colliders via gluon fusion including QCD corrections*, [hep-ph/9510347](#).
- [39] R. V. Harlander and W. B. Kilgore, *Next-to-Next-to-Leading Order Higgs Production at Hadron Colliders*, *Phys. Rev. Lett.* **88** (2002) 201801, [[hep-ph/0201206](#)].
- [40] R. V. Harlander, S. Liebler, and H. Mantler, *SusHi: A program for the calculation of Higgs production in gluon fusion and bottom-quark annihilation in the Standard Model and the MSSM*, *Comput. Phys. Commun.* **184** (2013) 1605–1617, [[arXiv:1212.3249](#)].
- [41] R. V. Harlander and M. Steinhauser, *Hadronic Higgs production and decay in supersymmetry at next-to-leading order*, *Phys. Lett. B* **574** (2003) 258–268, [[hep-ph/0307346](#)].
- [42] R. V. Harlander and M. Steinhauser, *Supersymmetric Higgs production in gluon fusion at next-to-leading order*, *JHEP* **09** (2004) 066, [[hep-ph/0409010](#)].
- [43] R. Harlander and M. Steinhauser, *Effects of SUSY QCD in hadronic Higgs production at next-to-next-to-leading order*, *Phys. Rev. D* **68** (2003) 111701, [[hep-ph/0308210](#)].
- [44] R. Harlander and W. B. Kilgore, *Higgs boson production in bottom quark fusion at next-to-next-to-leading order*, *Phys. Rev. D* **68** (2003) 013001, [[hep-ph/0304035](#)].
- [45] U. Aglietti, R. Bonciani, G. Degrassi, and A. Vicini, *Two loop light fermion contribution to Higgs production and decays*, *Phys. Lett. B* **595** (2004) 432–441, [[hep-ph/0404071](#)].
- [46] R. Bonciani, G. Degrassi, and A. Vicini, *On the Generalized Harmonic Polylogarithms of One Complex Variable*, *Comput. Phys. Commun.* **182** (2011) 1253–1264, [[arXiv:1007.1891](#)].
- [47] G. Degrassi and P. Slavich, *NLO QCD bottom corrections to Higgs boson production in the MSSM*, *JHEP* **11** (2010) 044, [[arXiv:1007.3465](#)].
- [48] G. Degrassi, S. Di Vita, and P. Slavich, *NLO QCD corrections to pseudoscalar Higgs production in the MSSM*, *JHEP* **08** (2011) 128, [[arXiv:1107.0914](#)].
- [49] G. Degrassi, S. Di Vita, and P. Slavich, *On the NLO QCD Corrections to the Production of the Heaviest Neutral Higgs Scalar in the MSSM*, *Eur. Phys. J. C* **72** (2012) 2032, [[arXiv:1204.1016](#)].
- [50] S. Heinemeyer, W. Hollik, and G. Weiglein, *FeynHiggs: A Program for the calculation of the masses of the neutral CP even Higgs bosons in the MSSM*, *Comput. Phys. Commun.* **124** (2000) 76–89, [[hep-ph/9812320](#)].
- [51] S. Heinemeyer, W. Hollik, and G. Weiglein, *The Masses of the neutral CP - even Higgs bosons in the MSSM: Accurate analysis at the two loop level*, *Eur. Phys. J. C* **9** (1999) 343–366, [[hep-ph/9812472](#)].
- [52] G. Degrassi, S. Heinemeyer, W. Hollik, P. Slavich, and G. Weiglein, *Towards high precision predictions for the MSSM Higgs sector*, *Eur. Phys. J. C* **28** (2003) 133–143, [[hep-ph/0212020](#)].
- [53] M. Frank et al., *The Higgs boson masses and mixings of the complex MSSM in the Feynman-diagrammatic approach*, *JHEP* **02** (2007) 047, [[hep-ph/0611326](#)].
- [54] R. Harlander and P. Kant, *Higgs production and decay: Analytic results at next-to-leading order QCD*, *JHEP* **12** (2005) 015, [[hep-ph/0509189](#)].
- [55] S. Dittmaier, M. Krämer and M. Spira, *Higgs radiation off bottom quarks at the Tevatron and the LHC*, *Phys. Rev. D* **70** (2004) 074010, [[hep-ph/0309204](#)].

- [56] S. Dawson, C. B. Jackson, L. Reina and D. Wackerlo, *Exclusive Higgs boson production with bottom quarks at hadron colliders*, *Phys. Rev. D* **69** (2004) 074027, [[hep-ph/0311067](#)].
- [57] R. Harlander, M. Krämer, and M. Schumacher, *Bottom-quark associated Higgs-boson production: reconciling the four- and five-flavour scheme approach*, [arXiv:1112.3478](#).
- [58] S. Alioli, P. Nason, C. Oleari, and E. Re, *NLO Higgs boson production via gluon fusion matched with shower in POWHEG*, *JHEP* **04** (2009) 002, [[arXiv:0812.0578](#)].
- [59] T. Gleisberg et al., *Event generation with SHERPA 1.1*, *JHEP* **02** (2009) 007, [[arXiv:0811.4622](#)].
- [60] H.-L. Lai et al., *New parton distributions for collider physics*, *Phys. Rev. D* **82** (2010) 074024, [[arXiv:1007.2241](#)].
- [61] M. L. Mangano, M. Moretti, F. Piccinini, R. Pittau and A. D. Polosa, *ALPGEN, a generator for hard multiparton processes in hadronic collisions*, *JHEP* **07** (2003) 001, [[hep-ph/0206293](#)].
- [62] T. Sjöstrand, S. Mrenna and P. Skands, *PYTHIA 6.4 physics and manual*, *JHEP* **05** (2006) 026, [[hep-ph/0603175](#)].
- [63] T. Sjöstrand, S. Mrenna and P. Skands, *A Brief Introduction to PYTHIA 8.1*, *Comput. Phys. Commun.* **178** (2008) 852–867, [[arXiv:0710.3820](#)].
- [64] G. Corcella et al., *HERWIG 6.5: an event generator for hadron emission reactions with interfering gluons (including supersymmetric processes)*, *JHEP* **01** (2001) 010, [[hep-ph/0011363](#)].
- [65] S. Frixione and B. R. Webber, *Matching NLO QCD computations and parton shower simulations*, *JHEP* **06** (2002) 029, [[hep-ph/0204244](#)].
- [66] B. P. Kersevan and E. Richter-Was, *The Monte Carlo event generator AcerMC version 2.0 with interfaces to PYTHIA 6.2 and HERWIG 6.5*, [hep-ph/0405247](#).
- [67] J. Pumplin, D. Stump, J. Huston, H. Lai, P. M. Nadolsky, et al., *New generation of parton distributions with uncertainties from global QCD analysis*, *JHEP* **07** (2002) 012, [[hep-ph/0201195](#)].
- [68] S. Jadach, J. H. Kuhn and Z. Was, *TAUOLA - a library of Monte Carlo programs to simulate decays of polarized τ leptons*, *Comput. Phys. Commun.* **64** (1990) 275–299.
- [69] E. Barberio, B. V. Eijk and Z. Was, *PHOTOS - a universal Monte Carlo for QED radiative corrections in decays*, *Comput. Phys. Commun.* **66** (1991) 115–128.
- [70] Z. Czyczula, T. Przedzinski, and Z. Was, *TauSpinner Program for Studies on Spin Effect in tau Production at the LHC*, *Eur. Phys. J. C* **72** (2012) 1988, [[arXiv:1201.0117](#)].
- [71] ATLAS Collaboration, *Electron efficiency measurements with the ATLAS detector using the 2012 LHC proton-proton collision data*, [ATLAS-CONF-2014-032](#), available at <http://cdsweb.cern.ch/record/1706245>.
- [72] ATLAS Collaboration, *Measurement of the muon reconstruction performance of the ATLAS detector using 2011 and 2012 LHC proton-proton collision data*, [arXiv:1407.3935](#).
- [73] M. Cacciari, G. P. Salam and G. Soyez, *The anti- k_t jet clustering algorithm*, *JHEP* **04** (2008) 063, [[arXiv:0802.1189](#)].
- [74] W. Lampl et al., *Calorimeter clustering algorithms: Description and performance*, [ATL-LARG-PUB-2008-002](#), CERN, Geneva Switzerland (2008).

- [75] ATLAS Collaboration, *Jet energy measurement and its systematic uncertainty in proton-proton collisions at $\sqrt{s} = 7$ TeV with the ATLAS detector*, [arXiv:1406.0076](https://arxiv.org/abs/1406.0076).
- [76] ATLAS Collaboration, *Calibration of b-tagging using dileptonic top pair events in a combinatorial likelihood approach with the ATLAS experiment*, [ATLAS-CONF-2014-004](#), available at <http://cds.cern.ch/record/1664335>.
- [77] ATLAS Collaboration, *Calibration of the performance of b-tagging for c and light-flavour jets in the 2012 ATLAS data*, [ATLAS-CONF-2014-046](#), available at <http://cds.cern.ch/record/1741020>.
- [78] ATLAS Collaboration, *Identification of the Hadronic Decays of Tau Leptons in 2012 Data with the ATLAS Detector*, [ATLAS-CONF-2013-064](#), available at <http://cds.cern.ch/record/1562839>.
- [79] ATLAS Collaboration, *Performance of missing transverse momentum reconstruction in proton–proton collisions at 7 TeV with ATLAS*, *Eur. Phys. J. C* **72** (2012) 1844, [[arXiv:1108.5602](https://arxiv.org/abs/1108.5602)].
- [80] A. Elagin, P. Murat, A. Pranko and A. Safonov, *A new mass reconstruction technique for resonances decaying to di- τ* , *Nucl. Instrum. Meth. A* **654** (2011) 481–489, [[arXiv:1012.4686](https://arxiv.org/abs/1012.4686)].
- [81] C. Anastasiou, L. J. Dixon, K. Melnikov, and F. Petriello, *High precision QCD at hadron colliders: Electroweak gauge boson rapidity distributions at NNLO*, *Phys. Rev. D* **69** (2004) 094008, [[hep-ph/0312266](https://arxiv.org/abs/hep-ph/0312266)].
- [82] LHC Higgs Cross Section Working Group, *Handbook of LHC Higgs Cross Sections: 1. Inclusive Observables*, [arXiv:1101.0593](https://arxiv.org/abs/1101.0593).
- [83] ATLAS Collaboration, *Improved luminosity determination in pp collisions at $\sqrt{s} = 7$ TeV using the ATLAS detector at the LHC*, *Eur. Phys. J. C* **73** (2013) 2518, [[arXiv:1302.4393](https://arxiv.org/abs/1302.4393)].
- [84] ATLAS Collaboration, *Performance of the ATLAS tau trigger in 2011*, [ATLAS-CONF-2013-006](#), available at <http://cds.cern.ch/record/1510157>.
- [85] ATLAS Collaboration, *Determination of the tau energy scale and the associated systematic uncertainty in proton-proton collisions at $\sqrt{s} = 8$ TeV with the ATLAS detector at the LHC in 2012*, [ATLAS-CONF-2013-044](#), available at <http://cds.cern.ch/record/1544036>.
- [86] ATLAS Collaboration, *Jet energy resolution in proton-proton collisions at $\sqrt{s} = 7$ TeV recorded in 2010 with the ATLAS detector*, *Eur. Phys. J. C* **73** (2013) 2306, [[arXiv:1210.6210](https://arxiv.org/abs/1210.6210)].
- [87] ATLAS Collaboration, *Performance of Missing Transverse Momentum Reconstruction in ATLAS studied in Proton-Proton Collisions recorded in 2012 at 8 TeV*, [ATLAS-CONF-2013-082](#), available at <http://cdsweb.cern.ch/record/1570993>.
- [88] ATLAS Collaboration, *Electron reconstruction and identification efficiency measurements with the ATLAS detector using the 2011 LHC proton-proton collision data*, [arXiv:1404.2240](https://arxiv.org/abs/1404.2240).
- [89] ATLAS Collaboration, *Electron and photon energy calibration with the ATLAS detector using LHC Run 1 data*, [arXiv:1407.5063](https://arxiv.org/abs/1407.5063).
- [90] A. L. Read, *Presentation of search results: the CL_s technique*, *J. Phys. G* **28** (2002) 2693–2704.

- [91] G. Cowan, K. Cranmer, E. Gross and O. Vitells, *Asymptotic formulae for likelihood-based tests of new physics*, *Eur. Phys. J. C* **71** (2011) 1554, [[arXiv:1007.1727](https://arxiv.org/abs/1007.1727)].

The ATLAS Collaboration

G. Aad⁸⁵, B. Abbott¹¹³, J. Abdallah¹⁵², S. Abdel Khalek¹¹⁷, O. Abdinov¹¹, R. Aben¹⁰⁷, B. Abi¹¹⁴, M. Abolins⁹⁰, O.S. AbouZeid¹⁵⁹, H. Abramowicz¹⁵⁴, H. Abreu¹⁵³, R. Abreu³⁰, Y. Abulaiti^{147a,147b}, B.S. Acharya^{165a,165b,a}, L. Adamczyk^{38a}, D.L. Adams²⁵, J. Adelman¹⁷⁷, S. Adomeit¹⁰⁰, T. Adye¹³¹, T. Agatonovic-Jovin^{13a}, J.A. Aguilar-Saavedra^{126a,126f}, M. Agustoni¹⁷, S.P. Ahlen²², F. Ahmadov^{65,b}, G. Aielli^{134a,134b}, H. Akerstedt^{147a,147b}, T.P.A. Åkesson⁸¹, G. Akimoto¹⁵⁶, A.V. Akimov⁹⁶, G.L. Alberghi^{20a,20b}, J. Albert¹⁷⁰, S. Albrand⁵⁵, M.J. Alconada Verzini⁷¹, M. Aleksa³⁰, I.N. Aleksandrov⁶⁵, C. Alexa^{26a}, G. Alexander¹⁵⁴, G. Alexandre⁴⁹, T. Alexopoulos¹⁰, M. Alhroob¹¹³, G. Alimonti^{91a}, L. Alio⁸⁵, J. Alison³¹, B.M.M. Allbrooke¹⁸, L.J. Allison⁷², P.P. Allport⁷⁴, A. Aloisio^{104a,104b}, A. Alonso³⁶, F. Alonso⁷¹, C. Alpigiani⁷⁶, A. Altheimer³⁵, B. Alvarez Gonzalez⁹⁰, M.G. Alviggi^{104a,104b}, K. Amako⁶⁶, Y. Amaral Coutinho^{24a}, C. Amelung²³, D. Amidei⁸⁹, S.P. Amor Dos Santos^{126a,126c}, A. Amorim^{126a,126b}, S. Amoroso⁴⁸, N. Amram¹⁵⁴, G. Amundsen²³, C. Anastopoulos¹⁴⁰, L.S. Ancu⁴⁹, N. Andari³⁰, T. Andeen³⁵, C.F. Anders^{58b}, G. Anders³⁰, K.J. Anderson³¹, A. Andreazza^{91a,91b}, V. Andrei^{58a}, X.S. Anduaga⁷¹, S. Angelidakis⁹, I. Angelozzi¹⁰⁷, P. Anger⁴⁴, A. Angerami³⁵, F. Anghinolfi³⁰, A.V. Anisenkov^{109,c}, N. Anjos¹², A. Annovi⁴⁷, A. Antonaki⁹, M. Antonelli⁴⁷, A. Antonov⁹⁸, J. Antos^{145b}, F. Anulli^{133a}, M. Aoki⁶⁶, L. Aperio Bella¹⁸, R. Apolle^{120,d}, G. Arabidze⁹⁰, I. Aracena¹⁴⁴, Y. Arai⁶⁶, J.P. Araque^{126a}, A.T.H. Arce⁴⁵, F.A. Arduh⁷¹, J-F. Arguin⁹⁵, S. Argyropoulos⁴², M. Arik^{19a}, A.J. Armbruster³⁰, O. Arnaez³⁰, V. Arnal⁸², H. Arnold⁴⁸, M. Arratia²⁸, O. Arslan²¹, A. Artamonov⁹⁷, G. Artoni²³, S. Asai¹⁵⁶, N. Asbah⁴², A. Ashkenazi¹⁵⁴, B. Åsman^{147a,147b}, L. Asquith⁶, K. Assamagan²⁵, R. Astalos^{145a}, M. Atkinson¹⁶⁶, N.B. Atlay¹⁴², B. Auerbach⁶, K. Augsten¹²⁸, M. Aurousseau^{146b}, G. Avolio³⁰, B. Axen¹⁵, G. Azuelos^{95,e}, Y. Azuma¹⁵⁶, M.A. Baak³⁰, A.E. Baas^{58a}, C. Bacci^{135a,135b}, H. Bachacou¹³⁷, K. Bachas¹⁵⁵, M. Backes³⁰, M. Backhaus³⁰, J. Backus Mayes¹⁴⁴, E. Badescu^{26a}, P. Bagiacchi^{133a,133b}, P. Bagnaia^{133a,133b}, Y. Bai^{33a}, T. Bain³⁵, J.T. Baines¹³¹, O.K. Baker¹⁷⁷, P. Balek¹²⁹, F. Balli¹³⁷, E. Banas³⁹, Sw. Banerjee¹⁷⁴, A.A.E. Bannoura¹⁷⁶, V. Bansal¹⁷⁰, H.S. Bansil¹⁸, L. Barak¹⁷³, S.P. Baranov⁹⁶, E.L. Barberio⁸⁸, D. Barberis^{50a,50b}, M. Barbero⁸⁵, T. Barillari¹⁰¹, M. Barisonzi¹⁷⁶, T. Barklow¹⁴⁴, N. Barlow²⁸, S.L. Barnes⁸⁴, B.M. Barnett¹³¹, R.M. Barnett¹⁵, Z. Barnovska⁵, A. Baroncelli^{135a}, G. Barone⁴⁹, A.J. Barr¹²⁰, F. Barreiro⁸², J. Barreiro Guimarães da Costa⁵⁷, R. Bartoldus¹⁴⁴, A.E. Barton⁷², P. Bartos^{145a}, V. Bartsch¹⁵⁰, A. Bassalat¹¹⁷, A. Basye¹⁶⁶, R.L. Bates⁵³, S.J. Batista¹⁵⁹, J.R. Batley²⁸, M. Battaglia¹³⁸, M. Battistin³⁰, F. Bauer¹³⁷, H.S. Bawa^{144,f}, M.D. Beattie⁷², T. Beau⁸⁰, P.H. Beauchemin¹⁶², R. Beccherle^{124a,124b}, P. Bechtle²¹, H.P. Beck¹⁷, K. Becker¹⁷⁶, S. Becker¹⁰⁰, M. Beckingham¹⁷¹, C. Becot¹¹⁷, A.J. Beddall^{19c}, A. Beddall^{19c}, S. Bedikian¹⁷⁷, V.A. Bednyakov⁶⁵, C.P. Bee¹⁴⁹, L.J. Beemster¹⁰⁷, T.A. Beermann¹⁷⁶, M. Begel²⁵, K. Behr¹²⁰, C. Belanger-Champagne⁸⁷, P.J. Bell⁴⁹, W.H. Bell⁴⁹, G. Bella¹⁵⁴, L. Bellagamba^{20a}, A. Bellerive²⁹, M. Bellomo⁸⁶, K. Belotskiy⁹⁸, O. Beltramello³⁰, O. Benary¹⁵⁴, D. Bencheikoun^{136a}, K. Bendtz^{147a,147b}, N. Benekos¹⁶⁶, Y. Benhammou¹⁵⁴, E. Benhar Noccioli⁴⁹, J.A. Benitez Garcia^{160b}, D.P. Benjamin⁴⁵, J.R. Bensinger²³,

S. Bentvelsen¹⁰⁷, D. Berge¹⁰⁷, E. Bergeaas Kuutmann¹⁶⁷, N. Berger⁵, F. Berghaus¹⁷⁰,
 J. Beringer¹⁵, C. Bernard²², P. Bernat⁷⁸, C. Bernius⁷⁹, F.U. Bernlochner¹⁷⁰, T. Berry⁷⁷,
 P. Berta¹²⁹, C. Bertella⁸⁵, G. Bertoli^{147a,147b}, F. Bertolucci^{124a,124b}, C. Bertsche¹¹³,
 D. Bertsche¹¹³, M.I. Besana^{91a}, G.J. Besjes¹⁰⁶, O. Bessidskaia^{147a,147b}, M. Bessner⁴²,
 N. Besson¹³⁷, C. Betancourt⁴⁸, S. Bethke¹⁰¹, W. Bhimji⁴⁶, R.M. Bianchi¹²⁵,
 L. Bianchini²³, M. Bianco³⁰, O. Biebel¹⁰⁰, S.P. Bieniek⁷⁸, K. Bierwagen⁵⁴, J. Biesiada¹⁵,
 M. Biglietti^{135a}, J. Bilbao De Mendizabal⁴⁹, H. Bilokon⁴⁷, M. Bindi⁵⁴, S. Binet¹¹⁷,
 A. Bingul^{19c}, C. Bini^{133a,133b}, C.W. Black¹⁵¹, J.E. Black¹⁴⁴, K.M. Black²²,
 D. Blackburn¹³⁹, R.E. Blair⁶, J.-B. Blanchard¹³⁷, T. Blazek^{145a}, I. Bloch⁴², C. Blocker²³,
 W. Blum^{83,*}, U. Blumenschein⁵⁴, G.J. Bobbink¹⁰⁷, V.S. Bobrovnikov^{109,c},
 S.S. Bocchetta⁸¹, A. Bocci⁴⁵, C. Bock¹⁰⁰, C.R. Boddy¹²⁰, M. Boehler⁴⁸, T.T. Boek¹⁷⁶,
 J.A. Bogaerts³⁰, A.G. Bogdanchikov¹⁰⁹, A. Bogouch^{92,*}, C. Bohm^{147a}, J. Bohm¹²⁷,
 V. Boisvert⁷⁷, T. Bold^{38a}, V. Boldea^{26a}, A.S. Boldyrev⁹⁹, M. Bomben⁸⁰, M. Bona⁷⁶,
 M. Boonekamp¹³⁷, A. Borisov¹³⁰, G. Borissov⁷², M. Borri⁸⁴, S. Borroni⁴², J. Bortfeldt¹⁰⁰,
 V. Bortolotto^{60a}, K. Bos¹⁰⁷, D. Boscherini^{20a}, M. Bosman¹², H. Boterenbrood¹⁰⁷,
 J. Boudreau¹²⁵, J. Bouffard², E.V. Bouhova-Thacker⁷², D. Boumediene³⁴,
 C. Bourdarios¹¹⁷, N. Bousson¹¹⁴, S. Boutouil^{136d}, A. Boveia³¹, J. Boyd³⁰, I.R. Boyko⁶⁵,
 I. Bozic^{13a}, J. Bracinik¹⁸, A. Brandt⁸, G. Brandt¹⁵, O. Brandt^{58a}, U. Bratzler¹⁵⁷,
 B. Brau⁸⁶, J.E. Brau¹¹⁶, H.M. Braun^{176,*}, S.F. Brazzale^{165a,165c}, B. Brelier¹⁵⁹,
 K. Brendlinger¹²², A.J. Brennan⁸⁸, R. Brenner¹⁶⁷, S. Bressler¹⁷³, K. Bristow^{146c},
 T.M. Bristow⁴⁶, D. Britton⁵³, F.M. Brochu²⁸, I. Brock²¹, R. Brock⁹⁰, C. Bromberg⁹⁰,
 J. Bronner¹⁰¹, G. Brooijmans³⁵, T. Brooks⁷⁷, W.K. Brooks^{32b}, J. Brosamer¹⁵,
 E. Brost¹¹⁶, J. Brown⁵⁵, P.A. Bruckman de Renstrom³⁹, D. Bruncko^{145b}, R. Bruneliere⁴⁸,
 S. Brunet⁶¹, A. Bruni^{20a}, G. Bruni^{20a}, M. Bruschi^{20a}, L. Bryngemark⁸¹, T. Buanes¹⁴,
 Q. Buat¹⁴³, F. Bucci⁴⁹, P. Buchholz¹⁴², R.M. Buckingham¹²⁰, A.G. Buckley⁵³,
 S.I. Buda^{26a}, I.A. Budagov⁶⁵, F. Buehrer⁴⁸, L. Bugge¹¹⁹, M.K. Bugge¹¹⁹, O. Bulekov⁹⁸,
 A.C. Bundock⁷⁴, H. Burckhart³⁰, S. Burdin⁷⁴, B. Burghgrave¹⁰⁸, S. Burke¹³¹,
 I. Burmeister⁴³, E. Busato³⁴, D. Büscher⁴⁸, V. Büscher⁸³, P. Bussey⁵³, C.P. Buszello¹⁶⁷,
 B. Butler⁵⁷, J.M. Butler²², A.I. Butt³, C.M. Buttar⁵³, J.M. Butterworth⁷⁸, P. Butti¹⁰⁷,
 W. Buttlinger²⁸, A. Buzatu⁵³, M. Byszewski¹⁰, S. Cabrera Urbán¹⁶⁸, D. Caforio^{20a,20b},
 O. Cakir^{4a}, P. Calafiura¹⁵, A. Calandri¹³⁷, G. Calderini⁸⁰, P. Calfayan¹⁰⁰, R. Calkins¹⁰⁸,
 L.P. Caloba^{24a}, D. Calvet³⁴, S. Calvet³⁴, R. Camacho Toro⁴⁹, S. Camarda⁴²,
 D. Cameron¹¹⁹, L.M. Caminada¹⁵, R. Caminal Armadans¹², S. Campana³⁰,
 M. Campanelli⁷⁸, A. Campoverde¹⁴⁹, V. Canale^{104a,104b}, A. Canepa^{160a}, M. Cano Bret⁷⁶,
 J. Cantero⁸², R. Cantrill^{126a}, T. Cao⁴⁰, M.D.M. Capeans Garrido³⁰, I. Caprini^{26a},
 M. Caprini^{26a}, M. Capua^{37a,37b}, R. Caputo⁸³, R. Cardarelli^{134a}, T. Carli³⁰, G. Carlino^{104a},
 L. Carminati^{91a,91b}, S. Caron¹⁰⁶, E. Carquin^{32a}, G.D. Carrillo-Montoya^{146c}, J.R. Carter²⁸,
 J. Carvalho^{126a,126c}, D. Casadei⁷⁸, M.P. Casado¹², M. Casolino¹²,
 E. Castaneda-Miranda^{146b}, A. Castelli¹⁰⁷, V. Castillo Gimenez¹⁶⁸, N.F. Castro^{126a},
 P. Catastini⁵⁷, A. Catinaccio³⁰, J.R. Catmore¹¹⁹, A. Cattai³⁰, G. Cattani^{134a,134b},
 J. Caudron⁸³, V. Cavaliere¹⁶⁶, D. Cavalli^{91a}, M. Cavalli-Sforza¹², V. Cavasinni^{124a,124b},
 F. Ceradini^{135a,135b}, B.C. Cerio⁴⁵, K. Cerny¹²⁹, A.S. Cerqueira^{24b}, A. Cerri¹⁵⁰,
 L. Cerrito⁷⁶, F. Cerutti¹⁵, M. Cerv³⁰, A. Cervelli¹⁷, S.A. Cetin^{19b}, A. Chafaq^{136a},

D. Chakraborty¹⁰⁸, I. Chalupkova¹²⁹, P. Chang¹⁶⁶, B. Chapleau⁸⁷, J.D. Chapman²⁸,
 D. Charfeddine¹¹⁷, D.G. Charlton¹⁸, C.C. Chau¹⁵⁹, C.A. Chavez Barajas¹⁵⁰,
 S. Cheatham⁸⁷, A. Chegwidden⁹⁰, S. Chekanov⁶, S.V. Chekulaev^{160a}, G.A. Chelkov^{65,g},
 M.A. Chelstowska⁸⁹, C. Chen⁶⁴, H. Chen²⁵, K. Chen¹⁴⁹, L. Chen^{33d,h}, S. Chen^{33c},
 X. Chen^{33f}, Y. Chen⁶⁷, Y. Chen³⁵, H.C. Cheng⁸⁹, Y. Cheng³¹, A. Cheplakov⁶⁵,
 R. Cherkaoui El Moursli^{136e}, V. Chernyatin^{25,*}, E. Cheu⁷, L. Chevalier¹³⁷, V. Chiarella⁴⁷,
 G. Chiefari^{104a,104b}, J.T. Childers⁶, A. Chilingarov⁷², G. Chiodini^{73a}, A.S. Chisholm¹⁸,
 R.T. Chislett⁷⁸, A. Chitan^{26a}, M.V. Chizhov⁶⁵, S. Chouridou⁹, B.K.B. Chow¹⁰⁰,
 D. Chromek-Burckhart³⁰, M.L. Chu¹⁵², J. Chudoba¹²⁷, J.J. Chwastowski³⁹, L. Chytka¹¹⁵,
 G. Ciapetti^{133a,133b}, A.K. Ciftci^{4a}, R. Ciftci^{4a}, D. Cinca⁵³, V. Cindro⁷⁵, A. Ciocio¹⁵,
 Z.H. Citron¹⁷³, M. Citterio^{91a}, M. Ciubancan^{26a}, A. Clark⁴⁹, P.J. Clark⁴⁶, R.N. Clarke¹⁵,
 W. Cleland¹²⁵, J.C. Clemens⁸⁵, C. Clement^{147a,147b}, Y. Coadou⁸⁵, M. Cobal^{165a,165c},
 A. Coccaro¹³⁹, J. Cochran⁶⁴, L. Coffey²³, J.G. Cogan¹⁴⁴, B. Cole³⁵, S. Cole¹⁰⁸,
 A.P. Colijn¹⁰⁷, J. Collot⁵⁵, T. Colombo^{58c}, G. Compostella¹⁰¹, P. Conde Muiño^{126a,126b},
 E. Coniavitis⁴⁸, S.H. Connell^{146b}, I.A. Connolly⁷⁷, S.M. Consonni^{91a,91b}, V. Consorti⁴⁸,
 S. Constantinescu^{26a}, C. Conta^{121a,121b}, G. Conti⁵⁷, F. Conventi^{104a,i}, M. Cooke¹⁵,
 B.D. Cooper⁷⁸, A.M. Cooper-Sarkar¹²⁰, N.J. Cooper-Smith⁷⁷, K. Copic¹⁵,
 T. Cornelissen¹⁷⁶, M. Corradi^{20a}, F. Corriveau^{87,j}, A. Corso-Radu¹⁶⁴,
 A. Cortes-Gonzalez¹², G. Cortiana¹⁰¹, G. Costa^{91a}, M.J. Costa¹⁶⁸, D. Costanzo¹⁴⁰,
 D. Côté⁸, G. Cottin²⁸, G. Cowan⁷⁷, B.E. Cox⁸⁴, K. Cranmer¹¹⁰, G. Cree²⁹,
 S. Crépé-Renaudin⁵⁵, F. Crescioli⁸⁰, W.A. Cribbs^{147a,147b}, M. Crispin Ortuzar¹²⁰,
 M. Cristinziani²¹, V. Croft¹⁰⁶, G. Crosetti^{37a,37b}, C.-M. Cuciuc^{26a},
 T. Cuhadar Donszelmann¹⁴⁰, J. Cummings¹⁷⁷, M. Curatolo⁴⁷, C. Cuthbert¹⁵¹,
 H. Czirr¹⁴², P. Czodrowski³, S. D'Auria⁵³, M. D'Onofrio⁷⁴,
 M.J. Da Cunha Sargedas De Sousa^{126a,126b}, C. Da Via⁸⁴, W. Dabrowski^{38a},
 A. Dafinca¹²⁰, T. Dai⁸⁹, O. Dale¹⁴, F. Dallaire⁹⁵, C. Dallapiccola⁸⁶, M. Dam³⁶,
 A.C. Daniells¹⁸, M. Dano Hoffmann¹³⁷, V. Dao⁴⁸, G. Darbo^{50a}, S. Darmora⁸,
 J. Dassoulas⁴², A. Dattagupta⁶¹, W. Davey²¹, C. David¹⁷⁰, T. Davidek¹²⁹, E. Davies^{120,d},
 M. Davies¹⁵⁴, O. Davignon⁸⁰, A.R. Davison⁷⁸, P. Davison⁷⁸, Y. Davygora^{58a}, E. Dawe¹⁴³,
 I. Dawson¹⁴⁰, R.K. Daya-Ishmukhametova⁸⁶, K. De⁸, R. de Asmundis^{104a},
 S. De Castro^{20a,20b}, S. De Cecco⁸⁰, N. De Groot¹⁰⁶, P. de Jong¹⁰⁷, H. De la Torre⁸²,
 F. De Lorenzi⁶⁴, L. De Nooij¹⁰⁷, D. De Pedis^{133a}, A. De Salvo^{133a}, U. De Sanctis¹⁵⁰,
 A. De Santo¹⁵⁰, J.B. De Vivie De Regie¹¹⁷, W.J. Dearnaley⁷², R. Debbe²⁵,
 C. Debenedetti¹³⁸, B. Dechenaux⁵⁵, D.V. Dedovich⁶⁵, I. Deigaard¹⁰⁷, J. Del Peso⁸²,
 T. Del Prete^{124a,124b}, F. Deliot¹³⁷, C.M. Delitzsch⁴⁹, M. Deliyergiyev⁷⁵, A. Dell'Acqua³⁰,
 L. Dell'Asta²², M. Dell'Orso^{124a,124b}, M. Della Pietra^{104a,i}, D. della Volpe⁴⁹,
 M. Delmastro⁵, P.A. Delsart⁵⁵, C. Deluca¹⁰⁷, D.A. DeMarco¹⁵⁹, S. Demers¹⁷⁷,
 M. Demichev⁶⁵, A. Demilly⁸⁰, S.P. Denisov¹³⁰, D. Derendarz³⁹, J.E. Derkaoui^{136d},
 F. Derue⁸⁰, P. Dervan⁷⁴, K. Desch²¹, C. Deterre⁴², P.O. Deviveiros¹⁰⁷, A. Dewhurst¹³¹,
 S. Dhaliwal¹⁰⁷, A. Di Ciaccio^{134a,134b}, L. Di Ciaccio⁵, A. Di Domenico^{133a,133b},
 C. Di Donato^{104a,104b}, A. Di Girolamo³⁰, B. Di Girolamo³⁰, A. Di Mattia¹⁵³,
 B. Di Micco^{135a,135b}, R. Di Nardo⁴⁷, A. Di Simone⁴⁸, R. Di Sipio^{20a,20b}, D. Di Valentino²⁹,
 F.A. Dias⁴⁶, M.A. Diaz^{32a}, E.B. Diehl⁸⁹, J. Dietrich⁴², T.A. Dietzsch^{58a}, S. Diglio⁸⁵,

A. Dimitrievska^{13a}, J. Dingfelder²¹, P. Dita^{26a}, S. Dita^{26a}, F. Dittus³⁰, F. Djama⁸⁵,
 T. Djobava^{51b}, J.I. Djuvsland^{58a}, M.A.B. do Vale^{24c}, A. Do Valle Wemans^{126a,126g},
 D. Dobos³⁰, C. Doglioni⁴⁹, T. Doherty⁵³, T. Dohmae¹⁵⁶, J. Dolejsi¹²⁹, Z. Dolezal¹²⁹,
 B.A. Dolgoshein^{98,*}, M. Donadelli^{24d}, S. Donati^{124a,124b}, P. Dondero^{121a,121b}, J. Donini³⁴,
 J. Dopke¹³¹, A. Doria^{104a}, M.T. Dova⁷¹, A.T. Doyle⁵³, M. Dris¹⁰, J. Dubbert⁸⁹,
 S. Dube¹⁵, E. Dubreuil³⁴, E. Duchovni¹⁷³, G. Duckeck¹⁰⁰, O.A. Ducu^{26a}, D. Duda¹⁷⁶,
 A. Dudarev³⁰, F. Dudziak⁶⁴, L. Duflot¹¹⁷, L. Duguid⁷⁷, M. Dührssen³⁰, M. Dunford^{58a},
 H. Duran Yildiz^{4a}, M. Düren⁵², A. Durglishvili^{51b}, M. Dwuznik^{38a}, M. Dyndal^{38a},
 J. Ebke¹⁰⁰, W. Edson², N.C. Edwards⁴⁶, W. Ehrenfeld²¹, T. Eifert¹⁴⁴, G. Eigen¹⁴,
 K. Einsweiler¹⁵, T. Ekelof¹⁶⁷, M. El Kacimi^{136c}, M. Ellert¹⁶⁷, S. Elles⁵, F. Ellinghaus⁸³,
 N. Ellis³⁰, J. Elmsheuser¹⁰⁰, M. Elsing³⁰, D. Emeliyanov¹³¹, Y. Enari¹⁵⁶, O.C. Endner⁸³,
 M. Endo¹¹⁸, R. Engelmann¹⁴⁹, J. Erdmann¹⁷⁷, A. Ereditato¹⁷, D. Eriksson^{147a},
 G. Ernis¹⁷⁶, J. Ernst², M. Ernst²⁵, J. Ernwein¹³⁷, D. Errede¹⁶⁶, S. Errede¹⁶⁶, E. Ertel⁸³,
 M. Escalier¹¹⁷, H. Esch⁴³, C. Escobar¹²⁵, B. Esposito⁴⁷, A.I. Etienvre¹³⁷, E. Etzion¹⁵⁴,
 H. Evans⁶¹, A. Ezhilov¹²³, L. Fabbri^{20a,20b}, G. Facini³¹, R.M. Fakhrutdinov¹³⁰,
 S. Falciano^{133a}, R.J. Falla⁷⁸, J. Faltova¹²⁹, Y. Fang^{33a}, M. Fanti^{91a,91b}, A. Farbin⁸,
 A. Farilla^{135a}, T. Farooque¹², S. Farrell¹⁵, S.M. Farrington¹⁷¹, P. Farthouat³⁰,
 F. Fassi^{136e}, P. Fassnacht³⁰, D. Fassouliotis⁹, A. Favareto^{50a,50b}, L. Fayard¹¹⁷,
 P. Federic^{145a}, O.L. Fedin^{123,k}, W. Fedorko¹⁶⁹, M. Fehling-Kaschek⁴⁸, S. Feigl³⁰,
 L. Feligioni⁸⁵, C. Feng^{33d}, E.J. Feng⁶, H. Feng⁸⁹, A.B. Fenyuk¹³⁰, S. Fernandez Perez³⁰,
 S. Ferrag⁵³, J. Ferrando⁵³, A. Ferrari¹⁶⁷, P. Ferrari¹⁰⁷, R. Ferrari^{121a},
 D.E. Ferreira de Lima⁵³, A. Ferrer¹⁶⁸, D. Ferrere⁴⁹, C. Ferretti⁸⁹,
 A. Ferretto Parodi^{50a,50b}, M. Fiascaris³¹, F. Fiedler⁸³, A. Filipčič⁷⁵, M. Filipuzzi⁴²,
 F. Filthaut¹⁰⁶, M. Fincke-Keeler¹⁷⁰, K.D. Finelli¹⁵¹, M.C.N. Fiolhais^{126a,126c},
 L. Fiorini¹⁶⁸, A. Firan⁴⁰, A. Fischer², J. Fischer¹⁷⁶, W.C. Fisher⁹⁰, E.A. Fitzgerald²³,
 M. Flechl⁴⁸, I. Fleck¹⁴², P. Fleischmann⁸⁹, S. Fleischmann¹⁷⁶, G.T. Fletcher¹⁴⁰,
 G. Fletcher⁷⁶, T. Flick¹⁷⁶, A. Floderus⁸¹, L.R. Flores Castillo^{60a}, A.C. Florez Bustos^{160b},
 M.J. Flowerdew¹⁰¹, A. Formica¹³⁷, A. Forti⁸⁴, D. Fortin^{160a}, D. Fournier¹¹⁷, H. Fox⁷²,
 S. Fracchia¹², P. Francavilla⁸⁰, M. Franchini^{20a,20b}, S. Franchino³⁰, D. Francis³⁰,
 L. Franconi¹¹⁹, M. Franklin⁵⁷, S. Franz⁶², M. Fraternali^{121a,121b}, S.T. French²⁸,
 C. Friedrich⁴², F. Friedrich⁴⁴, D. Froidevaux³⁰, J.A. Frost²⁸, C. Fukunaga¹⁵⁷,
 E. Fullana Torregrosa⁸³, B.G. Fulsom¹⁴⁴, J. Fuster¹⁶⁸, C. Gabaldon⁵⁵, O. Gabizon¹⁷⁶,
 A. Gabrielli^{20a,20b}, A. Gabrielli^{133a,133b}, S. Gadatsch¹⁰⁷, S. Gadomski⁴⁹,
 G. Gagliardi^{50a,50b}, P. Gagnon⁶¹, C. Galea¹⁰⁶, B. Galhardo^{126a,126c}, E.J. Gallas¹²⁰,
 V. Gallo¹⁷, B.J. Gallop¹³¹, P. Gallus¹²⁸, G. Galster³⁶, K.K. Gan¹¹¹, J. Gao^{33b,h},
 Y.S. Gao^{144,f}, F.M. Garay Walls⁴⁶, F. Garberson¹⁷⁷, C. García¹⁶⁸,
 J.E. García Navarro¹⁶⁸, M. Garcia-Sciveres¹⁵, R.W. Gardner³¹, N. Garelli¹⁴⁴,
 V. Garonne³⁰, C. Gatti⁴⁷, G. Gaudio^{121a}, B. Gaur¹⁴², L. Gauthier⁹⁵, P. Gauzzi^{133a,133b},
 I.L. Gavrilenko⁹⁶, C. Gay¹⁶⁹, G. Gaycken²¹, E.N. Gazis¹⁰, P. Ge^{33d}, Z. Gecse¹⁶⁹,
 C.N.P. Gee¹³¹, D.A.A. Geerts¹⁰⁷, Ch. Geich-Gimbel²¹, K. Gellerstedt^{147a,147b},
 C. Gemme^{50a}, A. Gemmell⁵³, M.H. Genest⁵⁵, S. Gentile^{133a,133b}, M. George⁵⁴,
 S. George⁷⁷, D. Gerbaudo¹⁶⁴, A. Gershon¹⁵⁴, H. Ghazlane^{136b}, N. Ghodbane³⁴,
 B. Giacobbe^{20a}, S. Giagu^{133a,133b}, V. Giangioffe¹², P. Giannetti^{124a,124b}, F. Gianotti³⁰,

B. Gibbard²⁵, S.M. Gibson⁷⁷, M. Gilchriese¹⁵, T.P.S. Gillam²⁸, D. Gillberg³⁰, G. Gilles³⁴,
 D.M. Gingrich^{3,e}, N. Giokaris⁹, M.P. Giordani^{165a,165c}, R. Giordano^{104a,104b},
 F.M. Giorgi^{20a}, F.M. Giorgi¹⁶, P.F. Giraud¹³⁷, D. Giugni^{91a}, C. Giuliani⁴⁸, M. Giulini^{58b},
 B.K. Gjelsten¹¹⁹, S. Gkaitatzis¹⁵⁵, I. Gkialas^{155,l}, E.L. Gkougkousis¹¹⁷, L.K. Gladilin⁹⁹,
 C. Glasman⁸², J. Glatzer³⁰, P.C.F. Glaysher⁴⁶, A. Glazov⁴², G.L. Glonti⁶⁵,
 M. Goblirsch-Kolb¹⁰¹, J.R. Goddard⁷⁶, J. Godlewski³⁰, C. Goeringer⁸³, S. Goldfarb⁸⁹,
 T. Golling¹⁷⁷, D. Golubkov¹³⁰, A. Gomes^{126a,126b,126d}, L.S. Gomez Fajardo⁴²,
 R. Gonçalo^{126a}, J. Goncalves Pinto Firmino Da Costa¹³⁷, L. Gonella²¹,
 S. González de la Hoz¹⁶⁸, G. Gonzalez Parra¹², S. Gonzalez-Sevilla⁴⁹, L. Goossens³⁰,
 P.A. Gorbounov⁹⁷, H.A. Gordon²⁵, I. Gorelov¹⁰⁵, B. Gorini³⁰, E. Gorini^{73a,73b},
 A. Gorišek⁷⁵, E. Gornicki³⁹, A.T. Goshaw⁶, C. Gössling⁴³, M.I. Gostkin⁶⁵,
 M. Gouighri^{136a}, D. Goujdami^{136c}, M.P. Goulette⁴⁹, A.G. Goussiou¹³⁹, C. Goy⁵,
 H.M.X. Grabas¹³⁸, L. Graber⁵⁴, I. Grabowska-Bold^{38a}, P. Grafström^{20a,20b}, K-J. Grahn⁴²,
 J. Gramling⁴⁹, E. Gramstad¹¹⁹, S. Grancagnolo¹⁶, V. Grassi¹⁴⁹, V. Gratchev¹²³,
 H.M. Gray³⁰, E. Graziani^{135a}, O.G. Grebenyuk¹²³, Z.D. Greenwood^{79,m}, K. Gregersen⁷⁸,
 I.M. Gregor⁴², P. Grenier¹⁴⁴, J. Griffiths⁸, A.A. Grillo¹³⁸, K. Grimm⁷², S. Grinstein^{12,n},
 Ph. Gris³⁴, Y.V. Grishkevich⁹⁹, J.-F. Grivaz¹¹⁷, J.P. Grohs⁴⁴, A. Grohsjean⁴²,
 E. Gross¹⁷³, J. Grosse-Knetter⁵⁴, G.C. Grossi^{134a,134b}, J. Groth-Jensen¹⁷³, Z.J. Grout¹⁵⁰,
 L. Guan^{33b}, J. Guenther¹²⁸, F. Guescini⁴⁹, D. Guest¹⁷⁷, O. Gueta¹⁵⁴, C. Guicheney³⁴,
 E. Guido^{50a,50b}, T. Guillemin¹¹⁷, S. Guindon², U. Gul⁵³, C. Gumpert⁴⁴, J. Guo³⁵,
 S. Gupta¹²⁰, P. Gutierrez¹¹³, N.G. Gutierrez Ortiz⁵³, C. Gutschow⁷⁸, N. Guttman¹⁵⁴,
 C. Guyot¹³⁷, C. Gwenlan¹²⁰, C.B. Gwilliam⁷⁴, A. Haas¹¹⁰, C. Haber¹⁵, H.K. Hadavand⁸,
 N. Haddad^{136e}, P. Haefner²¹, S. Hageböck²¹, Z. Hajduk³⁹, H. Hakobyan¹⁷⁸, M. Haleem⁴²,
 D. Hall¹²⁰, G. Halladjian⁹⁰, K. Hamacher¹⁷⁶, P. Hamal¹¹⁵, K. Hamano¹⁷⁰, M. Hamer⁵⁴,
 A. Hamilton^{146a}, S. Hamilton¹⁶², G.N. Hamity^{146c}, P.G. Hamnett⁴², L. Han^{33b},
 K. Hanagaki¹¹⁸, K. Hanawa¹⁵⁶, M. Hance¹⁵, P. Hanke^{58a}, R. Hanna¹³⁷, J.B. Hansen³⁶,
 J.D. Hansen³⁶, P.H. Hansen³⁶, K. Hara¹⁶¹, A.S. Hard¹⁷⁴, T. Harenberg¹⁷⁶, F. Hariri¹¹⁷,
 S. Harkusha⁹², D. Harper⁸⁹, R.D. Harrington⁴⁶, O.M. Harris¹³⁹, P.F. Harrison¹⁷¹,
 F. Hartjes¹⁰⁷, M. Hasegawa⁶⁷, S. Hasegawa¹⁰³, Y. Hasegawa¹⁴¹, A. Hasib¹¹³,
 S. Hassani¹³⁷, S. Haug¹⁷, M. Hauschild³⁰, R. Hauser⁹⁰, L. Hauswald⁴⁴, M. Havranek¹²⁷,
 C.M. Hawkes¹⁸, R.J. Hawkings³⁰, A.D. Hawkins⁸¹, T. Hayashi¹⁶¹, D. Hayden⁹⁰,
 C.P. Hays¹²⁰, H.S. Hayward⁷⁴, S.J. Haywood¹³¹, S.J. Head¹⁸, T. Heck⁸³, V. Hedberg⁸¹,
 L. Heelan⁸, S. Heim¹²², T. Heim¹⁷⁶, B. Heinemann¹⁵, L. Heinrich¹¹⁰, J. Hejbal¹²⁷,
 L. Helary²², C. Heller¹⁰⁰, M. Heller³⁰, S. Hellman^{147a,147b}, D. Hellmich²¹, C. Helsens³⁰,
 J. Henderson¹²⁰, R.C.W. Henderson⁷², Y. Heng¹⁷⁴, C. Hengler⁴², A. Henrichs¹⁷⁷,
 A.M. Henriques Correia³⁰, S. Henrot-Versille¹¹⁷, G.H. Herbert¹⁶,
 Y. Hernández Jiménez¹⁶⁸, R. Herrberg-Schubert¹⁶, G. Herten⁴⁸, R. Hertenberger¹⁰⁰,
 L. Hervas³⁰, G.G. Hesketh⁷⁸, N.P. Hessey¹⁰⁷, R. Hickling⁷⁶, E. Higón-Rodriguez¹⁶⁸,
 E. Hill¹⁷⁰, J.C. Hill²⁸, K.H. Hiller⁴², S. Hillert²¹, S.J. Hillier¹⁸, I. Hinchliffe¹⁵, E. Hines¹²²,
 M. Hirose¹⁵⁸, D. Hirschbuehl¹⁷⁶, J. Hobbs¹⁴⁹, N. Hod¹⁰⁷, M.C. Hodgkinson¹⁴⁰,
 P. Hodgson¹⁴⁰, A. Hoecker³⁰, M.R. Hoeferkamp¹⁰⁵, F. Hoenig¹⁰⁰, J. Hoffman⁴⁰,
 D. Hoffmann⁸⁵, M. Hohlfeld⁸³, T.R. Holmes¹⁵, T.M. Hong¹²²,
 L. Hooft van Huysduynen¹¹⁰, W.H. Hopkins¹¹⁶, Y. Horii¹⁰³, J-Y. Hostachy⁵⁵, S. Hou¹⁵²,

A. Hoummada^{136a}, J. Howard¹²⁰, J. Howarth⁴², M. Hrabovsky¹¹⁵, I. Hristova¹⁶,
 J. Hrvnac¹¹⁷, T. Hryna'ova⁵, C. Hsu^{146c}, P.J. Hsu⁸³, S.-C. Hsu¹³⁹, D. Hu³⁵, X. Hu⁸⁹,
 Y. Huang⁴², Z. Hubacek³⁰, F. Hubaut⁸⁵, F. Huegging²¹, T.B. Huffman¹²⁰,
 E.W. Hughes³⁵, G. Hughes⁷², M. Huhtinen³⁰, T.A. Hülsing⁸³, M. Hurwitz¹⁵,
 N. Huseynov^{65,b}, J. Huston⁹⁰, J. Huth⁵⁷, G. Iacobucci⁴⁹, G. Iakovidis¹⁰, I. Ibragimov¹⁴²,
 L. Iconomidou-Fayard¹¹⁷, E. Ideal¹⁷⁷, Z. Idrissi^{136e}, P. Iengo^{104a}, O. Igonkina¹⁰⁷,
 T. Iizawa¹⁷², Y. Ikegami⁶⁶, K. Ikematsu¹⁴², M. Ikeno⁶⁶, Y. Ilchenko^{31,o}, D. Iliadis¹⁵⁵,
 N. Ilic¹⁵⁹, Y. Inamaru⁶⁷, T. Ince¹⁰¹, P. Ioannou⁹, M. Iodice^{135a}, K. Iordanidou⁹,
 V. Ippolito⁵⁷, A. Irles Quiles¹⁶⁸, C. Isaksson¹⁶⁷, M. Ishino⁶⁸, M. Ishitsuka¹⁵⁸,
 R. Ishmukhametov¹¹¹, C. Issever¹²⁰, S. Isti^{19a}, J.M. Iturbe Ponce⁸⁴, R. Iuppa^{134a,134b},
 J. Ivarsson⁸¹, W. Iwanski³⁹, H. Iwasaki⁶⁶, J.M. Izen⁴¹, V. Izzo^{104a}, B. Jackson¹²²,
 M. Jackson⁷⁴, P. Jackson¹, M.R. Jaekel³⁰, V. Jain², K. Jakobs⁴⁸, S. Jakobsen³⁰,
 T. Jakoubek¹²⁷, J. Jakubek¹²⁸, D.O. Jamin¹⁵², D.K. Jana⁷⁹, E. Jansen⁷⁸, H. Jansen³⁰,
 J. Janssen²¹, M. Janus¹⁷¹, G. Jarlskog⁸¹, N. Javadov^{65,b}, T. Javurek⁴⁸, L. Jeanty¹⁵,
 J. Jejelava^{51a,p}, G.-Y. Jeng¹⁵¹, D. Jennens⁸⁸, P. Jenni^{48,q}, J. Jentzsch⁴³, C. Jeske¹⁷¹,
 S. Jézéquel⁵, H. Ji¹⁷⁴, J. Jia¹⁴⁹, Y. Jiang^{33b}, M. Jimenez Belenguer⁴², S. Jin^{33a},
 A. Jinaru^{26a}, O. Jinnouchi¹⁵⁸, M.D. Joergensen³⁶, K.E. Johansson^{147a,147b},
 P. Johansson¹⁴⁰, K.A. Johns⁷, K. Jon-And^{147a,147b}, G. Jones¹⁷¹, R.W.L. Jones⁷²,
 T.J. Jones⁷⁴, J. Jongmanns^{58a}, P.M. Jorge^{126a,126b}, K.D. Joshi⁸⁴, J. Jovicevic¹⁴⁸,
 X. Ju¹⁷⁴, C.A. Jung⁴³, R.M. Jungst³⁰, P. Jussel⁶², A. Juste Rozas^{12,n}, M. Kaci¹⁶⁸,
 A. Kaczmarska³⁹, M. Kado¹¹⁷, H. Kagan¹¹¹, M. Kagan¹⁴⁴, E. Kajomovitz⁴⁵,
 C.W. Kalderon¹²⁰, S. Kama⁴⁰, A. Kamenshchikov¹³⁰, N. Kanaya¹⁵⁶, M. Kaneda³⁰,
 S. Kaneti²⁸, V.A. Kantserov⁹⁸, J. Kanzaki⁶⁶, B. Kaplan¹¹⁰, A. Kapliy³¹, D. Kar⁵³,
 K. Karakostas¹⁰, N. Karastathis¹⁰, M.J. Kareem⁵⁴, M. Karnevskiy⁸³, S.N. Karpov⁶⁵,
 Z.M. Karpova⁶⁵, K. Karthik¹¹⁰, V. Kartvelishvili⁷², A.N. Karyukhin¹³⁰, L. Kashif¹⁷⁴,
 G. Kasieczka^{58b}, R.D. Kass¹¹¹, A. Kastanas¹⁴, Y. Kataoka¹⁵⁶, A. Katre⁴⁹, J. Katzy⁴²,
 V. Kaushik⁷, K. Kawagoe⁷⁰, T. Kawamoto¹⁵⁶, G. Kawamura⁵⁴, S. Kazama¹⁵⁶,
 V.F. Kazanin¹⁰⁹, M.Y. Kazarinov⁶⁵, R. Keeler¹⁷⁰, R. Kehoe⁴⁰, M. Keil⁵⁴, J.S. Keller⁴²,
 J.J. Kempster⁷⁷, H. Keoshkerian⁵, O. Kepka¹²⁷, B.P. Kerševan⁷⁵, S. Kersten¹⁷⁶,
 K. Kessoku¹⁵⁶, J. Keung¹⁵⁹, F. Khalil-zada¹¹, H. Khandanyan^{147a,147b}, A. Khanov¹¹⁴,
 A. Khodinov⁹⁸, A. Khomich^{58a}, T.J. Khoo²⁸, G. Khoriauli²¹, A. Khoroshilov¹⁷⁶,
 V. Khovanskiy⁹⁷, E. Khramov⁶⁵, J. Khubua^{51b}, H.Y. Kim⁸, H. Kim^{147a,147b}, S.H. Kim¹⁶¹,
 N. Kimura¹⁷², O. Kind¹⁶, B.T. King⁷⁴, M. King¹⁶⁸, R.S.B. King¹²⁰, S.B. King¹⁶⁹,
 J. Kirk¹³¹, A.E. Kiryunin¹⁰¹, T. Kishimoto⁶⁷, D. Kisielewska^{38a}, F. Kiss⁴⁸, K. Kiuchi¹⁶¹,
 E. Kladiva^{145b}, M. Klein⁷⁴, U. Klein⁷⁴, K. Kleinknecht⁸³, P. Klimek^{147a,147b},
 A. Klimentov²⁵, R. Klingenberg⁴³, J.A. Klinger⁸⁴, T. Klioutchnikova³⁰, P.F. Klok¹⁰⁶,
 E.-E. Kluge^{58a}, P. Kluit¹⁰⁷, S. Kluth¹⁰¹, E. Knerner⁶², E.B.F.G. Knoops⁸⁵, A. Knue⁵³,
 D. Kobayashi¹⁵⁸, T. Kobayashi¹⁵⁶, M. Kobel⁴⁴, M. Kocian¹⁴⁴, P. Kodys¹²⁹, T. Koffas²⁹,
 E. Koffeman¹⁰⁷, L.A. Kogan¹²⁰, S. Kohlmann¹⁷⁶, Z. Kohout¹²⁸, T. Kohriki⁶⁶, T. Koi¹⁴⁴,
 H. Kolanoski¹⁶, I. Koletsou⁵, J. Koll⁹⁰, A.A. Komar^{96,*}, Y. Komori¹⁵⁶, T. Kondo⁶⁶,
 N. Kondrashova⁴², K. Köneke⁴⁸, A.C. König¹⁰⁶, S. König⁸³, T. Kono^{66,r},
 R. Konoplich^{110,s}, N. Konstantinidis⁷⁸, R. Kopeliansky¹⁵³, S. Koperny^{38a}, L. Köpke⁸³,
 A.K. Kopp⁴⁸, K. Korcyl³⁹, K. Kordas¹⁵⁵, A. Korn⁷⁸, A.A. Korol^{109,c}, I. Korolkov¹²,

E.V. Korolkova¹⁴⁰, V.A. Korotkov¹³⁰, O. Kortner¹⁰¹, S. Kortner¹⁰¹, V.V. Kostyukhin²¹,
 V.M. Kotov⁶⁵, A. Kotwal⁴⁵, C. Kourkoumelis⁹, V. Kouskoura¹⁵⁵, A. Koutsman^{160a},
 R. Kowalewski¹⁷⁰, T.Z. Kowalski^{38a}, W. Kozanecki¹³⁷, A.S. Kozhin¹³⁰,
 V.A. Kramarenko⁹⁹, G. Kramberger⁷⁵, D. Krasnopevtsev⁹⁸, M.W. Krasny⁸⁰,
 A. Krasznahorkay³⁰, J.K. Kraus²¹, A. Kravchenko²⁵, S. Kreiss¹¹⁰, M. Kretz^{58c},
 J. Kretzschmar⁷⁴, K. Kreutzfeldt⁵², P. Krieger¹⁵⁹, K. Kroeninger⁵⁴, H. Kroha¹⁰¹,
 J. Kroll¹²², J. Kroseberg²¹, J. Krstic^{13a}, U. Kruchonak⁶⁵, H. Krüger²¹, T. Kruker¹⁷,
 N. Krumnack⁶⁴, Z.V. Krumshteyn⁶⁵, A. Kruse¹⁷⁴, M.C. Kruse⁴⁵, M. Kruskal²²,
 T. Kubota⁸⁸, H. Kucuk⁷⁸, S. Kuday^{4c}, S. Kuehn⁴⁸, A. Kugel^{58c}, A. Kuhl¹³⁸, T. Kuhl⁴²,
 V. Kukhtin⁶⁵, Y. Kulchitsky⁹², S. Kuleshov^{32b}, M. Kuna^{133a,133b}, J. Kunkle¹²²,
 A. Kupco¹²⁷, H. Kurashige⁶⁷, Y.A. Kurochkin⁹², R. Kurumida⁶⁷, V. Kus¹²⁷,
 E.S. Kuwertz¹⁴⁸, M. Kuze¹⁵⁸, J. Kvita¹¹⁵, A. La Rosa⁴⁹, L. La Rotonda^{37a,37b},
 C. Lacasta¹⁶⁸, F. Lacava^{133a,133b}, J. Lacey²⁹, H. Lacker¹⁶, D. Lacour⁸⁰, V.R. Lacuesta¹⁶⁸,
 E. Ladygin⁶⁵, R. Lafaye⁵, B. Laforge⁸⁰, T. Lagouri¹⁷⁷, S. Lai⁴⁸, H. Laier^{58a},
 L. Lambourne⁷⁸, S. Lammers⁶¹, C.L. Lampen⁷, W. Lampl⁷, E. Lançon¹³⁷, U. Landgraf⁴⁸,
 M.P.J. Landon⁷⁶, V.S. Lang^{58a}, A.J. Lankford¹⁶⁴, F. Lanni²⁵, K. Lantzsch³⁰,
 S. Laplace⁸⁰, C. Lapoire²¹, J.F. Laporte¹³⁷, T. Lari^{91a}, F. Lasagni Manghi^{20a,20b},
 M. Lassnig³⁰, P. Laurelli⁴⁷, W. Lavrijsen¹⁵, A.T. Law¹³⁸, P. Laycock⁷⁴, O. Le Dortz⁸⁰,
 E. Le Guirriec⁸⁵, E. Le Menedeu¹², T. LeCompte⁶, F. Ledroit-Guillon⁵⁵, C.A. Lee^{146b},
 H. Lee¹⁰⁷, J.S.H. Lee¹¹⁸, S.C. Lee¹⁵², L. Lee¹, G. Lefebvre⁸⁰, M. Lefebvre¹⁷⁰,
 F. Legger¹⁰⁰, C. Leggett¹⁵, A. Lehan⁷⁴, G. Lehmann Miotto³⁰, X. Lei⁷, W.A. Leight²⁹,
 A. Leisos¹⁵⁵, A.G. Leister¹⁷⁷, M.A.L. Leite^{24d}, R. Leitner¹²⁹, D. Lellouch¹⁷³,
 B. Lemmer⁵⁴, K.J.C. Leney⁷⁸, T. Lenz²¹, G. Lenzen¹⁷⁶, B. Lenzi³⁰, R. Leone⁷,
 S. Leone^{124a,124b}, C. Leonidopoulos⁴⁶, S. Leontsinis¹⁰, C. Leroy⁹⁵, C.G. Lester²⁸,
 C.M. Lester¹²², M. Levchenko¹²³, J. Levêque⁵, D. Levin⁸⁹, L.J. Levinson¹⁷³, M. Levy¹⁸,
 A. Lewis¹²⁰, G.H. Lewis¹¹⁰, A.M. Leyko²¹, M. Leyton⁴¹, B. Li^{33b,t}, B. Li⁸⁵, H. Li¹⁴⁹,
 H.L. Li³¹, L. Li⁴⁵, L. Li^{33e}, S. Li⁴⁵, Y. Li^{33c,u}, Z. Liang¹³⁸, H. Liao³⁴, B. Liberti^{134a},
 P. Lichard³⁰, K. Lie¹⁶⁶, J. Liebal²¹, W. Liebig¹⁴, C. Limbach²¹, A. Limosani¹⁵¹,
 S.C. Lin^{152,v}, T.H. Lin⁸³, F. Linde¹⁰⁷, B.E. Lindquist¹⁴⁹, J.T. Linnemann⁹⁰, E. Lipeles¹²²,
 A. Lipniacka¹⁴, M. Lisovy⁴², T.M. Liss¹⁶⁶, D. Lissauer²⁵, A. Lister¹⁶⁹, A.M. Litke¹³⁸,
 B. Liu¹⁵², D. Liu¹⁵², J.B. Liu^{33b}, K. Liu^{33b,w}, L. Liu⁸⁹, M. Liu⁴⁵, M. Liu^{33b}, Y. Liu^{33b},
 M. Livan^{121a,121b}, A. Lleres⁵⁵, J. Llorente Merino⁸², S.L. Lloyd⁷⁶, F. Lo Sterzo¹⁵²,
 E. Lobodzinska⁴², P. Loch⁷, W.S. Lockman¹³⁸, F.K. Loebinger⁸⁴,
 A.E. Loevschall-Jensen³⁶, A. Loginov¹⁷⁷, T. Lohse¹⁶, K. Lohwasser⁴², M. Lokajicek¹²⁷,
 V.P. Lombardo⁵, B.A. Long²², J.D. Long⁸⁹, R.E. Long⁷², L. Lopes^{126a},
 D. Lopez Mateos⁵⁷, B. Lopez Paredes¹⁴⁰, I. Lopez Paz¹², J. Lorenz¹⁰⁰,
 N. Lorenzo Martinez⁶¹, M. Losada¹⁶³, P. Loscutoff¹⁵, X. Lou⁴¹, A. Lounis¹¹⁷, J. Love⁶,
 P.A. Love⁷², A.J. Lowe^{144,f}, F. Lu^{33a}, N. Lu⁸⁹, H.J. Lubatti¹³⁹, C. Luci^{133a,133b},
 A. Lucotte⁵⁵, F. Luehring⁶¹, W. Lukas⁶², L. Luminari^{133a}, O. Lundberg^{147a,147b},
 B. Lund-Jensen¹⁴⁸, M. Lungwitz⁸³, D. Lynn²⁵, R. Lysak¹²⁷, E. Lytken⁸¹, H. Ma²⁵,
 L.L. Ma^{33d}, G. Maccarrone⁴⁷, A. Macchiolo¹⁰¹, J. Machado Miguens^{126a,126b},
 D. Macina³⁰, D. Madaffari⁸⁵, R. Madar⁴⁸, H.J. Maddocks⁷², W.F. Mader⁴⁴,
 A. Madsen¹⁶⁷, M. Maeno⁸, T. Maeno²⁵, A. Maeviskiy⁹⁹, E. Magradze⁵⁴, K. Mahboubi⁴⁸,

J. Mahlstedt¹⁰⁷, S. Mahmoud⁷⁴, C. Maiani¹³⁷, C. Maidantchik^{24a}, A.A. Maier¹⁰¹,
A. Maio^{126a,126b,126d}, S. Majewski¹¹⁶, Y. Makida⁶⁶, N. Makovec¹¹⁷, P. Mal^{137,x},
B. Malaescu⁸⁰, Pa. Malecki³⁹, V.P. Maleev¹²³, F. Malek⁵⁵, U. Mallik⁶³, D. Malon⁶,
C. Malone¹⁴⁴, S. Maltezos¹⁰, V.M. Malyshev¹⁰⁹, S. Malyukov³⁰, J. Mamuzic^{13b},
B. Mandelli³⁰, L. Mandelli^{91a}, I. Mandić⁷⁵, R. Mandrysch⁶³, J. Maneira^{126a,126b},
A. Manfredini¹⁰¹, L. Manhaes de Andrade Filho^{24b}, J.A. Manjarres Ramos^{160b},
A. Mann¹⁰⁰, P.M. Manning¹³⁸, A. Manousakis-Katsikakis⁹, B. Mansoulie¹³⁷,
R. Mantifel⁸⁷, L. Mapelli³⁰, L. March^{146c}, J.F. Marchand²⁹, G. Marchiori⁸⁰,
M. Marcisovsky¹²⁷, C.P. Marino¹⁷⁰, M. Marjanovic^{13a}, C.N. Marques^{126a},
F. Marroquim^{24a}, S.P. Marsden⁸⁴, Z. Marshall¹⁵, L.F. Marti¹⁷, S. Marti-Garcia¹⁶⁸,
B. Martin³⁰, B. Martin⁹⁰, T.A. Martin¹⁷¹, V.J. Martin⁴⁶, B. Martin dit Latour¹⁴,
H. Martinez¹³⁷, M. Martinez^{12,n}, S. Martin-Haugh¹³¹, A.C. Martyniuk⁷⁸, M. Marx¹³⁹,
F. Marzano^{133a}, A. Marzin³⁰, L. Masetti⁸³, T. Mashimo¹⁵⁶, R. Mashinistov⁹⁶, J. Masik⁸⁴,
A.L. Maslennikov^{109,c}, I. Massa^{20a,20b}, L. Massa^{20a,20b}, N. Massol⁵, P. Mastrandrea¹⁴⁹,
A. Mastroberardino^{37a,37b}, T. Masubuchi¹⁵⁶, P. Mättig¹⁷⁶, J. Mattmann⁸³, J. Maurer^{26a},
S.J. Maxfield⁷⁴, D.A. Maximov^{109,c}, R. Mazini¹⁵², L. Mazzaferro^{134a,134b},
G. Mc Goldrick¹⁵⁹, S.P. Mc Kee⁸⁹, A. McCarn⁸⁹, R.L. McCarthy¹⁴⁹, T.G. McCarthy²⁹,
N.A. McCubbin¹³¹, K.W. McFarlane^{56,*}, J.A. Mcfayden⁷⁸, G. Mchedlidze⁵⁴,
S.J. McMahon¹³¹, R.A. McPherson^{170,j}, J. Mechnich¹⁰⁷, M. Medinnis⁴², S. Meehan³¹,
S. Mehlhase¹⁰⁰, A. Mehta⁷⁴, K. Meier^{58a}, C. Meineck¹⁰⁰, B. Meirose⁸¹, C. Melachrinos³¹,
B.R. Mellado Garcia^{146c}, F. Meloni¹⁷, A. Mengarelli^{20a,20b}, S. Menke¹⁰¹, E. Meoni¹⁶²,
K.M. Mercurio⁵⁷, S. Mergelmeyer²¹, N. Meric¹³⁷, P. Mermod⁴⁹, L. Merola^{104a,104b},
C. Meroni^{91a}, F.S. Merritt³¹, H. Merritt¹¹¹, A. Messina^{30,y}, J. Metcalfe²⁵, A.S. Mete¹⁶⁴,
C. Meyer⁸³, C. Meyer¹²², J-P. Meyer¹³⁷, J. Meyer³⁰, R.P. Middleton¹³¹, S. Migas⁷⁴,
L. Mijović²¹, G. Mikenberg¹⁷³, M. Mikestikova¹²⁷, M. Mikuž⁷⁵, A. Milic³⁰, D.W. Miller³¹,
C. Mills⁴⁶, A. Milov¹⁷³, D.A. Milstead^{147a,147b}, D. Milstein¹⁷³, A.A. Minaenko¹³⁰,
Y. Minami¹⁵⁶, I.A. Minashvili⁶⁵, A.I. Mincer¹¹⁰, B. Mindur^{38a}, M. Mineev⁶⁵, Y. Ming¹⁷⁴,
L.M. Mir¹², G. Mirabelli^{133a}, T. Mitani¹⁷², J. Mitrevski¹⁰⁰, V.A. Mitsou¹⁶⁸, A. Miucci⁴⁹,
P.S. Miyagawa¹⁴⁰, J.U. Mjörnmark⁸¹, T. Moa^{147a,147b}, K. Mochizuki⁸⁵, S. Mohapatra³⁵,
W. Mohr⁴⁸, S. Molander^{147a,147b}, R. Moles-Valls¹⁶⁸, K. Mönig⁴², C. Monini⁵⁵, J. Monk³⁶,
E. Monnier⁸⁵, J. Montejo Berlingen¹², F. Monticelli⁷¹, S. Monzani^{133a,133b}, R.W. Moore³,
N. Morange⁶³, D. Moreno⁸³, M. Moreno Llácer⁵⁴, P. Morettini^{50a}, M. Morgenstern⁴⁴,
M. Morii⁵⁷, V. Morisbak¹¹⁹, S. Moritz⁸³, A.K. Morley¹⁴⁸, G. Mornacchi³⁰, J.D. Morris⁷⁶,
L. Morvaj¹⁰³, H.G. Moser¹⁰¹, M. Mosidze^{51b}, J. Moss¹¹¹, K. Motohashi¹⁵⁸, R. Mount¹⁴⁴,
E. Mountricha²⁵, S.V. Mouraviev^{96,*}, E.J.W. Moyse⁸⁶, S. Muanza⁸⁵, R.D. Mudd¹⁸,
F. Mueller^{58a}, J. Mueller¹²⁵, K. Mueller²¹, T. Mueller²⁸, T. Mueller⁸³,
D. Muenstermann⁴⁹, Y. Munwes¹⁵⁴, J.A. Murillo Quijada¹⁸, W.J. Murray^{171,131},
H. Musheghyan⁵⁴, E. Musto¹⁵³, A.G. Myagkov^{130,z}, M. Myska¹²⁸, O. Nackenhorst⁵⁴,
J. Nadal⁵⁴, K. Nagai¹²⁰, R. Nagai¹⁵⁸, Y. Nagai⁸⁵, K. Nagano⁶⁶, A. Nagarkar¹¹¹,
Y. Nagasaka⁵⁹, K. Nagata¹⁶¹, M. Nagel¹⁰¹, A.M. Nairz³⁰, Y. Nakahama³⁰,
K. Nakamura⁶⁶, T. Nakamura¹⁵⁶, I. Nakano¹¹², H. Namasivayam⁴¹, G. Nanava²¹,
R.F. Naranjo Garcia⁴², R. Narayan^{58b}, T. Nattermann²¹, T. Naumann⁴², G. Navarro¹⁶³,
R. Nayyar⁷, H.A. Neal⁸⁹, P.Yu. Nechaeva⁹⁶, T.J. Neep⁸⁴, P.D. Nef¹⁴⁴, A. Negri^{121a,121b},

G. Negri³⁰, M. Negrini^{20a}, S. Nektarijevic⁴⁹, C. Nellist¹¹⁷, A. Nelson¹⁶⁴, T.K. Nelson¹⁴⁴,
 S. Nemecek¹²⁷, P. Nemethy¹¹⁰, A.A. Nepomuceno^{24a}, M. Nessi^{30,aa}, M.S. Neubauer¹⁶⁶,
 M. Neumann¹⁷⁶, R.M. Neves¹¹⁰, P. Nevski²⁵, P.R. Newman¹⁸, D.H. Nguyen⁶,
 R.B. Nickerson¹²⁰, R. Nicolaidou¹³⁷, B. Nicquevert³⁰, J. Nielsen¹³⁸, N. Nikiforou³⁵,
 A. Nikiforov¹⁶, V. Nikolaenko^{130,z}, I. Nikolic-Audit⁸⁰, K. Nikolics⁴⁹, K. Nikolopoulos¹⁸,
 P. Nilsson²⁵, Y. Ninomiya¹⁵⁶, A. Nisati^{133a}, R. Nisius¹⁰¹, T. Nobe¹⁵⁸, L. Nodulman⁶,
 M. Nomachi¹¹⁸, I. Nomidis²⁹, S. Norberg¹¹³, M. Nordberg³⁰, O. Novgorodova⁴⁴,
 S. Nowak¹⁰¹, M. Nozaki⁶⁶, L. Nozka¹¹⁵, K. Ntekas¹⁰, G. Nunes Hanninger⁸⁸,
 T. Nunnemann¹⁰⁰, E. Nurse⁷⁸, F. Nuti⁸⁸, B.J. O'Brien⁴⁶, F. O'grady⁷, D.C. O'Neil¹⁴³,
 V. O'Shea⁵³, F.G. Oakham^{29,e}, H. Oberlack¹⁰¹, T. Obermann²¹, J. Ocariz⁸⁰, A. Ochi⁶⁷,
 M.I. Ochoa⁷⁸, S. Oda⁷⁰, S. Odaka⁶⁶, H. Ogren⁶¹, A. Oh⁸⁴, S.H. Oh⁴⁵, C.C. Ohm¹⁵,
 H. Ohman¹⁶⁷, H. Oide³⁰, W. Okamura¹¹⁸, H. Okawa²⁵, Y. Okumura³¹, T. Okuyama¹⁵⁶,
 A. Olariu^{26a}, A.G. Olchevski⁶⁵, S.A. Olivares Pino⁴⁶, D. Oliveira Damazio²⁵,
 E. Oliver Garcia¹⁶⁸, A. Olszewski³⁹, J. Olszowska³⁹, A. Onofre^{126a,126e}, P.U.E. Onyisi^{31,o},
 C.J. Oram^{160a}, M.J. Oreglia³¹, Y. Oren¹⁵⁴, D. Orestano^{135a,135b}, N. Orlando^{73a,73b},
 C. Oropeza Barrera⁵³, R.S. Orr¹⁵⁹, B. Osculati^{50a,50b}, R. Ospanov¹²²,
 G. Otero y Garzon²⁷, H. Otono⁷⁰, M. Ouchrif^{136d}, E.A. Ouellette¹⁷⁰, F. Ould-Saada¹¹⁹,
 A. Ouraou¹³⁷, K.P. Oussoren¹⁰⁷, Q. Ouyang^{33a}, A. Ovcharova¹⁵, M. Owen⁸⁴,
 V.E. Ozcan^{19a}, N. Ozturk⁸, K. Pachal¹²⁰, A. Pacheco Pages¹², C. Padilla Aranda¹²,
 M. Pagáčová⁴⁸, S. Pagan Griso¹⁵, E. Paganis¹⁴⁰, C. Pahl¹⁰¹, F. Paige²⁵, P. Pais⁸⁶,
 K. Pajchel¹¹⁹, G. Palacino^{160b}, S. Palestini³⁰, M. Palka^{38b}, D. Pallin³⁴, A. Palma^{126a,126b},
 J.D. Palmer¹⁸, Y.B. Pan¹⁷⁴, E. Panagiotopoulou¹⁰, J.G. Panduro Vazquez⁷⁷, P. Pani¹⁰⁷,
 N. Panikashvili⁸⁹, S. Panitkin²⁵, D. Pantea^{26a}, L. Paolozzi^{134a,134b},
 Th.D. Papadopoulou¹⁰, K. Papageorgiou^{155,l}, A. Paramonov⁶, D. Paredes Hernandez¹⁵⁵,
 M.A. Parker²⁸, F. Parodi^{50a,50b}, J.A. Parsons³⁵, U. Parzefall⁴⁸, E. Pasqualucci^{133a},
 S. Passaggio^{50a}, A. Passeri^{135a}, F. Pastore^{135a,135b,*}, Fr. Pastore⁷⁷, G. Pásztor²⁹,
 S. Pataraia¹⁷⁶, N.D. Patel¹⁵¹, J.R. Pater⁸⁴, S. Patricelli^{104a,104b}, T. Pauly³⁰, J. Pearce¹⁷⁰,
 L.E. Pedersen³⁶, M. Pedersen¹¹⁹, S. Pedraza Lopez¹⁶⁸, R. Pedro^{126a,126b},
 S.V. Peleganchuk¹⁰⁹, D. Pelikan¹⁶⁷, H. Peng^{33b}, B. Penning³¹, J. Penwell⁶¹,
 D.V. Perepelitsa²⁵, E. Perez Codina^{160a}, M.T. Pérez García-Estañ¹⁶⁸, L. Perini^{91a,91b},
 H. Pernegger³⁰, S. Perrella^{104a,104b}, R. Perrino^{73a}, R. Peschke⁴², V.D. Peshekhonov⁶⁵,
 K. Peters³⁰, R.F.Y. Peters⁸⁴, B.A. Petersen³⁰, T.C. Petersen³⁶, E. Petit⁴²,
 A. Petridis^{147a,147b}, C. Petridou¹⁵⁵, E. Petrolo^{133a}, F. Petrucci^{135a,135b}, N.E. Pettersson¹⁵⁸,
 R. Pezoa^{32b}, P.W. Phillips¹³¹, G. Piacquadio¹⁴⁴, E. Pianori¹⁷¹, A. Picazio⁴⁹, E. Piccaro⁷⁶,
 M. Piccinini^{20a,20b}, R. Piegai²⁷, D.T. Pignotti¹¹¹, J.E. Pilcher³¹, A.D. Pilkington⁷⁸,
 J. Pina^{126a,126b,126d}, M. Pinamonti^{165a,165c,ab}, A. Pinder¹²⁰, J.L. Pinfold³, A. Pingel³⁶,
 B. Pinto^{126a}, S. Pires⁸⁰, M. Pitt¹⁷³, C. Pizio^{91a,91b}, L. Plazak^{145a}, M.-A. Pleier²⁵,
 V. Pleskot¹²⁹, E. Plotnikova⁶⁵, P. Plucinski^{147a,147b}, D. Pluth⁶⁴, S. Poddar^{58a},
 F. Podlyski³⁴, R. Poettgen⁸³, L. Poggiali¹¹⁷, D. Pohl²¹, M. Pohl⁴⁹, G. Polesello^{121a},
 A. Policicchio^{37a,37b}, R. Polifka¹⁵⁹, A. Polini^{20a}, C.S. Pollard⁴⁵, V. Polychronakos²⁵,
 K. Pommès³⁰, L. Pontecorvo^{133a}, B.G. Pope⁹⁰, G.A. Popenciu^{26b}, D.S. Popovic^{13a},
 A. Poppleton³⁰, X. Portell Bueso¹², S. Pospisil¹²⁸, K. Potamianos¹⁵, I.N. Potrap⁶⁵,
 C.J. Potter¹⁵⁰, C.T. Potter¹¹⁶, G. Poulard³⁰, J. Poveda⁶¹, V. Pozdnyakov⁶⁵,

P. Pralavorio⁸⁵, A. Pranko¹⁵, S. Prasad³⁰, R. Pravahan⁸, S. Prell⁶⁴, D. Price⁸⁴, J. Price⁷⁴, L.E. Price⁶, D. Prieur¹²⁵, M. Primavera^{73a}, M. Proissl⁴⁶, K. Prokofiev⁴⁷, F. Prokoshin^{32b}, E. Protopapadaki¹³⁷, S. Protopopescu²⁵, J. Proudfoot⁶, M. Przybycien^{38a}, H. Przysiezniak⁵, E. Ptacek¹¹⁶, D. Puddu^{135a,135b}, E. Pueschel⁸⁶, D. Puldon¹⁴⁹, M. Purohit^{25,ac}, P. Puzo¹¹⁷, J. Qian⁸⁹, G. Qin⁵³, Y. Qin⁸⁴, A. Quadt⁵⁴, D.R. Quarrie¹⁵, W.B. Quayle^{165a,165b}, M. Queitsch-Maitland⁸⁴, D. Quilty⁵³, A. Qureshi^{160b}, V. Radeka²⁵, V. Radescu⁴², S.K. Radhakrishnan¹⁴⁹, P. Radloff¹¹⁶, P. Rados⁸⁸, F. Ragusa^{91a,91b}, G. Rahal¹⁷⁹, S. Rajagopalan²⁵, M. Rammensee³⁰, A.S. Randle-Conde⁴⁰, C. Rangel-Smith¹⁶⁷, K. Rao¹⁶⁴, F. Rauscher¹⁰⁰, T.C. Rave⁴⁸, T. Ravenscroft⁵³, M. Raymond³⁰, A.L. Read¹¹⁹, N.P. Readloff⁷⁴, D.M. Rebuzzi^{121a,121b}, A. Redelbach¹⁷⁵, G. Redlinger²⁵, R. Reece¹³⁸, K. Reeves⁴¹, L. Rehnisch¹⁶, H. Reisin²⁷, M. Relich¹⁶⁴, C. Rembser³⁰, H. Ren^{33a}, Z.L. Ren¹⁵², A. Renaud¹¹⁷, M. Rescigno^{133a}, S. Resconi^{91a}, O.L. Rezanova^{109,c}, P. Reznicek¹²⁹, R. Rezvani⁹⁵, R. Richter¹⁰¹, M. Ridel⁸⁰, P. Rieck¹⁶, J. Rieger⁵⁴, M. Rijssenbeek¹⁴⁹, A. Rimoldi^{121a,121b}, L. Rinaldi^{20a}, E. Ritsch⁶², I. Riu¹², F. Rizatdinova¹¹⁴, E. Rizvi⁷⁶, S.H. Robertson^{87,j}, A. Robichaud-Veronneau⁸⁷, D. Robinson²⁸, J.E.M. Robinson⁸⁴, A. Robson⁵³, C. Roda^{124a,124b}, L. Rodrigues³⁰, S. Roe³⁰, O. Røhne¹¹⁹, S. Rolli¹⁶², A. Romaniouk⁹⁸, M. Romano^{20a,20b}, E. Romero Adam¹⁶⁸, N. Rompotis¹³⁹, M. Ronzani⁴⁸, L. Roos⁸⁰, E. Ros¹⁶⁸, S. Rosati^{133a}, K. Rosbach⁴⁹, M. Rose⁷⁷, P. Rose¹³⁸, P.L. Rosendahl¹⁴, O. Rosenthal¹⁴², V. Rossetti^{147a,147b}, E. Rossi^{104a,104b}, L.P. Rossi^{50a}, R. Rosten¹³⁹, M. Rotaru^{26a}, I. Roth¹⁷³, J. Rothberg¹³⁹, D. Rousseau¹¹⁷, C.R. Royon¹³⁷, A. Rozanov⁸⁵, Y. Rozen¹⁵³, X. Ruan^{146c}, F. Rubbo¹², I. Rubinskiy⁴², V.I. Rud⁹⁹, C. Rudolph⁴⁴, M.S. Rudolph¹⁵⁹, F. Rühr⁴⁸, A. Ruiz-Martinez³⁰, Z. Rurikova⁴⁸, N.A. Rusakovich⁶⁵, A. Ruschke¹⁰⁰, J.P. Rutherford⁷, N. Ruthmann⁴⁸, Y.F. Ryabov¹²³, M. Rybar¹²⁹, G. Rybkin¹¹⁷, N.C. Ryder¹²⁰, A.F. Saavedra¹⁵¹, G. Sabato¹⁰⁷, S. Sacerdoti²⁷, A. Saddique³, I. Sadeh¹⁵⁴, H.F-W. Sadrozinski¹³⁸, R. Sadykov⁶⁵, F. Safai Tehrani^{133a}, H. Sakamoto¹⁵⁶, Y. Sakurai¹⁷², G. Salamanna^{135a,135b}, A. Salamon^{134a}, M. Saleem¹¹³, D. Salek¹⁰⁷, P.H. Sales De Bruin¹³⁹, D. Salihagic¹⁰¹, A. Salnikov¹⁴⁴, J. Salt¹⁶⁸, D. Salvatore^{37a,37b}, F. Salvatore¹⁵⁰, A. Salvucci¹⁰⁶, A. Salzburger³⁰, D. Sampsonidis¹⁵⁵, A. Sanchez^{104a,104b}, J. Sánchez¹⁶⁸, V. Sanchez Martinez¹⁶⁸, H. Sandaker¹⁴, R.L. Sandbach⁷⁶, H.G. Sander⁸³, M.P. Sanders¹⁰⁰, M. Sandhoff¹⁷⁶, T. Sandoval²⁸, C. Sandoval¹⁶³, R. Sandstroem¹⁰¹, D.P.C. Sankey¹³¹, A. Sansoni⁴⁷, C. Santoni³⁴, R. Santonico^{134a,134b}, H. Santos^{126a}, I. Santoyo Castillo¹⁵⁰, K. Sapp¹²⁵, A. Sapronov⁶⁵, J.G. Saraiva^{126a,126d}, B. Sarrazin²¹, G. Sartisohn¹⁷⁶, O. Sasaki⁶⁶, Y. Sasaki¹⁵⁶, G. Sauvage^{5,*}, E. Sauvan⁵, P. Savard^{159,e}, D.O. Savu³⁰, C. Sawyer¹²⁰, L. Sawyer^{79,m}, D.H. Saxon⁵³, J. Saxon¹²², C. Sbarra^{20a}, A. Sbrizzi^{20a,20b}, T. Scanlon⁷⁸, D.A. Scannicchio¹⁶⁴, M. Scarella¹⁵¹, V. Scarfone^{37a,37b}, J. Schaarschmidt¹⁷³, P. Schacht¹⁰¹, D. Schaefer³⁰, R. Schaefer⁴², S. Schaepe²¹, S. Schaetzl^{58b}, U. Schäfer⁸³, A.C. Schaffer¹¹⁷, D. Schaile¹⁰⁰, R.D. Schamberger¹⁴⁹, V. Scharf^{58a}, V.A. Schegelsky¹²³, D. Scheirich¹²⁹, M. Schernau¹⁶⁴, M.I. Scherzer³⁵, C. Schiavi^{50a,50b}, J. Schieck¹⁰⁰, C. Schillo⁴⁸, M. Schioppa^{37a,37b}, S. Schlenker³⁰, E. Schmidt⁴⁸, K. Schmieden³⁰, C. Schmitt⁸³, S. Schmitt^{58b}, B. Schneider¹⁷, Y.J. Schnellbach⁷⁴, U. Schnoor⁴⁴, L. Schoeffel¹³⁷, A. Schoening^{58b}, B.D. Schoenrock⁹⁰, A.L.S. Schorlemmer⁵⁴, M. Schott⁸³, D. Schouten^{160a}, J. Schovancova²⁵, S. Schramm¹⁵⁹,

M. Schreyer¹⁷⁵, C. Schroeder⁸³, N. Schuh⁸³, M.J. Schultens²¹, H.-C. Schultz-Coulon^{58a},
 H. Schulz¹⁶, M. Schumacher⁴⁸, B.A. Schumm¹³⁸, Ph. Schune¹³⁷, C. Schwanenberger⁸⁴,
 A. Schwartzman¹⁴⁴, T.A. Schwarz⁸⁹, Ph. Schwegler¹⁰¹, Ph. Schwemling¹³⁷,
 R. Schwienhorst⁹⁰, J. Schwindling¹³⁷, T. Schwindt²¹, M. Schwoerer⁵, F.G. Sciacca¹⁷,
 E. Scifo¹¹⁷, G. Sciolla²³, W.G. Scott¹³¹, F. Scuri^{124a,124b}, F. Scutti²¹, J. Searcy⁸⁹,
 G. Sedov⁴², E. Sedykh¹²³, P. Seema²¹, S.C. Seidel¹⁰⁵, A. Seiden¹³⁸, F. Seifert¹²⁸,
 J.M. Seixas^{24a}, G. Sekhniadze^{104a}, S.J. Sekula⁴⁰, K.E. Selbach⁴⁶, D.M. Seliverstov^{123,*},
 G. Sellers⁷⁴, N. Semprini-Cesari^{20a,20b}, C. Serfon³⁰, L. Serin¹¹⁷, L. Serkin⁵⁴, T. Serre⁸⁵,
 R. Seuster^{160a}, H. Severini¹¹³, T. Sfiligoj⁷⁵, F. Sforza¹⁰¹, A. Sfyrla³⁰, E. Shabalina⁵⁴,
 M. Shamim¹¹⁶, L.Y. Shan^{33a}, R. Shang¹⁶⁶, J.T. Shank²², M. Shapiro¹⁵, P.B. Shatalov⁹⁷,
 K. Shaw^{165a,165b}, C.Y. Shehu¹⁵⁰, P. Sherwood⁷⁸, L. Shi^{152,ad}, S. Shimizu⁶⁷,
 C.O. Shimmin¹⁶⁴, M. Shimojima¹⁰², M. Shiyakova⁶⁵, A. Shmeleva⁹⁶, M.J. Shochet³¹,
 D. Short¹²⁰, S. Shrestha⁶⁴, E. Shulga⁹⁸, M.A. Shupe⁷, S. Shushkevich⁴², P. Sicho¹²⁷,
 O. Sidiropoulou¹⁵⁵, D. Sidorov¹¹⁴, A. Sidoti^{133a}, F. Siegert⁴⁴, Dj. Sijacki^{13a},
 J. Silva^{126a,126d}, Y. Silver¹⁵⁴, D. Silverstein¹⁴⁴, S.B. Silverstein^{147a}, V. Simak¹²⁸,
 O. Simard⁵, Lj. Simic^{13a}, S. Simion¹¹⁷, E. Simioni⁸³, B. Simmons⁷⁸, R. Simoniello^{91a,91b},
 P. Sinervo¹⁵⁹, N.B. Sinev¹¹⁶, G. Siragusa¹⁷⁵, A. Sircar⁷⁹, A.N. Sisakyan^{65,*},
 S.Yu. Sivoklokov⁹⁹, J. Sjölin^{147a,147b}, T.B. Sjursen¹⁴, H.P. Skottowe⁵⁷, K.Yu. Skovpen¹⁰⁹,
 P. Skubic¹¹³, M. Slater¹⁸, T. Slavicek¹²⁸, M. Slawinska¹⁰⁷, K. Sliwa¹⁶², V. Smakhtin¹⁷³,
 B.H. Smart⁴⁶, L. Smestad¹⁴, S.Yu. Smirnov⁹⁸, Y. Smirnov⁹⁸, L.N. Smirnova^{99,ae},
 O. Smirnova⁸¹, K.M. Smith⁵³, M. Smizanska⁷², K. Smolek¹²⁸, A.A. Snesarev⁹⁶,
 G. Snidero⁷⁶, S. Snyder²⁵, R. Sobie^{170,j}, F. Socher⁴⁴, A. Soffer¹⁵⁴, D.A. Soh^{152,ad},
 C.A. Solans³⁰, M. Solar¹²⁸, J. Solc¹²⁸, E.Yu. Soldatov⁹⁸, U. Soldevila¹⁶⁸,
 A.A. Solodkov¹³⁰, A. Soloshenko⁶⁵, O.V. Solovyanov¹³⁰, V. Solovyev¹²³, P. Sommer⁴⁸,
 H.Y. Song^{33b}, N. Soni¹, A. Sood¹⁵, A. Sopczak¹²⁸, B. Sopko¹²⁸, V. Sopko¹²⁸, V. Sorin¹²,
 M. Sosebee⁸, R. Soualah^{165a,165c}, P. Soueid⁹⁵, A.M. Soukharev^{109,c}, D. South⁴²,
 S. Spagnolo^{73a,73b}, F. Spano⁷⁷, W.R. Spearman⁵⁷, F. Spettel¹⁰¹, R. Spighi^{20a}, G. Spigo³⁰,
 L.A. Spiller⁸⁸, M. Spousta¹²⁹, T. Spreitzer¹⁵⁹, B. Spurlock⁸, R.D. St. Denis^{53,*},
 S. Staerz⁴⁴, J. Stahlman¹²², R. Stamen^{58a}, S. Stamm¹⁶, E. Stanecka³⁹, R.W. Stanek⁶,
 C. Stanescu^{135a}, M. Stanescu-Bellu⁴², M.M. Stanitzki⁴², S. Stapnes¹¹⁹,
 E.A. Starchenko¹³⁰, J. Stark⁵⁵, P. Staroba¹²⁷, P. Starovoitov⁴², R. Staszewski³⁹,
 P. Stavina^{145a,*}, P. Steinberg²⁵, B. Stelzer¹⁴³, H.J. Stelzer³⁰, O. Stelzer-Chilton^{160a},
 H. Stenzel⁵², S. Stern¹⁰¹, G.A. Stewart⁵³, J.A. Stillings²¹, M.C. Stockton⁸⁷, M. Stoebe⁸⁷,
 G. Stoicea^{26a}, P. Stolte⁵⁴, S. Stonjek¹⁰¹, A.R. Stradling⁸, A. Straessner⁴⁴,
 M.E. Stramaglia¹⁷, J. Strandberg¹⁴⁸, S. Strandberg^{147a,147b}, A. Strandlie¹¹⁹,
 E. Strauss¹⁴⁴, M. Strauss¹¹³, P. Strizenec^{145b}, R. Ströhmer¹⁷⁵, D.M. Strom¹¹⁶,
 R. Stroynowski⁴⁰, A. Strubig¹⁰⁶, S.A. Stucci¹⁷, B. Stugu¹⁴, N.A. Styles⁴², D. Su¹⁴⁴,
 J. Su¹²⁵, R. Subramaniam⁷⁹, A. Succurro¹², Y. Sugaya¹¹⁸, C. Suhr¹⁰⁸, M. Suk¹²⁸,
 V.V. Sulin⁹⁶, S. Sultansoy^{4d}, T. Sumida⁶⁸, S. Sun⁵⁷, X. Sun^{33a}, J.E. Sundermann⁴⁸,
 K. Suruliz¹⁴⁰, G. Susinno^{37a,37b}, M.R. Sutton¹⁵⁰, Y. Suzuki⁶⁶, M. Svatos¹²⁷,
 S. Swedish¹⁶⁹, M. Swiatlowski¹⁴⁴, I. Sykora^{145a}, T. Sykora¹²⁹, D. Ta⁹⁰, C. Taccini^{135a,135b},
 K. Tackmann⁴², J. Taenzer¹⁵⁹, A. Taffard¹⁶⁴, R. Tafirout^{160a}, N. Taiblum¹⁵⁴, H. Takai²⁵,
 R. Takashima⁶⁹, H. Takeda⁶⁷, T. Takeshita¹⁴¹, Y. Takubo⁶⁶, M. Talby⁸⁵,

A.A. Talyshov^{109,c}, J.Y.C. Tam¹⁷⁵, K.G. Tan⁸⁸, J. Tanaka¹⁵⁶, R. Tanaka¹¹⁷, S. Tanaka¹³²,
 S. Tanaka⁶⁶, A.J. Tanasijczuk¹⁴³, B.B. Tannenwald¹¹¹, N. Tannoury²¹, S. Tapprogge⁸³,
 S. Tarem¹⁵³, F. Tarrade²⁹, G.F. Tartarelli^{91a}, P. Tas¹²⁹, M. Tasevsky¹²⁷, T. Tashiro⁶⁸,
 E. Tassi^{37a,37b}, A. Tavares Delgado^{126a,126b}, Y. Tayalati^{136d}, F.E. Taylor⁹⁴, G.N. Taylor⁸⁸,
 W. Taylor^{160b}, F.A. Teischinger³⁰, M. Teixeira Dias Castanheira⁷⁶, P. Teixeira-Dias⁷⁷,
 K.K. Temming⁴⁸, H. Ten Kate³⁰, P.K. Teng¹⁵², J.J. Teoh¹¹⁸, S. Terada⁶⁶, K. Terashi¹⁵⁶,
 J. Terron⁸², S. Terzo¹⁰¹, M. Testa⁴⁷, R.J. Teuscher^{159,j}, J. Therhaag²¹,
 T. Theveneaux-Pelzer³⁴, J.P. Thomas¹⁸, J. Thomas-Wilsker⁷⁷, E.N. Thompson³⁵,
 P.D. Thompson¹⁸, P.D. Thompson¹⁵⁹, R.J. Thompson⁸⁴, A.S. Thompson⁵³,
 L.A. Thomsen³⁶, E. Thomson¹²², M. Thomson²⁸, W.M. Thong⁸⁸, R.P. Thun^{89,*},
 F. Tian³⁵, M.J. Tibbetts¹⁵, V.O. Tikhomirov^{96,af}, Yu.A. Tikhonov^{109,c}, S. Timoshenko⁹⁸,
 E. Tiouchichine⁸⁵, P. Tipton¹⁷⁷, S. Tisserant⁸⁵, T. Todorov⁵, S. Todorova-Nova¹²⁹,
 J. Tojo⁷⁰, S. Tokár^{145a}, K. Tokushuku⁶⁶, K. Tollefson⁹⁰, E. Tolley⁵⁷, L. Tomlinson⁸⁴,
 M. Tomoto¹⁰³, L. Tompkins³¹, K. Toms¹⁰⁵, N.D. Topilin⁶⁵, E. Torrence¹¹⁶, H. Torres¹⁴³,
 E. Torró Pastor¹⁶⁸, J. Toth^{85,ag}, F. Touchard⁸⁵, D.R. Tovey¹⁴⁰, H.L. Tran¹¹⁷,
 T. Trefzger¹⁷⁵, L. Tremblet³⁰, A. Tricoli³⁰, I.M. Trigger^{160a}, S. Trincaz-Duvold⁸⁰,
 M.F. Tripiana¹², W. Trischuk¹⁵⁹, B. Trocmé⁵⁵, C. Troncon^{91a}, M. Trottier-McDonald¹⁵,
 M. Trovatelli^{135a,135b}, P. True⁹⁰, M. Trzebinski³⁹, A. Trzupek³⁹, C. Tsarouchas³⁰,
 J.C-L. Tseng¹²⁰, P.V. Tsiareshka⁹², D. Tsionou¹³⁷, G. Tsipolitis¹⁰, N. Tsirintanis⁹,
 S. Tsiskaridze¹², V. Tsiskaridze⁴⁸, E.G. Tskhadadze^{51a}, I.I. Tsukerman⁹⁷, V. Tsulaia¹⁵,
 S. Tsuno⁶⁶, D. Tsybychev¹⁴⁹, A. Tudorache^{26a}, V. Tudorache^{26a}, A.N. Tuna¹²²,
 S.A. Tupputi^{20a,20b}, S. Turchikhin^{99,ae}, D. Turecek¹²⁸, I. Turk Cakir^{4c}, R. Turra^{91a,91b},
 A.J. Turvey⁴⁰, P.M. Tuts³⁵, A. Tykhanov⁴⁹, M. Tylmad^{147a,147b}, M. Tyndel¹³¹,
 K. Uchida²¹, I. Ueda¹⁵⁶, R. Ueno²⁹, M. Ughetto⁸⁵, M. Ugland¹⁴, M. Uhlenbrock²¹,
 F. Ukegawa¹⁶¹, G. Unal³⁰, A. Undrus²⁵, G. Unel¹⁶⁴, F.C. Ungaro⁴⁸, Y. Unno⁶⁶,
 C. Unverdorben¹⁰⁰, D. Urbaniec³⁵, P. Urquijo⁸⁸, G. Usai⁸, A. Usanova⁶², L. Vacavant⁸⁵,
 V. Vacek¹²⁸, B. Vachon⁸⁷, N. Valencic¹⁰⁷, S. Valentinetto^{20a,20b}, A. Valero¹⁶⁸, L. Valery³⁴,
 S. Valkar¹²⁹, E. Valladolid Gallego¹⁶⁸, S. Vallecorsa⁴⁹, J.A. Valls Ferrer¹⁶⁸,
 W. Van Den Wollenberg¹⁰⁷, P.C. Van Der Deijl¹⁰⁷, R. van der Geer¹⁰⁷,
 H. van der Graaf¹⁰⁷, R. Van Der Leeuw¹⁰⁷, D. van der Ster³⁰, N. van Eldik³⁰,
 P. van Gemmeren⁶, J. Van Nieuwkoop¹⁴³, I. van Vulpene¹⁰⁷, M.C. van Woerden³⁰,
 M. Vanadia^{133a,133b}, W. Vandelli³⁰, R. Vanguri¹²², A. Vaniachine⁶, P. Vankov⁴²,
 F. Vannucci⁸⁰, G. Vardanyan¹⁷⁸, R. Vari^{133a}, E.W. Varnes⁷, T. Varol⁸⁶, D. Varouchas⁸⁰,
 A. Vartapetian⁸, K.E. Varvell¹⁵¹, F. Vazeille³⁴, T. Vazquez Schroeder⁵⁴, J. Veatch⁷,
 F. Veloso^{126a,126c}, T. Velz²¹, S. Veneziano^{133a}, A. Ventura^{73a,73b}, D. Ventura⁸⁶,
 M. Venturi¹⁷⁰, N. Venturi¹⁵⁹, A. Venturini²³, V. Vercesi^{121a}, M. Verducci^{133a,133b},
 W. Verkerke¹⁰⁷, J.C. Vermeulen¹⁰⁷, A. Vest⁴⁴, M.C. Vetterli^{143,e}, O. Viazlo⁸¹,
 I. Vichou¹⁶⁶, T. Vickey^{146c,ah}, O.E. Vickey Boeriu^{146c}, G.H.A. Viehhauser¹²⁰, S. Viel¹⁶⁹,
 R. Vigne³⁰, M. Villa^{20a,20b}, M. Villaplana Perez^{91a,91b}, E. Vilucchi⁴⁷, M.G. Vinchter²⁹,
 V.B. Vinogradov⁶⁵, J. Virzi¹⁵, I. Vivarelli¹⁵⁰, F. Vives Vaque³, S. Vlachos¹⁰,
 D. Vladoiu¹⁰⁰, M. Vlasak¹²⁸, A. Vogel²¹, M. Vogel^{32a}, P. Vokac¹²⁸, G. Volpi^{124a,124b},
 M. Volpi⁸⁸, H. von der Schmitt¹⁰¹, H. von Radziewski⁴⁸, E. von Toerne²¹, V. Vorobel¹²⁹,
 K. Vorobev⁹⁸, M. Vos¹⁶⁸, R. Voss³⁰, J.H. Vossebeld⁷⁴, N. Vranjes¹³⁷,

M. Vranjes Milosavljevic^{13a}, V. Vrba¹²⁷, M. Vreeswijk¹⁰⁷, T. Vu Anh⁴⁸, R. Vuillermet³⁰, I. Vukotic³¹, Z. Vykydal¹²⁸, P. Wagner²¹, W. Wagner¹⁷⁶, H. Wahlberg⁷¹, S. Wahrmund⁴⁴, J. Wakabayashi¹⁰³, J. Walder⁷², R. Walker¹⁰⁰, W. Walkowiak¹⁴², R. Wall¹⁷⁷, P. Waller⁷⁴, B. Walsh¹⁷⁷, C. Wang^{152,ai}, C. Wang⁴⁵, F. Wang¹⁷⁴, H. Wang¹⁵, H. Wang⁴⁰, J. Wang⁴², J. Wang^{33a}, K. Wang⁸⁷, R. Wang¹⁰⁵, S.M. Wang¹⁵², T. Wang²¹, X. Wang¹⁷⁷, C. Wanotayaroj¹¹⁶, A. Warburton⁸⁷, C.P. Ward²⁸, D.R. Wardrope⁷⁸, M. Warsinsky⁴⁸, A. Washbrook⁴⁶, C. Wasicki⁴², P.M. Watkins¹⁸, A.T. Watson¹⁸, I.J. Watson¹⁵¹, M.F. Watson¹⁸, G. Watts¹³⁹, S. Watts⁸⁴, B.M. Waugh⁷⁸, S. Webb⁸⁴, M.S. Weber¹⁷, S.W. Weber¹⁷⁵, J.S. Webster³¹, A.R. Weidberg¹²⁰, B. Weinert⁶¹, J. Weingarten⁵⁴, C. Weiser⁴⁸, H. Weits¹⁰⁷, P.S. Wells³⁰, T. Wenaus²⁵, D. Wendland¹⁶, Z. Weng^{152,ad}, T. Wengler³⁰, S. Wenig³⁰, N. Wermes²¹, M. Werner⁴⁸, P. Werner³⁰, M. Wessels^{58a}, J. Wetter¹⁶², K. Whalen²⁹, A. White⁸, M.J. White¹, R. White^{32b}, S. White^{124a,124b}, D. Whiteson¹⁶⁴, D. Wicke¹⁷⁶, F.J. Wickens¹³¹, W. Wiedenmann¹⁷⁴, M. Wielers¹³¹, P. Wienemann²¹, C. Wiglesworth³⁶, L.A.M. Wiik-Fuchs²¹, P.A. Wijeratne⁷⁸, A. Wildauer¹⁰¹, M.A. Wildt^{42,aj}, H.G. Wilkens³⁰, H.H. Williams¹²², S. Williams²⁸, C. Willis⁹⁰, S. Willocq⁸⁶, A. Wilson⁸⁹, J.A. Wilson¹⁸, I. Wingerter-Seez⁵, F. Winkelmeier¹¹⁶, B.T. Winter²¹, M. Wittgen¹⁴⁴, T. Wittig⁴³, J. Wittkowski¹⁰⁰, S.J. Wollstadt⁸³, M.W. Wolter³⁹, H. Wolters^{126a,126c}, B.K. Wosiek³⁹, J. Wotschack³⁰, M.J. Woudstra⁸⁴, K.W. Wozniak³⁹, M. Wright⁵³, M. Wu⁵⁵, S.L. Wu¹⁷⁴, X. Wu⁴⁹, Y. Wu⁸⁹, E. Wulf³⁵, T.R. Wyatt⁸⁴, B.M. Wynne⁴⁶, S. Xella³⁶, M. Xiao¹³⁷, D. Xu^{33a}, L. Xu^{33b,ak}, B. Yabsley¹⁵¹, S. Yacoob^{146b,al}, R. Yakabe⁶⁷, M. Yamada⁶⁶, H. Yamaguchi¹⁵⁶, Y. Yamaguchi¹¹⁸, A. Yamamoto⁶⁶, K. Yamamoto⁶⁴, S. Yamamoto¹⁵⁶, T. Yamamura¹⁵⁶, T. Yamanaka¹⁵⁶, K. Yamauchi¹⁰³, Y. Yamazaki⁶⁷, Z. Yan²², H. Yang^{33e}, H. Yang¹⁷⁴, U.K. Yang⁸⁴, Y. Yang¹¹¹, S. Yanush⁹³, L. Yao^{33a}, W-M. Yao¹⁵, Y. Yasu⁶⁶, E. Yatsenko⁴², K.H. Yau Wong²¹, J. Ye⁴⁰, S. Ye²⁵, I. Yeletskikh⁶⁵, A.L. Yen⁵⁷, E. Yildirim⁴², M. Yilmaz^{4b}, R. Yoosoofmiya¹²⁵, K. Yorita¹⁷², R. Yoshida⁶, K. Yoshihara¹⁵⁶, C. Young¹⁴⁴, C.J.S. Young³⁰, S. Youssef²², D.R. Yu¹⁵, J. Yu⁸, J.M. Yu⁸⁹, J. Yu¹¹⁴, L. Yuan⁶⁷, A. Yurkewicz¹⁰⁸, I. Yusuff^{28,am}, B. Zabinski³⁹, R. Zaidan⁶³, A.M. Zaitsev^{130,z}, A. Zaman¹⁴⁹, S. Zambito²³, L. Zanello^{133a,133b}, D. Zanzi⁸⁸, C. Zeitnitz¹⁷⁶, M. Zeman¹²⁸, A. Zemla^{38a}, K. Zengel²³, O. Zenin¹³⁰, T. Ženiš^{145a}, D. Zerwas¹¹⁷, G. Zevi della Porta⁵⁷, D. Zhang⁸⁹, F. Zhang¹⁷⁴, H. Zhang⁹⁰, J. Zhang⁶, L. Zhang¹⁵², X. Zhang^{33d}, Z. Zhang¹¹⁷, Y. Zhao^{33d}, Z. Zhao^{33b}, A. Zhemchugov⁶⁵, J. Zhong¹²⁰, B. Zhou⁸⁹, L. Zhou³⁵, N. Zhou¹⁶⁴, C.G. Zhu^{33d}, H. Zhu^{33a}, J. Zhu⁸⁹, Y. Zhu^{33b}, X. Zhuang^{33a}, K. Zhukov⁹⁶, A. Zibell¹⁷⁵, D. Ziemińska⁶¹, N.I. Zimine⁶⁵, C. Zimmermann⁸³, R. Zimmermann²¹, S. Zimmermann²¹, S. Zimmermann⁴⁸, Z. Zinonos⁵⁴, M. Ziolkowski¹⁴², G. Zobernig¹⁷⁴, A. Zoccoli^{20a,20b}, M. zur Nedden¹⁶, G. Zurzolo^{104a,104b}, V. Zutshi¹⁰⁸, L. Zwalski³⁰.

¹ Department of Physics, University of Adelaide, Adelaide, Australia

² Physics Department, SUNY Albany, Albany NY, United States of America

³ Department of Physics, University of Alberta, Edmonton AB, Canada

⁴ ^(a) Department of Physics, Ankara University, Ankara; ^(b) Department of Physics, Gazi University, Ankara; ^(c) Istanbul Aydin University, Istanbul; ^(d) Division of Physics, TOBB University of Economics and Technology, Ankara, Turkey

- ⁵ LAPP, CNRS/IN2P3 and Université de Savoie, Annecy-le-Vieux, France
- ⁶ High Energy Physics Division, Argonne National Laboratory, Argonne IL, United States of America
- ⁷ Department of Physics, University of Arizona, Tucson AZ, United States of America
- ⁸ Department of Physics, The University of Texas at Arlington, Arlington TX, United States of America
- ⁹ Physics Department, University of Athens, Athens, Greece
- ¹⁰ Physics Department, National Technical University of Athens, Zografou, Greece
- ¹¹ Institute of Physics, Azerbaijan Academy of Sciences, Baku, Azerbaijan
- ¹² Institut de Física d'Altes Energies and Departament de Física de la Universitat Autònoma de Barcelona, Barcelona, Spain
- ¹³ ^(a) Institute of Physics, University of Belgrade, Belgrade; ^(b) Vinca Institute of Nuclear Sciences, University of Belgrade, Belgrade, Serbia
- ¹⁴ Department for Physics and Technology, University of Bergen, Bergen, Norway
- ¹⁵ Physics Division, Lawrence Berkeley National Laboratory and University of California, Berkeley CA, United States of America
- ¹⁶ Department of Physics, Humboldt University, Berlin, Germany
- ¹⁷ Albert Einstein Center for Fundamental Physics and Laboratory for High Energy Physics, University of Bern, Bern, Switzerland
- ¹⁸ School of Physics and Astronomy, University of Birmingham, Birmingham, United Kingdom
- ¹⁹ ^(a) Department of Physics, Bogazici University, Istanbul; ^(b) Department of Physics, Dogus University, Istanbul; ^(c) Department of Physics Engineering, Gaziantep University, Gaziantep, Turkey
- ²⁰ ^(a) INFN Sezione di Bologna; ^(b) Dipartimento di Fisica e Astronomia, Università di Bologna, Bologna, Italy
- ²¹ Physikalisches Institut, University of Bonn, Bonn, Germany
- ²² Department of Physics, Boston University, Boston MA, United States of America
- ²³ Department of Physics, Brandeis University, Waltham MA, United States of America
- ²⁴ ^(a) Universidade Federal do Rio De Janeiro COPPE/EE/IF, Rio de Janeiro; ^(b) Federal University of Juiz de Fora (UFJF), Juiz de Fora; ^(c) Federal University of Sao Joao del Rei (UFSJ), Sao Joao del Rei; ^(d) Instituto de Fisica, Universidade de Sao Paulo, Sao Paulo, Brazil
- ²⁵ Physics Department, Brookhaven National Laboratory, Upton NY, United States of America
- ²⁶ ^(a) National Institute of Physics and Nuclear Engineering, Bucharest; ^(b) National Institute for Research and Development of Isotopic and Molecular Technologies, Physics Department, Cluj Napoca; ^(c) University Politehnica Bucharest, Bucharest; ^(d) West University in Timisoara, Timisoara, Romania
- ²⁷ Departamento de Física, Universidad de Buenos Aires, Buenos Aires, Argentina
- ²⁸ Cavendish Laboratory, University of Cambridge, Cambridge, United Kingdom
- ²⁹ Department of Physics, Carleton University, Ottawa ON, Canada
- ³⁰ CERN, Geneva, Switzerland

- ³¹ Enrico Fermi Institute, University of Chicago, Chicago IL, United States of America
- ³² ^(a) Departamento de Física, Pontificia Universidad Católica de Chile, Santiago; ^(b) Departamento de Física, Universidad Técnica Federico Santa María, Valparaíso, Chile
- ³³ ^(a) Institute of High Energy Physics, Chinese Academy of Sciences, Beijing; ^(b) Department of Modern Physics, University of Science and Technology of China, Anhui; ^(c) Department of Physics, Nanjing University, Jiangsu; ^(d) School of Physics, Shandong University, Shandong; ^(e) Physics Department, Shanghai Jiao Tong University, Shanghai; ^(f) Physics Department, Tsinghua University, Beijing 100084, China
- ³⁴ Laboratoire de Physique Corpusculaire, Clermont Université and Université Blaise Pascal and CNRS/IN2P3, Clermont-Ferrand, France
- ³⁵ Nevis Laboratory, Columbia University, Irvington NY, United States of America
- ³⁶ Niels Bohr Institute, University of Copenhagen, Kobenhavn, Denmark
- ³⁷ ^(a) INFN Gruppo Collegato di Cosenza, Laboratori Nazionali di Frascati; ^(b) Dipartimento di Fisica, Università della Calabria, Rende, Italy
- ³⁸ ^(a) AGH University of Science and Technology, Faculty of Physics and Applied Computer Science, Krakow; ^(b) Marian Smoluchowski Institute of Physics, Jagiellonian University, Krakow, Poland
- ³⁹ The Henryk Niewodniczanski Institute of Nuclear Physics, Polish Academy of Sciences, Krakow, Poland
- ⁴⁰ Physics Department, Southern Methodist University, Dallas TX, United States of America
- ⁴¹ Physics Department, University of Texas at Dallas, Richardson TX, United States of America
- ⁴² DESY, Hamburg and Zeuthen, Germany
- ⁴³ Institut für Experimentelle Physik IV, Technische Universität Dortmund, Dortmund, Germany
- ⁴⁴ Institut für Kern- und Teilchenphysik, Technische Universität Dresden, Dresden, Germany
- ⁴⁵ Department of Physics, Duke University, Durham NC, United States of America
- ⁴⁶ SUPA - School of Physics and Astronomy, University of Edinburgh, Edinburgh, United Kingdom
- ⁴⁷ INFN Laboratori Nazionali di Frascati, Frascati, Italy
- ⁴⁸ Fakultät für Mathematik und Physik, Albert-Ludwigs-Universität, Freiburg, Germany
- ⁴⁹ Section de Physique, Université de Genève, Geneva, Switzerland
- ⁵⁰ ^(a) INFN Sezione di Genova; ^(b) Dipartimento di Fisica, Università di Genova, Genova, Italy
- ⁵¹ ^(a) E. Andronikashvili Institute of Physics, Iv. Javakhishvili Tbilisi State University, Tbilisi; ^(b) High Energy Physics Institute, Tbilisi State University, Tbilisi, Georgia
- ⁵² II Physikalisches Institut, Justus-Liebig-Universität Giessen, Giessen, Germany
- ⁵³ SUPA - School of Physics and Astronomy, University of Glasgow, Glasgow, United Kingdom
- ⁵⁴ II Physikalisches Institut, Georg-August-Universität, Göttingen, Germany
- ⁵⁵ Laboratoire de Physique Subatomique et de Cosmologie, Université Grenoble-Alpes,

- CNRS/IN2P3, Grenoble, France
- ⁵⁶ Department of Physics, Hampton University, Hampton VA, United States of America
- ⁵⁷ Laboratory for Particle Physics and Cosmology, Harvard University, Cambridge MA, United States of America
- ⁵⁸ ^(a) Kirchhoff-Institut für Physik, Ruprecht-Karls-Universität Heidelberg, Heidelberg; ^(b) Physikalisches Institut, Ruprecht-Karls-Universität Heidelberg, Heidelberg; ^(c) ZITI Institut für technische Informatik, Ruprecht-Karls-Universität Heidelberg, Mannheim, Germany
- ⁵⁹ Faculty of Applied Information Science, Hiroshima Institute of Technology, Hiroshima, Japan
- ⁶⁰ ^(a) Department of Physics, The Chinese University of Hong Kong, Shatin, N.T., Hong Kong; ^(b) Department of Physics, The University of Hong Kong, Hong Kong; ^(c) Department of Physics, The Hong Kong University of Science and Technology, Clear Water Bay, Kowloon, Hong Kong, China
- ⁶¹ Department of Physics, Indiana University, Bloomington IN, United States of America
- ⁶² Institut für Astro- und Teilchenphysik, Leopold-Franzens-Universität, Innsbruck, Austria
- ⁶³ University of Iowa, Iowa City IA, United States of America
- ⁶⁴ Department of Physics and Astronomy, Iowa State University, Ames IA, United States of America
- ⁶⁵ Joint Institute for Nuclear Research, JINR Dubna, Dubna, Russia
- ⁶⁶ KEK, High Energy Accelerator Research Organization, Tsukuba, Japan
- ⁶⁷ Graduate School of Science, Kobe University, Kobe, Japan
- ⁶⁸ Faculty of Science, Kyoto University, Kyoto, Japan
- ⁶⁹ Kyoto University of Education, Kyoto, Japan
- ⁷⁰ Department of Physics, Kyushu University, Fukuoka, Japan
- ⁷¹ Instituto de Física La Plata, Universidad Nacional de La Plata and CONICET, La Plata, Argentina
- ⁷² Physics Department, Lancaster University, Lancaster, United Kingdom
- ⁷³ ^(a) INFN Sezione di Lecce; ^(b) Dipartimento di Matematica e Fisica, Università del Salento, Lecce, Italy
- ⁷⁴ Oliver Lodge Laboratory, University of Liverpool, Liverpool, United Kingdom
- ⁷⁵ Department of Physics, Jožef Stefan Institute and University of Ljubljana, Ljubljana, Slovenia
- ⁷⁶ School of Physics and Astronomy, Queen Mary University of London, London, United Kingdom
- ⁷⁷ Department of Physics, Royal Holloway University of London, Surrey, United Kingdom
- ⁷⁸ Department of Physics and Astronomy, University College London, London, United Kingdom
- ⁷⁹ Louisiana Tech University, Ruston LA, United States of America
- ⁸⁰ Laboratoire de Physique Nucléaire et de Hautes Energies, UPMC and Université Paris-Diderot and CNRS/IN2P3, Paris, France
- ⁸¹ Fysiska institutionen, Lunds universitet, Lund, Sweden

- ⁸² Departamento de Fisica Teorica C-15, Universidad Autonoma de Madrid, Madrid, Spain
- ⁸³ Institut für Physik, Universität Mainz, Mainz, Germany
- ⁸⁴ School of Physics and Astronomy, University of Manchester, Manchester, United Kingdom
- ⁸⁵ CPPM, Aix-Marseille Université and CNRS/IN2P3, Marseille, France
- ⁸⁶ Department of Physics, University of Massachusetts, Amherst MA, United States of America
- ⁸⁷ Department of Physics, McGill University, Montreal QC, Canada
- ⁸⁸ School of Physics, University of Melbourne, Victoria, Australia
- ⁸⁹ Department of Physics, The University of Michigan, Ann Arbor MI, United States of America
- ⁹⁰ Department of Physics and Astronomy, Michigan State University, East Lansing MI, United States of America
- ⁹¹ ^(a) INFN Sezione di Milano; ^(b) Dipartimento di Fisica, Università di Milano, Milano, Italy
- ⁹² B.I. Stepanov Institute of Physics, National Academy of Sciences of Belarus, Minsk, Republic of Belarus
- ⁹³ National Scientific and Educational Centre for Particle and High Energy Physics, Minsk, Republic of Belarus
- ⁹⁴ Department of Physics, Massachusetts Institute of Technology, Cambridge MA, United States of America
- ⁹⁵ Group of Particle Physics, University of Montreal, Montreal QC, Canada
- ⁹⁶ P.N. Lebedev Institute of Physics, Academy of Sciences, Moscow, Russia
- ⁹⁷ Institute for Theoretical and Experimental Physics (ITEP), Moscow, Russia
- ⁹⁸ National Research Nuclear University MEPhI, Moscow, Russia
- ⁹⁹ D.V.Skobeltsyn Institute of Nuclear Physics, M.V.Lomonosov Moscow State University, Moscow, Russia
- ¹⁰⁰ Fakultät für Physik, Ludwig-Maximilians-Universität München, München, Germany
- ¹⁰¹ Max-Planck-Institut für Physik (Werner-Heisenberg-Institut), München, Germany
- ¹⁰² Nagasaki Institute of Applied Science, Nagasaki, Japan
- ¹⁰³ Graduate School of Science and Kobayashi-Maskawa Institute, Nagoya University, Nagoya, Japan
- ¹⁰⁴ ^(a) INFN Sezione di Napoli; ^(b) Dipartimento di Fisica, Università di Napoli, Napoli, Italy
- ¹⁰⁵ Department of Physics and Astronomy, University of New Mexico, Albuquerque NM, United States of America
- ¹⁰⁶ Institute for Mathematics, Astrophysics and Particle Physics, Radboud University Nijmegen/Nikhef, Nijmegen, Netherlands
- ¹⁰⁷ Nikhef National Institute for Subatomic Physics and University of Amsterdam, Amsterdam, Netherlands
- ¹⁰⁸ Department of Physics, Northern Illinois University, DeKalb IL, United States of America

- ¹⁰⁹ Budker Institute of Nuclear Physics, SB RAS, Novosibirsk, Russia
¹¹⁰ Department of Physics, New York University, New York NY, United States of America
¹¹¹ Ohio State University, Columbus OH, United States of America
¹¹² Faculty of Science, Okayama University, Okayama, Japan
¹¹³ Homer L. Dodge Department of Physics and Astronomy, University of Oklahoma, Norman OK, United States of America
¹¹⁴ Department of Physics, Oklahoma State University, Stillwater OK, United States of America
¹¹⁵ Palacký University, RCPTM, Olomouc, Czech Republic
¹¹⁶ Center for High Energy Physics, University of Oregon, Eugene OR, United States of America
¹¹⁷ LAL, Université Paris-Sud and CNRS/IN2P3, Orsay, France
¹¹⁸ Graduate School of Science, Osaka University, Osaka, Japan
¹¹⁹ Department of Physics, University of Oslo, Oslo, Norway
¹²⁰ Department of Physics, Oxford University, Oxford, United Kingdom
¹²¹ ^(a) INFN Sezione di Pavia; ^(b) Dipartimento di Fisica, Università di Pavia, Pavia, Italy
¹²² Department of Physics, University of Pennsylvania, Philadelphia PA, United States of America
¹²³ Petersburg Nuclear Physics Institute, Gatchina, Russia
¹²⁴ ^(a) INFN Sezione di Pisa; ^(b) Dipartimento di Fisica E. Fermi, Università di Pisa, Pisa, Italy
¹²⁵ Department of Physics and Astronomy, University of Pittsburgh, Pittsburgh PA, United States of America
¹²⁶ ^(a) Laboratorio de Instrumentacao e Fisica Experimental de Particulas - LIP, Lisboa; ^(b) Faculdade de Ciências, Universidade de Lisboa, Lisboa; ^(c) Department of Physics, University of Coimbra, Coimbra; ^(d) Centro de Física Nuclear da Universidade de Lisboa, Lisboa; ^(e) Departamento de Fisica, Universidade do Minho, Braga; ^(f) Departamento de Fisica Teorica y del Cosmos and CAFPE, Universidad de Granada, Granada (Spain); ^(g) Dep Fisica and CEFITEC of Faculdade de Ciencias e Tecnologia, Universidade Nova de Lisboa, Caparica, Portugal
¹²⁷ Institute of Physics, Academy of Sciences of the Czech Republic, Praha, Czech Republic
¹²⁸ Czech Technical University in Prague, Praha, Czech Republic
¹²⁹ Faculty of Mathematics and Physics, Charles University in Prague, Praha, Czech Republic
¹³⁰ State Research Center Institute for High Energy Physics, Protvino, Russia
¹³¹ Particle Physics Department, Rutherford Appleton Laboratory, Didcot, United Kingdom
¹³² Ritsumeikan University, Kusatsu, Shiga, Japan
¹³³ ^(a) INFN Sezione di Roma; ^(b) Dipartimento di Fisica, Sapienza Università di Roma, Roma, Italy
¹³⁴ ^(a) INFN Sezione di Roma Tor Vergata; ^(b) Dipartimento di Fisica, Università di Roma Tor Vergata, Roma, Italy

- ¹³⁵ ^(a) INFN Sezione di Roma Tre; ^(b) Dipartimento di Matematica e Fisica, Università Roma Tre, Roma, Italy
- ¹³⁶ ^(a) Faculté des Sciences Ain Chock, Réseau Universitaire de Physique des Hautes Energies - Université Hassan II, Casablanca; ^(b) Centre National de l'Energie des Sciences Techniques Nucléaires, Rabat; ^(c) Faculté des Sciences Semlalia, Université Cadi Ayyad, LPHEA-Marrakech; ^(d) Faculté des Sciences, Université Mohamed Premier and LPTPM, Oujda; ^(e) Faculté des sciences, Université Mohammed V-Agdal, Rabat, Morocco
- ¹³⁷ DSM/IRFU (Institut de Recherches sur les Lois Fondamentales de l'Univers), CEA Saclay (Commissariat à l'Energie Atomique et aux Energies Alternatives), Gif-sur-Yvette, France
- ¹³⁸ Santa Cruz Institute for Particle Physics, University of California Santa Cruz, Santa Cruz CA, United States of America
- ¹³⁹ Department of Physics, University of Washington, Seattle WA, United States of America
- ¹⁴⁰ Department of Physics and Astronomy, University of Sheffield, Sheffield, United Kingdom
- ¹⁴¹ Department of Physics, Shinshu University, Nagano, Japan
- ¹⁴² Fachbereich Physik, Universität Siegen, Siegen, Germany
- ¹⁴³ Department of Physics, Simon Fraser University, Burnaby BC, Canada
- ¹⁴⁴ SLAC National Accelerator Laboratory, Stanford CA, United States of America
- ¹⁴⁵ ^(a) Faculty of Mathematics, Physics & Informatics, Comenius University, Bratislava; ^(b) Department of Subnuclear Physics, Institute of Experimental Physics of the Slovak Academy of Sciences, Kosice, Slovak Republic
- ¹⁴⁶ ^(a) Department of Physics, University of Cape Town, Cape Town; ^(b) Department of Physics, University of Johannesburg, Johannesburg; ^(c) School of Physics, University of the Witwatersrand, Johannesburg, South Africa
- ¹⁴⁷ ^(a) Department of Physics, Stockholm University; ^(b) The Oskar Klein Centre, Stockholm, Sweden
- ¹⁴⁸ Physics Department, Royal Institute of Technology, Stockholm, Sweden
- ¹⁴⁹ Departments of Physics & Astronomy and Chemistry, Stony Brook University, Stony Brook NY, United States of America
- ¹⁵⁰ Department of Physics and Astronomy, University of Sussex, Brighton, United Kingdom
- ¹⁵¹ School of Physics, University of Sydney, Sydney, Australia
- ¹⁵² Institute of Physics, Academia Sinica, Taipei, Taiwan
- ¹⁵³ Department of Physics, Technion: Israel Institute of Technology, Haifa, Israel
- ¹⁵⁴ Raymond and Beverly Sackler School of Physics and Astronomy, Tel Aviv University, Tel Aviv, Israel
- ¹⁵⁵ Department of Physics, Aristotle University of Thessaloniki, Thessaloniki, Greece
- ¹⁵⁶ International Center for Elementary Particle Physics and Department of Physics, The University of Tokyo, Tokyo, Japan
- ¹⁵⁷ Graduate School of Science and Technology, Tokyo Metropolitan University, Tokyo, Japan

- ¹⁵⁸ Department of Physics, Tokyo Institute of Technology, Tokyo, Japan
¹⁵⁹ Department of Physics, University of Toronto, Toronto ON, Canada
¹⁶⁰ ^(a) TRIUMF, Vancouver BC; ^(b) Department of Physics and Astronomy, York University, Toronto ON, Canada
¹⁶¹ Faculty of Pure and Applied Sciences, University of Tsukuba, Tsukuba, Japan
¹⁶² Department of Physics and Astronomy, Tufts University, Medford MA, United States of America
¹⁶³ Centro de Investigaciones, Universidad Antonio Narino, Bogota, Colombia
¹⁶⁴ Department of Physics and Astronomy, University of California Irvine, Irvine CA, United States of America
¹⁶⁵ ^(a) INFN Gruppo Collegato di Udine, Sezione di Trieste, Udine; ^(b) ICTP, Trieste; ^(c) Dipartimento di Chimica, Fisica e Ambiente, Università di Udine, Udine, Italy
¹⁶⁶ Department of Physics, University of Illinois, Urbana IL, United States of America
¹⁶⁷ Department of Physics and Astronomy, University of Uppsala, Uppsala, Sweden
¹⁶⁸ Instituto de Física Corpuscular (IFIC) and Departamento de Física Atómica, Molecular y Nuclear and Departamento de Ingeniería Electrónica and Instituto de Microelectrónica de Barcelona (IMB-CNM), University of Valencia and CSIC, Valencia, Spain
¹⁶⁹ Department of Physics, University of British Columbia, Vancouver BC, Canada
¹⁷⁰ Department of Physics and Astronomy, University of Victoria, Victoria BC, Canada
¹⁷¹ Department of Physics, University of Warwick, Coventry, United Kingdom
¹⁷² Waseda University, Tokyo, Japan
¹⁷³ Department of Particle Physics, The Weizmann Institute of Science, Rehovot, Israel
¹⁷⁴ Department of Physics, University of Wisconsin, Madison WI, United States of America
¹⁷⁵ Fakultät für Physik und Astronomie, Julius-Maximilians-Universität, Würzburg, Germany
¹⁷⁶ Fachbereich C Physik, Bergische Universität Wuppertal, Wuppertal, Germany
¹⁷⁷ Department of Physics, Yale University, New Haven CT, United States of America
¹⁷⁸ Yerevan Physics Institute, Yerevan, Armenia
¹⁷⁹ Centre de Calcul de l’Institut National de Physique Nucléaire et de Physique des Particules (IN2P3), Villeurbanne, France
^a Also at Department of Physics, King’s College London, London, United Kingdom
^b Also at Institute of Physics, Azerbaijan Academy of Sciences, Baku, Azerbaijan
^c Also at Novosibirsk State University, Novosibirsk, Russia
^d Also at Particle Physics Department, Rutherford Appleton Laboratory, Didcot, United Kingdom
^e Also at TRIUMF, Vancouver BC, Canada
^f Also at Department of Physics, California State University, Fresno CA, United States of America
^g Also at Tomsk State University, Tomsk, Russia
^h Also at CPPM, Aix-Marseille Université and CNRS/IN2P3, Marseille, France
ⁱ Also at Università di Napoli Parthenope, Napoli, Italy

- ^j Also at Institute of Particle Physics (IPP), Canada
- ^k Also at Department of Physics, St. Petersburg State Polytechnical University, St. Petersburg, Russia
- ^l Also at Department of Financial and Management Engineering, University of the Aegean, Chios, Greece
- ^m Also at Louisiana Tech University, Ruston LA, United States of America
- ⁿ Also at Institutio Catalana de Recerca i Estudis Avancats, ICREA, Barcelona, Spain
- ^o Also at Department of Physics, The University of Texas at Austin, Austin TX, United States of America
- ^p Also at Institute of Theoretical Physics, Ilia State University, Tbilisi, Georgia
- ^q Also at CERN, Geneva, Switzerland
- ^r Also at Ochadai Academic Production, Ochanomizu University, Tokyo, Japan
- ^s Also at Manhattan College, New York NY, United States of America
- ^t Also at Institute of Physics, Academia Sinica, Taipei, Taiwan
- ^u Also at LAL, Université Paris-Sud and CNRS/IN2P3, Orsay, France
- ^v Also at Academia Sinica Grid Computing, Institute of Physics, Academia Sinica, Taipei, Taiwan
- ^w Also at Laboratoire de Physique Nucléaire et de Hautes Energies, UPMC and Université Paris-Diderot and CNRS/IN2P3, Paris, France
- ^x Also at School of Physical Sciences, National Institute of Science Education and Research, Bhubaneswar, India
- ^y Also at Dipartimento di Fisica, Sapienza Università di Roma, Roma, Italy
- ^z Also at Moscow Institute of Physics and Technology State University, Dolgoprudny, Russia
- ^{aa} Also at Section de Physique, Université de Genève, Geneva, Switzerland
- ^{ab} Also at International School for Advanced Studies (SISSA), Trieste, Italy
- ^{ac} Also at Department of Physics and Astronomy, University of South Carolina, Columbia SC, United States of America
- ^{ad} Also at School of Physics and Engineering, Sun Yat-sen University, Guangzhou, China
- ^{ae} Also at Faculty of Physics, M.V.Lomonosov Moscow State University, Moscow, Russia
- ^{af} Also at National Research Nuclear University MEPhI, Moscow, Russia
- ^{ag} Also at Institute for Particle and Nuclear Physics, Wigner Research Centre for Physics, Budapest, Hungary
- ^{ah} Also at Department of Physics, Oxford University, Oxford, United Kingdom
- ^{ai} Also at Department of Physics, Nanjing University, Jiangsu, China
- ^{aj} Also at Institut für Experimentalphysik, Universität Hamburg, Hamburg, Germany
- ^{ak} Also at Department of Physics, The University of Michigan, Ann Arbor MI, United States of America
- ^{al} Also at Discipline of Physics, University of KwaZulu-Natal, Durban, South Africa
- ^{am} Also at University of Malaya, Department of Physics, Kuala Lumpur, Malaysia
- * Deceased